

**Chemoenzymatic and Template-Directed Synthesis of
Bioactive Macrocyclic Peptides**

Dissertation
zur Erlangung des Doktorgrades
der Naturwissenschaften
(Dr. rer. nat.)

dem
Fachbereich Chemie
der Philipps-Universität Marburg
vorgelegt von

Jan Grünewald

aus Fritzlar

Marburg/Lahn 2005

Vom Fachbereich Chemie

der Philipps-Universität Marburg als Dissertation

am 15. November 2005 angenommen.

Erstgutachter : Prof. Dr. M. A. Marahiel (Philipps-Universität, Marburg)

Zweitgutachter : Prof. Dr. T. Schrader (Philipps-Universität, Marburg)

Tag der Disputation: 15. Dezember 2005

To my parents...

Summary

Nonribosomal peptide synthetases (NRPS) are large multienzyme complexes, which simultaneously represent template and biosynthetic machinery for the production of structurally diverse peptidic products that feature high pharmacological and biological activities. A key determinant of nonribosomal peptide product activity is the common macrocyclic structure of many compounds. Macrocyclization is catalyzed in the last step of nonribosomal synthesis by thioesterase (TE) domain activity. The herein presented work describes the first biochemical characterization of a TE domain of a streptomycete, the thioesterase of the *S. coelicolor* calcium-dependent antibiotic (CDA) synthetase. This recombinant cyclase catalyzes macrolactone formation of linear peptidyl-thioesters based on a sequence analogous to natural CDA. For substrate mimics, the phosphopantetheine cofactor was successfully substituted by various thioester leaving groups. The best rates for cyclization were determined for the thiophenol leaving group, revealing that chemical reactivity is more important for enzyme acylation than cofactor recognition. Interestingly, CDA cyclase catalyzes the formation of two regioisomeric macrolactones, which arise from simultaneous nucleophilic attack of the two adjacent Thr₂ and Ser₁ residues onto the C-terminal Trp₁₁ of the acyl-enzyme intermediate. To further explore this relaxed regioselectivity of CDA TE, alterations to the peptide backbone and the fatty acyl chain were made. Substitution of either Thr₂ or Ser₁ by alanine led to selective formation of a decapeptide or undecapeptide lactone ring. However, the stereoselectivity of CDA cyclase was fully retained, thus accepting only L-configured Ser₁ and Thr₂ for cyclization. Elongation of the fatty acyl group by four methylene groups to the natural length (C₆) of CDA turned the relaxed regioselectivity into a strict regioselectivity, yielding solely the decapeptide lactone ring, along with decreased hydrolysis of the peptidyl-thioester substrate. This provides evidence for the crucial role of the lipid chain in controlling the regio- and chemoselectivity of TE-mediated macrocyclization.

CDA belongs to the group of acidic lipopeptides, which includes the clinically approved antibiotic daptomycin. To evaluate the capability of CDA cyclase for the chemoenzymatic generation of daptomycin, six daptomycin-specific residues were successively incorporated into linear CDA undecapeptidyl-thioesters. All these six substrates were efficiently cyclized by CDA TE. Simultaneous incorporation of all six of these residues into the peptide backbone and elongation of the N-terminus of CDA by two residues finally yielded a daptomycin derivative that lacked only the β -methyl group of L-3-methylglutamate. In accordance with acidic lipopeptide antibiotics, the bioactivity of the chemoenzymatic assembled daptomycin analogue is dependent on the presence of calcium ions. To identify calcium-binding sites in the lipo-tridecapeptide chain of the daptomycin analogue, all four acidic residues were successively substituted by either Asn or Gln. Bioactivity studies revealed that only Asp₇ and Asp₉ are essential for antimicrobial potency. Moreover, these two residues are strictly conserved among all other nonribosomal acidic lipopeptides and the calcium-binding EF-motif of ribosomally assembled calmodulin.

The final part of this work is dedicated to the selective detection of peptide cyclization by fluorescence resonance energy transfer (FRET). In this approach, peptide cyclization catalyzed by NRPS-derived TE domains brings the donor Trp and the acceptor Kyn (kynurenine) in sufficiently close proximity to enable efficient FRET. These fluorophores were readily incorporated into the peptide backbone by solid-phase peptide chemistry and show excellent spectral overlap between the donor emission and acceptor absorption. Application of this method provided a tool to track TE-mediated peptide cyclization in real-time. Furthermore, picomolar detection limits of cyclopeptides were realized, thereby facilitating kinetic studies of TE-mediated macrocyclization. The general utility of FRET-assisted detection of cyclopeptides was demonstrated for two cyclases, namely tyrocidine (Tyc) TE, and CDA TE. For the latter cyclase, this approach was combined with site-directed affinity labelling, opening the possibility for high-throughput enzymatic screening.

Chemoenzymatische und Templat-gerichtete Synthese von bioaktiven makrozyklischen Peptiden

Zusammenfassung

Nichtribosomale Peptidsynthetasen (NRPS) sind Multienzymkomplexe, die gleichzeitig Templat und biosynthetische Maschinerie für die Herstellung strukturell diverser peptidischer Produkte mit oftmals bedeutender pharmakologischer und biologischer Aktivität repräsentieren. Ein Schlüsselfaktor für die Bioaktivität nichtribosomaler Peptide ist die makrozyklische Struktur vieler dieser Verbindungen. Makrozyklisierung wird durch Thioesterase- (TE-) Domänen im letzten Schritt der nichtribosomalen Synthese katalysiert. Diese Arbeit beschreibt die erste biochemische Charakterisierung einer TE-Domäne eines Streptomyceten: Die Thioesterase des kalzium-abhängigen Antibiotikums (CDA) von *S. coelicolor*. Diese Zyklastase katalysiert die Ringbildung linearer Peptidylthioester, die auf einer zu CDA analogen Sequenz basieren. Hierzu wurde der natürliche Phosphopantethein-Kofaktor durch verschiedene Abgangsgruppen ersetzt. Die höchsten Zyklisierungsraten wurden für die Thiophenol-Abgangsgruppe erzielt. Chemische Reaktivität ist demnach für eine effiziente Enzym-Acylierung wichtiger als Kofaktorerkennung. Die CDA-Zyklastase katalysiert die Bildung zweier regioisomerer Laktone durch konzertierten Angriff der benachbarten Reste Thr₂ und Ser₁ auf das C-terminale Trp₁₁ des Acyl-Enzym-Intermediates. Um diese relaxierte Regioselektivität der CDA TE eingehender zu untersuchen, wurden Änderungen im Peptidrückgrat und der Fettsäure vorgenommen. Substitution von Thr₂ oder Ser₁ durch Alanin führte zur selektiven Bildung eines Dekapeptid- oder Undekapeptid-Ringes. Die Stereoselektivität der Zyklastase blieb voll erhalten, und nur L-konfiguriertes Ser₁ bzw. Thr₂ wurde toleriert. Elongation der Fettsäure um vier Methylenheiten auf die natürliche Länge (C₆) von CDA wandelte die relaxierte in eine strikte Regioselektivität um, was zur ausschließlichen Bildung des Dekapeptid-Laktone führte. Zudem wurde weniger Hydrolyse beobachtet. Diese Ergebnisse verdeutlichen den Einfluss der Fettsäure auf die Regio- und Chemo-selektivität der TE-vermittelten Makrozyklisierung.

CDA gehört, wie das klinisch zugelassene Antibiotikum Daptomycin, den sauren Lipopeptiden an. Um das Potential der CDA-Zyklastase zur chemoenzymatischen Synthese von Daptomycin abschätzen zu können, wurden sukzessive sechs Daptomycin-spezifische Reste in lineare CDA-Undekapeptidyl-Thioester eingebaut. Alle sechs Substrate wurden durch die CDA TE zyklisiert. Gleichzeitiger Einbau aller sechs Reste in das CDA-Peptidrückgrat und Verlängerung des N-Terminus um zwei Reste führte schließlich zur Synthese eines Daptomycin-Analogons, dem nur die β -Methylgruppe von L-3-Methylglutamat fehlte. In Übereinstimmung mit sauren Lipopeptiden war die Bioaktivität des chemoenzymatisch hergestellten Daptomycin-Derivats von der Anwesenheit von Kalzium abhängig. Um Kalzium-Bindungsstellen in dem Daptomycin-Analogon zu identifizieren, wurden sukzessive alle vier sauren Reste gegen Asn oder Gln ausgetauscht. Bioaktivitätstests wiesen die essentielle Bedeutung von Asp₇ und Asp₉ für die antimikrobielle Potenz nach. Zudem sind diese Reste in allen nichtribosomalen sauren Lipopeptiden und dem Kalzium-bindenden EF-Motiv ribosomal-hergestellten Calmodulins konserviert.

Der letzte Teil dieser Arbeit beschreibt die Detektion von Peptidzyklisierung durch Fluoreszenz-Resonanz-Energie-Transfer (FRET). Hierbei werden der Donor Trp und der Akzeptor Kyn (Kynurenin) durch TE-Domänen-katalysierte Peptidzyklisierung räumlich so nahe zusammengebracht, dass effizienter FRET ermöglicht wird. Die beiden Fluorophore konnten mittels Festphasensynthese in das Peptidrückgrat eingebaut werden und zeigen exzellente spektrale Überlappung zwischen Donor-Emission und Akzeptor-Absorption. Mittels dieser Methode konnte TE-vermittelte Zyklisierung in Echtzeit verfolgt werden. Zudem konnten Zylopeptide im picomolaren Bereich detektiert werden, was kinetische Studien TE-katalysierter Makrozyklisierung erleichterte. Die generelle Anwendbarkeit FRET-unterstützter Detektion von Zylopeptiden wurde für zwei Zyklastasen gezeigt: Tyrocidin (Tyc) TE und CDA TE. Bei letzterer wurde diese Methode mit ortsgerichtetem Affinitätslabeling kombiniert, was neue Möglichkeiten für das Hochdurchsatz-Enzymscreening eröffnete.

The majority of the work presented here has been published:

Grünwald, J., Marahiel, M. A. “Chemoenzymatic and template-directed synthesis of bioactive macrocyclic peptides“ *Microbiol. Mol. Biol. Rev.*, 2005, submitted.

Grünwald, J., Mahlert, C., Kopp, F., Marahiel, M. A. “Chemoenzymatic pathways towards novel peptide antibiotics“ *Curr. Med. Chem.*, 2005, submitted.

Grünwald, J., Marahiel, M. A. “Nonribosomally synthesized bacterial peptides” in *The handbook of peptides*. Elsevier, 2005, in revision.

Grünwald, J., Kopp, F., Mahlert, C., Linne, U., Sieber, S. A., Marahiel, M. A. “Fluorescence resonance energy transfer as a probe of peptide cyclization catalyzed by nonribosomal thioesterase domains” *Chem. & Biol.*, 2005, 12, 873-881.

Mahlert, C., Sieber, S. A., Grünwald, J., Marahiel, M. A. “Chemoenzymatic approach to enantiopure streptogramin B variants: Characterization of stereoselective pristinamycin I cyclase from *Streptomyces pristinaespiralis*” *J. Am. Chem. Soc.*, 2005, 127, 9571-9580.

Grünwald, J., Sieber, S. A., Mahlert, C., Linne, U., Marahiel, M. A. “Synthesis and derivatization of daptomycin: A chemoenzymatic route to acidic lipopeptide antibiotics” *J. Am. Chem. Soc.*, 2004, 126, 17025-17031.

Grünwald, J.*, Sieber, S. A.*, Marahiel, M. A. “Chemo- and regioselective peptide cyclization triggered by the N-terminal fatty acid chain length: The recombinant cyclase of the calcium-dependent antibiotic from *Streptomyces coelicolor*” *Biochemistry*, 2004, 43, 2915-2925.

*these authors contributed equally to this work

Table of Contents

TTABLE OF CONTENTS	7
1. ABBREVIATIONS	12
2. INTRODUCTION	16
2.1. STRUCTURAL RIGIDITY OF NONRIBOSOMALLY SYNTHESIZED PEPTIDES	17
2.2. DIVERSITY OF NONRIBOSOMAL PEPTIDES: THE ACIDIC LIPOPEPTIDE ANTIBIOTICS	19
2.3. PRODUCTION OF ACIDIC LIPOPEPTIDES BY NONRIBOSOMAL PEPTIDE SYNTHETASES (NRPSs).....	23
2.3.1. <i>Principles of Nonribosomal Peptide Synthesis: Dissecting the Modules into Domains</i>	25
2.3.2. <i>Proofreading of Nonribosomal Peptide Synthesis</i>	27
2.3.3. <i>Lipidation of Nonribosomally-Produced Peptides</i>	28
2.3.4. <i>Generation of D-Amino Acid Residues in NRPSs</i>	29
2.4. MACROCYCLIZATION CATALYZED BY NONRIBOSOMAL THIOESTERASE-DOMAINS	31
2.4.1. <i>Structural and Mechanistic Aspects of Peptide Cyclases</i>	34
2.4.2. <i>Autonomous Cyclization Activity of Excised TE Domains</i>	35
2.4.3. <i>Generality of TE-Catalyzed Peptide Cyclization</i>	37
2.4.4. <i>Chemoenzymatic approaches towards novel cyclopeptides</i>	39
2.5. DIVERSIFICATION AND RIGIDIFICATION OF PEPTIDES MEDIATED BY TAILORING ENZYMES	41
2.5.1. <i>C-, N-Methylation of Nonribosomal Peptides</i>	42
2.5.2. <i>Tailoring of Rigidity-Conferring Heterocyclic Elements</i>	45
2.5.3. <i>Rigidification of Peptide Scaffolds by Oxidative Cross-Linking</i>	46
2.6. MANIPULATION OF CARRIER PROTEINS BY POSTTRANSLATIONAL MODIFICATION.....	47
2.7. TASK.....	51
3. MATERIAL	52
3.1. CHEMICALS, ENZYMES AND GENERAL MATERIALS.....	52
3.2. EQUIPMENT	53
3.3. VECTOR SYSTEMS	54
3.3.1. <i>pQE60-vector</i>	54
3.3.2. <i>pQTEV-vector</i>	55
3.3.3. <i>pBAD202/D-TOPO</i>	56
3.4. MICROORGANISMS.....	57
3.4.1. <i>E. coli XLI-Blue</i>	57
3.4.2. <i>E. coli Top 10</i>	57
3.4.3. <i>E. coli BL21(DE3)</i>	57
3.4.4. <i>E. coli BL21(M15)</i>	58
3.5. MEDIA	58
4. METHODS	59
4.1. MOLECULAR BIOLOGY TECHNIQUES	59
4.1.1. <i>Construction of Recombinant Plasmids</i>	59
4.1.2. <i>DNA Sequencing</i>	60
4.2. PROTEIN METHODS.....	61
4.2.1. <i>Gene Expression</i>	61
4.2.1.1. Expression with the pQE60- and pQTEV-Vector Systems	61
4.2.1.2. Expression with the pBAD202/D-TOPO-Vector System.....	62
4.2.2. <i>Protein Purification</i>	62
4.2.2.1. Disruption of cell material.....	62
4.2.2.2. Ni ²⁺ -NTA affinity chromatography.....	63
4.2.2.3. Determination of Protein Concentrations	63
4.3. BIOCHEMICAL METHODS	64
4.3.1. <i>Cyclization Assays</i>	64
4.3.2. <i>Preparation of Linear and Cyclic Peptides for Bioassays and Fluorescence Measurements</i>	65
4.3.3. <i>Peptide Cyclization by the Immobilized CDA PCP-TE Didomain</i>	66
4.4. ANALYTICAL METHODS	66
4.4.1. <i>Biological Activity Assays</i>	66
4.4.2. <i>Mass Spectrometry</i>	67
4.5. FLUORESCENCE TECHNIQUES	71
4.5.1. <i>Real-time fluorescence measurements</i>	71

Table of Contents

4.6.	SOLID PHASE PEPTIDE SYNTHESIS (SPPS).....	72
4.6.1.	<i>Initiation: Loading of 2-chlorotritylchloride resin</i>	72
4.6.2.	<i>Elongation: Coupling of Fmoc amino acids</i>	73
4.6.3.	<i>Termination: Cleavage from the Resin</i>	75
4.7.	ORGANIC SYNTHESIS	75
4.7.1.	<i>Synthesis of Peptidyl-SNAC and Peptidyl-Thiophenol Substrates</i>	75
4.7.2.	<i>Synthesis of 4'-Phosphopantetheine (ppan)</i>	76
4.7.3.	<i>Synthesis of Peptidyl-CoA and Peptidyl-ppan Substrates</i>	76
4.7.4.	<i>Synthesis of N-(9-Fluorenylmethoxycarbonyl)-L-kynurenine</i>	76
4.7.5.	<i>Synthesis of Biotin CoA</i>	77
5.	RESULTS	78
5.1.	PEPTIDE CYCLIZATION CATALYZED BY THE RECOMBINANT THIOESTERASE DOMAIN OF THE CALCIUM-DEPENDENT ANTIBIOTIC	78
5.1.1.	<i>Overexpression of CDA TE as a Thioredoxin-Fusion Protein</i>	78
5.1.2.	<i>CDA Cyclase Catalyzes Ring Formation of a Synthetic CDA Analogue</i>	79
5.1.3.	<i>Selecting the Best Leaving Group for Macrolactonization Mediated by the CDA Cyclase</i>	84
5.1.4.	<i>Regioselectivity of CDA Cyclase</i>	86
5.1.5.	<i>Stereoselectivity of CDA Cyclase</i>	87
5.1.6.	<i>Extending the N-Terminal Acyl Chain of the CDA Thioester Substrate</i>	88
5.2.	EXPLORING THE SUBSTRATE TOLERANCE OF CDA CYCLASE TO PRODUCE DAPTOMYCIN	90
5.2.1.	<i>Single Amino Acid Substitutions</i>	90
5.2.2.	<i>Simultaneous Amino Acid Changes and Branch Point Movement</i>	93
5.2.3.	<i>Derivatization of Daptomycin and Bioactivity Studies</i>	96
5.3.	FRET-ASSISTED DETECTION OF PEPTIDE CYCLIZATION	100
5.3.1.	<i>Synthesis and Fluorescence Characteristics of Linear and Cyclic Daptomycin Peptides</i>	100
5.3.2.	<i>Examination of Distance-Dependent Interactions between Donor and Acceptor</i>	103
5.3.3.	<i>Real-Time Monitoring of Peptide Cyclization</i>	106
5.3.4.	<i>FRET Can Be Used to Measure Kinetics of Enzyme Mediated Peptide Cyclization</i>	109
5.3.5.	<i>FRET-Assisted Detection of Peptide Cyclization of Immobilized CDA Cyclase</i>	110
6.	DISCUSSION	112
6.1.	THE ENZYMOLOGY OF CDA CYCLASE	112
6.1.1.	<i>Enzymatic Cyclization of CDA: Substrate Recognition and Leaving Group Properties</i>	113
6.1.2.	<i>Exploring the Regioselectivity of CDA TE-Catalyzed Macrolactonization</i>	114
6.1.3.	<i>Probing the Stereoselectivity of CDA Cyclase</i>	116
6.1.4.	<i>Regioselective Peptide Cyclization Triggered by the Fatty Acid Chain Length</i>	117
6.2.	A CHEMOENZYMATIC ROUTE TO DAPTOMYCIN.....	119
6.2.1.	<i>Probing the Substrate Specificity of CDA Cyclase</i>	119
6.2.2.	<i>Chemoenzymatic Derivatization of Daptomycin</i>	122
6.3.	TE-CATALYZED PEPTIDE CYCLIZATION FOLLOWED BY FRET.....	124
6.3.1.	<i>Distance Dependence and Detection Limits</i>	124
6.3.2.	<i>FRET-Assisted Detection of Peptide Cyclization Combined with PCP-TE Tagging</i>	125
7.	LITERATURE	128
	ACKNOWLEDGEMENTS	137

Inhaltsverzeichnis

INHALTSVERZEICHNIS	7
1. ABKÜRZUNGEN	12
2. EINLEITUNG	16
2.1. STRUKTURELLE RIGIDITÄT VON NICHTTRIBOSOMAL-SYNTHEZISIERTEN PEPTIDEN	17
2.2. DIVERSITÄT VON NICHTTRIBOSOMALEN PEPTIDEN: DIE SAUREN LIPOPEPTID-ANTIBIOTIKA	19
2.3. HERSTELLUNG SAURER LIPOPEPTIDE DURCH NICHTTRIBOSOMALE PEPTIDSYNTHETASEN (NRPS)	23
2.3.1. <i>Prinzipien nichtribosomaler Peptidsynthese: Unterteilung der Module in Domänen</i>	25
2.3.2. <i>Fehlerkorrektur der nichtribosomalen Peptidsynthese</i>	27
2.3.3. <i>Lipidierung nichtribosomal-produzierter Peptide</i>	28
2.3.4. <i>Herstellung von D-Aminosäuren in NRPS</i>	29
2.4. MAKROZYKLISIERUNG DURCH NICHTTRIBOSOMALE THIOESTERASE-DOMÄNEN	31
2.4.1. <i>Strukturelle und mechanistische Aspekte von Peptidzyklasen</i>	34
2.4.2. <i>Autonome Zyklisierungsaktivität von isolierten TE-Domänen</i>	35
2.4.3. <i>Generalisierbarkeit TE-katalysierter Peptidzyklisierung</i>	37
2.4.4. <i>Chemoenzymatischer Ansatz für die Herstellung neuer Zyklopeptide</i>	39
2.5. DIVERSIFIZIERUNG UND RIGIDIFIZIERUNG VON PEPTIDEN DURCH TAILORING-ENZYME ...	41
2.5.1. <i>C-, N-Methylierung nichtribosomaler Peptide</i>	42
2.5.2. <i>Maßschneidern rigider heterozyklischer Elemente</i>	45
2.5.3. <i>Rigidifizierung von Peptidgerüsten durch oxidative Quervernetzung</i>	46
2.6. MANIPULATION VON CARRIER-PROTEINEN DURCH POSTTRANSLATIONALE MODIFIKATION.	47
2.7. AUFGABENSTELLUNG.....	51
3. MATERIALEN.....	52
3.1. CHEMIKALIEN, ENZYME UND SONSTIGE MATERIALIEN	52
3.2. AUSSTATTUNG	53
3.3. VEKTORSYSTEME	54
3.3.1. <i>pQE60-Vektor</i>	54
3.3.2. <i>pQTEV-Vektor</i>	55
3.3.3. <i>pBAD202/D-TOPO</i>	56
3.4. MIKROORGANISMEN	57
3.4.1. <i>E. coli XLI-Blue</i>	57
3.4.2. <i>E. coli Top 10</i>	57
3.4.3. <i>E. coli BL21(DE3)</i>	57
3.4.4. <i>E. coli BL21(M15)</i>	58
3.5. MEDIEN	58
4. METHODEN.....	59
4.1. MOLEKULARBIOLOGISCHE METHODEN	59
4.1.1. <i>Konstruktion rekombinanter Plasmide</i>	59
4.1.2. <i>DNA-Sequenzierung</i>	60
4.2. PROTEINTECHNIKEN	61
4.2.1. <i>Genexpression</i>	61
4.2.1.1. <i>Expression mit den pQE60- und pQTEV-Vektorsystemen</i>	61
4.2.1.2. <i>Expression mit dem pBAD202/D-TOPO-Vektorsystem</i>	62
4.2.2. <i>Proteinreinigung</i>	62
4.2.2.1. <i>Zellaufschluss</i>	62
4.2.2.2. <i>Ni²⁺-NTA-Affinitätschromatographie</i>	63
4.2.2.3. <i>Proteinkonzentrationsbestimmung</i>	63
4.3. BIOCHEMISCHE METHODEN	64
4.3.1. <i>Zyklisierungsassays</i>	64

4.3.2.	<i>Präparation linearer und zyklischer Peptide für Bioassays und Fluoreszenzmessungen</i>	65
4.3.3.	<i>Peptidzyklisierung durch die immobilisierte CDA PCP-TE-Didomäne</i>	66
4.4.	ANALYTISCHE METHODEN	66
4.4.1.	<i>Bioaktivitätsbestimmungen</i>	66
4.4.2.	<i>Massenspektrometrie</i>	67
4.5.	FLUORESCENZTECHNIKEN	71
4.5.1.	<i>Fluoreszenzmessungen in Echtzeit</i>	71
4.6.	FESTPHASENPEPTIDSYNTHESE (SPPS)	72
4.6.1.	<i>Initiation: Beladung des 2-Chlorotrylchlorid-Harzes</i>	72
4.6.2.	<i>Elongation: Kupplung der Fmoc-geschützten Aminosäuren</i>	73
4.6.3.	<i>Termination: Abspaltung vom Harz</i>	75
4.7.	ORGANISCHE SYNTHESE	75
4.7.1.	<i>Synthese von Peptidyl-SNAC- und Peptidyl-Thiophenol-Substraten</i>	75
4.7.2.	<i>Synthese von 4'-Phosphopantethein (ppan)</i>	76
4.7.3.	<i>Synthese von Peptidyl-CoA- und Peptidyl-ppan-Substraten</i>	76
4.7.4.	<i>Synthese von N-(9-Fluorenylmethoxycarbonyl)-L-kynurenin</i>	76
4.7.5.	<i>Synthese von Biotin-CoA</i>	77
5.	ERGEBNISSE	78
5.1.	PEPTIDZYKLISIERUNG KATALYSIERT DURCH DIE REKOMBINANTE THIOESTERASEDOMÄNE DES KALZIUM-ABHÄNGIGEN ANTIBIOTIKUMS	78
5.1.1.	<i>Überexpression der CDA TE als ein Thioredoxin-Fusionsprotein</i>	78
5.1.2.	<i>Die CDA-Zyklase katalysiert die Ringbildung synthetischer CDA-Analoga</i>	79
5.1.3.	<i>Bestimmung der besten Abgangsgruppe für die CDA-TE-vermittelte Makrolaktonisierung</i>	84
5.1.4.	<i>Regioselektivität der CDA-Zyklase</i>	86
5.1.5.	<i>Stereoselektivität der CDA-Zyklase</i>	87
5.1.6.	<i>Verlängerung der N-terminalen Acylkette des CDA-Thioestersubstrates</i>	88
5.2.	ERFORSCHUNG DER SUBSTRATTOLERANZ DER CDA-ZYKLASE IM HINBLICK AUF DAPTOMYCIN	90
5.2.1.	<i>Substitution einzelner Aminosäuren</i>	90
5.2.2.	<i>Konzertierte Aminosäure-Substitutionen und Veränderung des Verzweigungspunktes</i>	93
5.2.3.	<i>Derivatisierung von Daptomycin und Bioaktivitätsstudien</i>	96
5.3.	FRET-UNTERSTÜTZTE DETEKTION VON PEPTIDZYKLISIERUNG	100
5.3.1.	<i>Synthese und Fluoreszenz-Charakteristika linearer und zyklischer Daptomycin-Peptide</i>	100
5.3.2.	<i>Untersuchung der abstandsabhängigen Interaktionen zwischen Donor und Akzeptor</i>	103
5.3.3.	<i>Verfolgung von Peptidzyklisierung in Echtzeit</i>	106
5.3.4.	<i>FRET zur Messung von Peptidzyklisierungskinetiken</i>	109
5.3.5.	<i>FRET-unterstützte Detektion von Peptidzyklisierung katalysiert durch die immobilisierte CDA-Zyklase</i>	110
6.	DISKUSSION	112
6.1.	DIE ENZYMOLOGIE DER CDA-ZYKLASE	112
6.1.1.	<i>Enzymatische Zyklisierung von CDA: Substraterkennung und Abgangsgruppeneigenschaften</i>	113
6.1.2.	<i>Erforschung der Regioselektivität der CDA TE-katalysierten Makrolaktonisierung</i>	114
6.1.3.	<i>Erforschung der Stereoselektivität der CDA-Zyklase</i>	116
6.1.4.	<i>Regioselektive Peptidzyklisierung gesteuert durch die Länge der Fettsäure</i>	117
6.2.	EINE CHEMOENZYMATISCHE ROUTE ZU DAPTOMYCIN	119
6.2.1.	<i>Ermittlung der Substratspezifität der CDA Zyklase</i>	119
6.2.2.	<i>Chemoenzymatische Derivatisierung von Daptomycin</i>	122
6.3.	VERFOLGUNG TE-KATALYSIRTER PEPTIDZYKLISIERUNG MITTELS FRET	124
6.3.1.	<i>Abstandsabhängigkeit und Nachweisgrenzen</i>	124
6.3.2.	<i>FRET-unterstützte Detektion von Peptidzyklisierung kombiniert mit PCP-TE-Tagging</i>	125
7.	LITERATUR	128

Table of Contents

DANKSAGUNG..... 137

1. Abbreviations

aa	amino acid
Ac	acetyl
AcOH	acetic acid
ACP	acyl carrier protein
A-domain	adenylation domain
Aloc	allyloxycarbonyl
Amp	ampicillin
AMP	adenosine-5'-monophosphate
ADP	adenosine-5'-diphosphate
ATP	adenosine-5'-triphosphate
B	base
Boc	tert-butyloxycarbonyl
bp	base pairs
BSA	bovine serum albumin
calcd.	calculated
CDA	calcium dependent antibiotic
C-domain	condensation domain
CoA	coenzyme A
COM domain	communication-mediating domain
CP	carrier protein
cy	cyclic
Cy-domain	heterocyclization domain
Da	Dalton
DCC	dicyclohexylcarbodiimide
DCM	dichloromethane
DEBS	6-deoxyerythronolide B synthase
Dec	decanoyl
DHB	dihydroxybenzoyl
DMSO	dimethyl sulfoxide
DIPEA	diisopropylethylamine
DMF	N,N-dimethylformamide
dNTP	2'-desoxynucleosid-5'-triphosphate
E-domain	epimerization domain
EDTA	ethylene-diamino-tetraacetic acid
EK	enterokinase
Em	emission
ESI-MS	electron spray ionization – mass spectrometry
eq.	equivalent
Ex	excitation
FAAL	fatty acyl-AMP ligase
FAS	fatty acid synthase
Fen	fengycin
Fig.	Figure
FMN	flavin mononucleotide
Fmoc	9-fluorenylmethyloxycarbonyl
FPLC	fast performance liquid chromatography
FRET	fluorescence resonance energy transfer

1 Abbreviations

HBTU	2-(1H-benzotriazole-1-yl)-1,1,3,3-tetramethyluronium hexafluorophosphate
Hepes	2-N'-[N-(2-hydroxyethyl)-piperazinyl]-ethansulfonic acid
Hex	hexanoyl
HOBt	1-hydroxybenzotriazole
HPLC	high performance liquid chromatography
ICL	isochorismate lyase
IMAC	immobilized metal ion affinity chromatography
IPTG	isopropyl- β -D-thiogalactoside
Kan	kanamycin
kb	kilo base pairs
LB medium	Luria-Bertani medium
LC/MS	liquid chromatography/mass spectrometry
ln	linear
MALDI-TOF	matrix assisted laser desorption ionization-time of flight
MCS	multiple cloning site
MES	2-morpholinoethanesulfonic acid
MIC	minimal inhibitory concentration
MS	mass spectrometry
Myc	mycosubtilin
n. d.	not detected
N-Mt-domain	N-methylation domain
NMR	nuclear magnetic resonance
NRPS	nonribosomal peptide synthetases
NTA	nitrioltriacetate
OD	optical density
OSu	hydroxysuccinimide ester
Ox-domain	oxidation domain
PAGE	polyacrylamide gel electrophoresis
PCP	peptidyl carrier protein or thiolation domain
PCR	polymerase chain reaction
PEGA	poly(ethylene glycol)acrylamide copolymer
PKS	polyketide synthase
PLP	pyridoxal phosphate
PMP	pyridoxamine phosphate
ppan	4'-phosphopantetheine
PP _i	inorganic pyrophosphate
PyBOP	benzotriazole-1-yl-oxy-tris-pyrrolidino-phosphonium hexafluorophosphate
R-domain	reductase domain
rpm	rounds per minute
RT	room temperature
SAM	S-adenosylmethionine
S _B	streptogramin B
SDS	sodium dodecylsulfate
Sfp	4'-phosphopantetheine transferase involved in surfactin production
SNAC	N-acetylcysteamine
SPPS	solid phase peptide synthesis
Srf	surfactin
Syr	syringomycin
tBu	tert-butyl

1 Abbreviations

TCEP	tris(carboxyethyl)phosphine
T-domain	thiolation domain or peptidyl carrier protein
TE-domain	thioesterase domain
TFA	trifluoroacetic acid
TFE	trifluoroethanol
THF	tetrahydrofuran
TIPS	triisopropylsilane
t_R	retention time
Tris	tris-(hydroxymethyl)-aminomethane
Trt	trityl
Tyc	tyrocidine
V	volts
v/v	volume per volume
wt	wild type
w/v	weight per volume

Table 1.1: Amino acids: Abbreviations and molecular weights

amino acid	3-/1-letter code		MW [g/mol]
alanine	Ala	A	89
arginine	Arg	R	174
asparagine	Asn	N	132
aspartate	Asp	D	133
cysteine	Cys	C	121
2,3-diaminobutyrate	Dab		118
(Z)-dehydrotryptophan	dTrp		202
glutamine	Gln	Q	146
glutamate	Glu	E	147
glycine	Gly	G	75
histidine	His	H	155
3-hydroxyasparagine	hAsn		148
4-hydroxyphenylglycine	Hpg		167
isoleucine	Ile	I	131
kynurenine	Kyn	U	208
leucine	Leu	L	131
lysine	Lys	K	146
methionine	Met	M	149
3-methylaspartate	mAsp		147
3-methylglutamate	mGlu		161
3-methoxyaspartate	omAsp		163
ornithine	Orn	O	132
phenylalanine	Phe	F	165
phenylglycine	Phg		151
3-phosphohydroxyasparagine	pAsn		228
pipecolic acid	Pip		129
proline	Pro	P	115
sarcosine	Sar		89
serine	Ser	S	105
threonine	Thr	T	119
tryptophan	Trp	W	204
tyrosine	Tyr	Y	181
valine	Val	V	117

2. Introduction

Natural products that are produced by microorganisms have for decades attracted considerable attention for modern therapy. The bioactivity of these structurally complex substances reaches from antibiotic over immunosuppressive, cytostatic to antitumor [1]. Not only have these secondary metabolites been elaborated for their dedicated function over eons of evolution, they also represent promising scaffolds for the development of novel drug leads with improved or altered activities. Optimization can be achieved by the introduction of artificial modifications, which yields semisynthetic derivatives of existing structures, although total synthesis of complete natural product-based compounds is also envisioned [2, 3].

Peptidic products represent a large subclass of highly diverse natural products, many of which display therapeutically useful activity. They can be classified into different groups according to their synthesis pathway. The lantibiotics, for example, are ribosomally synthesized antimicrobial agents, that are posttranslationally modified to their biologically active forms [4]. Yet another and widespread class of therapeutically important peptides are produced nonribosomally by large multienzyme complexes, the nonribosomal peptide synthetases (NRPS) [5, 6]. In contrast to ribosomal peptide synthesis, nonribosomally assembled peptides contain not only the common 20 amino acids, but hundreds of different building blocks. Moreover, these secondary metabolite peptides contain unique structural features such as D-amino acids, N-terminally attached fatty acid chains, N- and C-methylated residues, N-formylated residues, heterocyclic elements, glycosylated amino acids as well as phosphorylated residues [5]. In recent research using both genetic and biochemical methods, experiments have revealed deep insights into the mechanism of nonribosomal peptide synthesis. In many cases it was possible to alter existing nonribosomally produced peptides by the combined action of chemical peptide synthesis and subsequent enzyme catalysis. This chemoenzymatic approach, along with a brief overview of the nonribosomal peptide synthesis machinery, will be discussed in more detail later in this introduction. Another focus of this

introduction is the labeling of NRPS-derived proteins by site-specific posttranslational modification.

2.1. Structural Rigidity of Nonribosomally Synthesized Peptides

Selected structures of some nonribosomally produced peptides are shown in Figure 2.1. A common feature of these compounds is their constraint structure, which ensures bioactivity by a precise orientation required for interaction with a dedicated molecular target [7]. In some cases, these constraints are imposed by heterocyclization. For instance, the iron-chelating siderophore vibriobactin **1** comprises two oxazoline rings, both of which originate from threonine residues [8]. This oxazoline ring can be further oxidized to yield oxazole, as found in the potent telomerase inhibitor telomestatin **2** [9]. In addition to oxazoles, telomestatin also contains a thiazoline ring that is synthesized by the heterocyclization of cysteine. In the case of the antibiotic bacitracin **3**, this heterocyclic element mediates a specific cation-dependent complexation of the phosphate group of the C₅₅ lipid carrier, leading to depletion of this carrier and subsequent blocking of bacterial cell wall synthesis [10, 11]. An additional strategy to modify and thus constrain the conformation of nonribosomal peptides is exemplified by the glycopeptide antibiotics of the vancomycin **4** and teicoplanin class [12]. These closely related compounds contain a homologous heptapeptide scaffold, whose backbone is constrained by extensive oxidative crosslinking. The joining of electron-rich aromatic rings by aryl ether linkages and direct C-C coupling convert these acyclic, floppy heptapeptides into rigid, cup-shaped structures. The constraint glycopeptides sequester the N-acetyl-D-Ala-D-Ala termini of bacterial peptidoglycan strands with five hydrogen bonds and inhibit the transglycosylation and/or transpeptidation steps of bacterial peptidoglycan synthesis [13, 14].

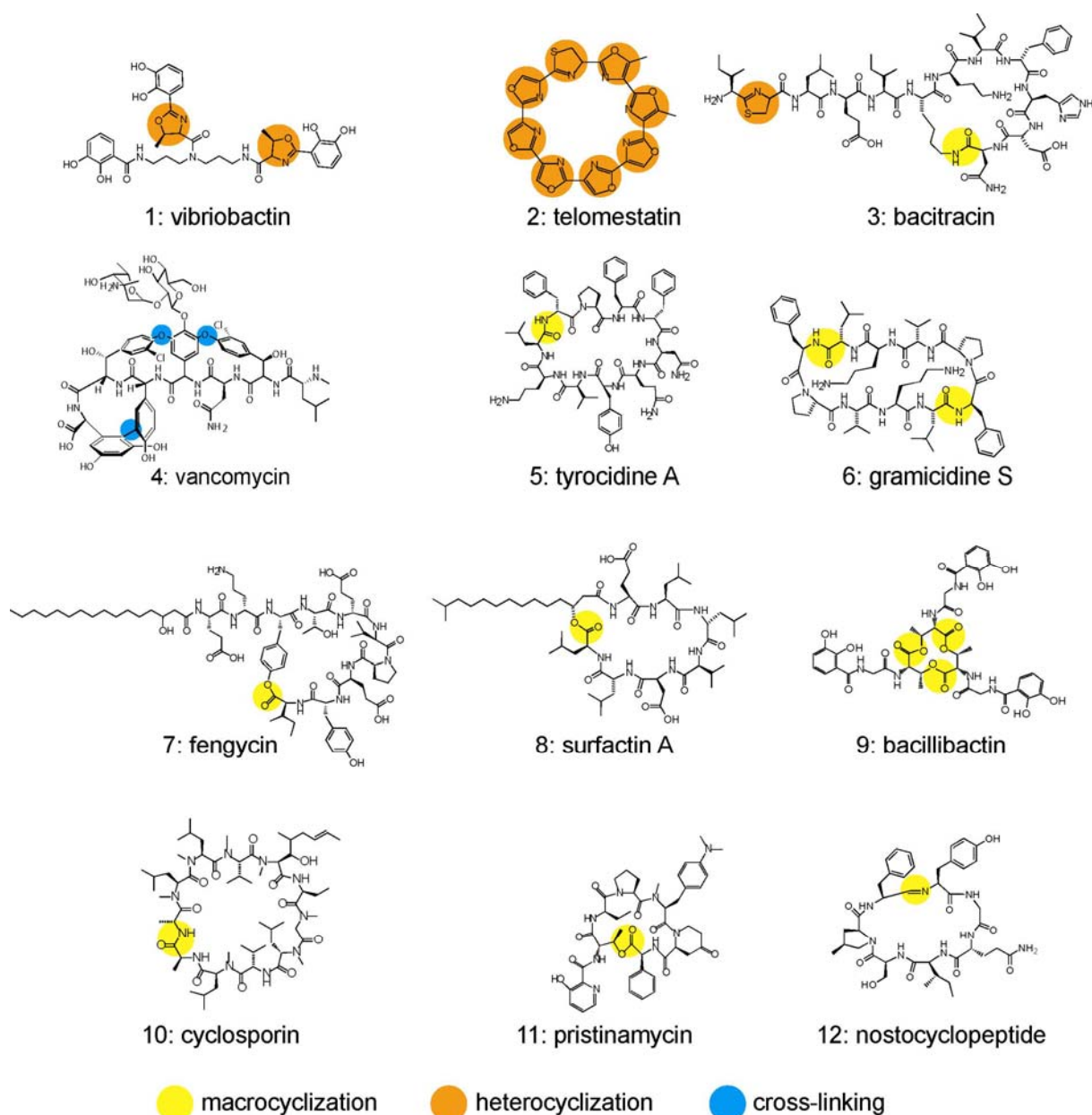


Figure 2.1: A selection of nonribosomally synthesized peptides. Characteristic structural features that confer rigidity to the peptide backbone are highlighted.

Macrocyclization is another common constraint of nonribosomally synthesized peptides whereby parts of the molecule distant in the linear peptide precursor are covalently linked to one another [7]. Many cyclization strategies are known so far, giving rise to the high diversity of nonribosomal cyclopeptides. For instance, the intramolecular capture by amines leads to peptidolactams, whereas cyclization via hydroxyl substituents leads to peptidolactones. The former strategy is observed for the peptide antibiotics tyrocidine A **5**, bacitracin **3** and gramicidin S **6** [15]. In the case of tyrocidine A, amide bond formation occurs head-to-tail

between the N-terminal amino group and the C-terminus of the decapeptide. The dodecapeptide bacitracin instead has a lariat structure, with the heptapeptide lactam ring arising from capture of the C-terminal carbonyl group by the ϵ -amino group of Lys₆. Moreover, the macrolactam gramicidin S is composed of two identical pentapeptides bridged head-to-tail yielding a symmetric dilactam ring. For macrolactones, analogous cyclization strategies lead to branched-cyclic structures as seen for the antifungal lipopeptide fengycin **7** and the biosurfactant surfactin A **8** [15]. The former depsipeptide is cyclized via the side chain of a hydroxy amino acid such as tyrosine, whereas the latter compound is cyclized via a β -hydroxylated fatty acid moiety. Finally, the iron-chelating siderophore bacillibactin **9** is a cyclic trilactone, that arises from cyclotrimerization of threonine [16].

2.2. Diversity of Nonribosomal Peptides: The Acidic Lipopeptide Antibiotics

The structural diversity of nonribosomally produced peptides is best exemplified for the class of acidic lipopeptide antibiotics, including the calcium-dependent antibiotic (CDA) from *Streptomyces coelicolor* [17], daptomycin from *Streptomyces roseosporus* [18], A54145 from *Streptomyces fradiae* [19] as well as friulimicins and amphomycins from *Actinoplanes friuliensis* [20]. All of these lipopeptides originate from streptomycetes, which produce over two-thirds of naturally derived antibiotics [21]. Each member of this class of lipopeptides can be subdivided into various individual compounds that differ in the structure of the N-terminally attached fatty acid moiety and/or the peptide backbone (Figure 2.2). For example, A54145 is a complex of eight lipopeptides which are acylated with either a 2-decanoyl, *n*-decanoyl or undecanoyl lipid side chain. These factors also contain four different cyclic peptide nuclei which vary in glutamate/3-methylglutamate (position 12) and/or valine/isoleucine (position 13) substitutions [19]. The diversity of acidic lipopeptide antibiotics is further amplified by the occurrence of D-configured as well as nonproteinogenic amino acids, including D-4-hydroxyphenylglycine, D-3-phosphohydroxyasparagine, 3-

2 Introduction

methylglutamate, D-pipecolic acid, kynurenine, and many more. Interestingly, all of the acidic lipopeptide antibiotics are comprised of a branched cyclic decapeptide lactone ring or lactam ring. The positions of the D-configured amino acids are strictly conserved in this macrocyclic scaffold. Moreover, two aspartic acid residues are found in equivalent ring positions of the macrolactone or macrolactam ring. Recently, a genomics-based approach revealed the existence of numerous uncharacterized lipopeptide biosynthetic gene clusters, indicating that much more antibiotics of this class have yet to be identified [22].

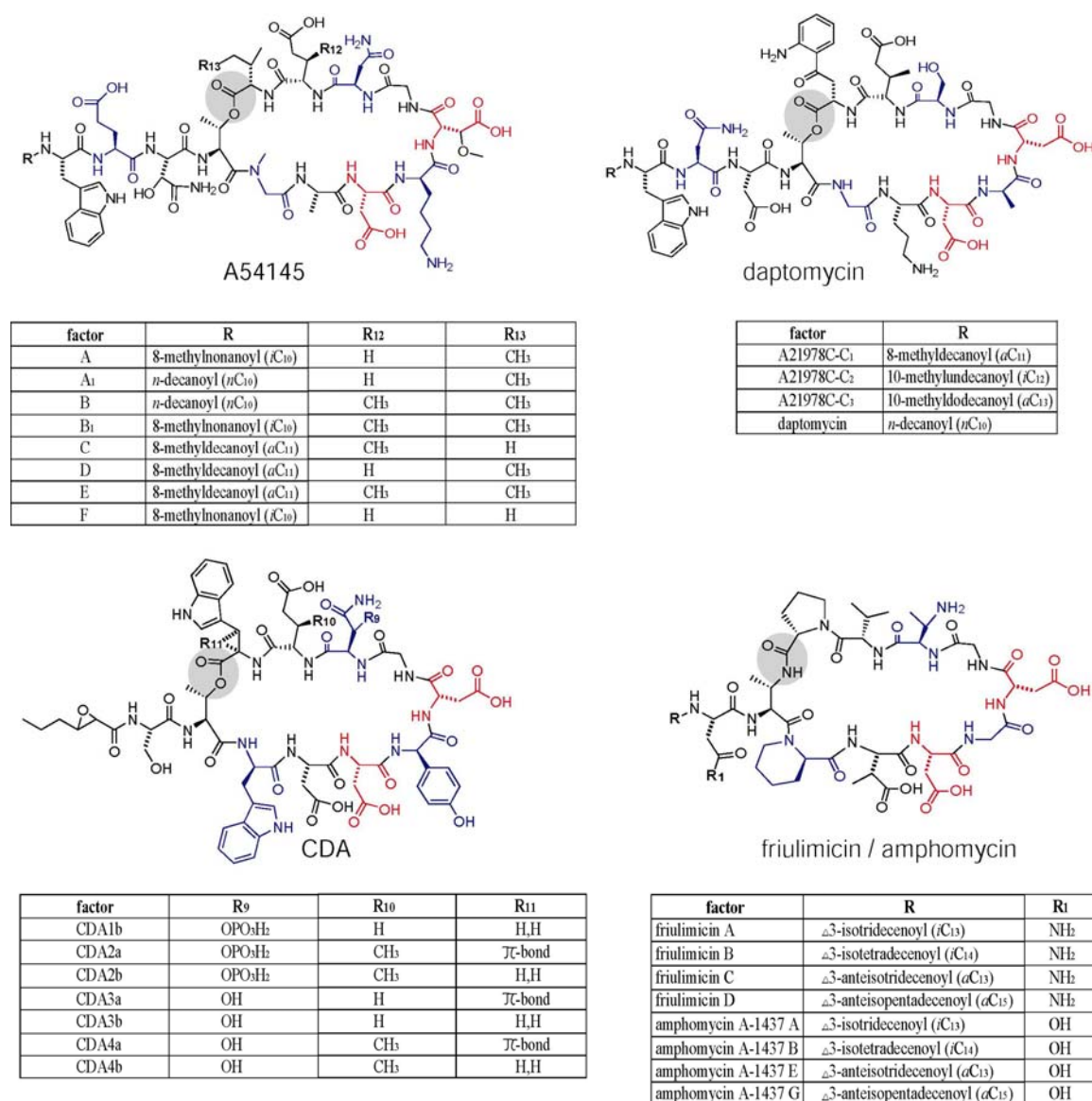


Figure 2.2: Diversity of acidic lipopeptide antibiotics. At least 27 compounds have been characterized so far. CDA is produced by *Streptomyces coelicolor*, friulimicins and amphomycins by *Actinoplanes friuliensis*, A54145 by *Streptomyces fradiae*, and daptomycin is derived from *Streptomyces roseosporus*. Conserved acidic residues are indicated in red and D-configured/achiral residues at equivalent positions are highlighted in blue.

2 Introduction

The therapeutic importance of the acidic lipopeptide antibiotics is best exemplified for daptomycin. This tridecapeptide is a member of the A21978C complex produced by *S. roseosporus* (Figure 2.2). Although the major components, A21978C₁₋₃, have 11-, 12- or 13-carbon fatty acids, the yield of daptomycin (10-carbon fatty acid) from fermentations is significantly increased by adding decanoic acid to the medium. Daptomycin, under the trade name CubicinTM, exhibits bactericidal activity against resistant pathogens for which there are very few therapeutic alternatives, such as vancomycin-resistant enterococci (VRE), methicillin-resistant *Staphylococcus aureus* and penicillin-resistant *Streptococcus pneumoniae* (PRSP) [23]. At present, spontaneous acquisition of resistance to daptomycin is rare, which might be due to a unique mechanism of action [18].

Although the mechanism of action of daptomycin is not yet fully understood, it has been clearly established that calcium ions play an essential role in antimicrobial potency [24, 25]. Based on detailed NMR studies, Jung et al. proposed that calcium binding to daptomycin increases its amphipathicity due to the redistribution of charged side chains toward the top of the ring structure and the clustering of the lipid chain with the hydrophobic Trp₁ and Kyn₁₃ residues at the bottom of the ring structure (Figure 2.3) [24]. These changes in the daptomycin structure also led to a 5% increase in the solvent-exposed hydrophobic surface. Furthermore, the total charge of the Ca²⁺-conjugated daptomycin (-1) is lower than for Ca²⁺-free daptomycin (-3) at neutral pH. Therefore, the increased amphipathicity and solvent exposed hydrophobic surface as well as the decreased total charge may facilitate interaction of Ca²⁺-conjugated daptomycin with either neutral or acidic bacterial membranes. Upon association with cytoplasmic membranes, a second Ca²⁺-dependent structural transition is proposed that promotes deeper insertion of daptomycin into the lipid bilayer [24]. This is followed by large membrane perturbations, including lipid flip-flop and membrane leakage. Formation of any of these structures presumably disrupts the functional integrity of the membrane leading to cell death of Gram-positive bacteria.

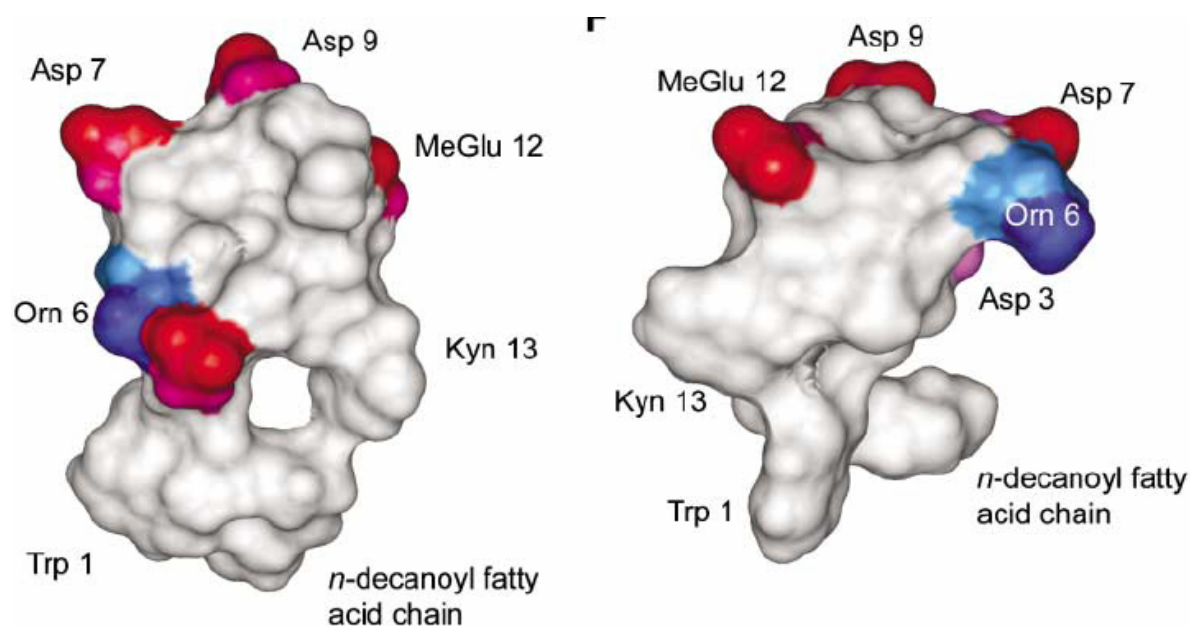


Figure 2.3: Surface representation of Ca²⁺-free (left) and Ca²⁺-conjugated (right) daptomycin [24]. Negative charges are indicated in red, positive charges in blue and uncharged regions in white.

Although some of the key structural prerequisites for daptomycin's antibacterial activity have been identified, the exact nature of the molecular targets within the cytoplasmic membrane has yet to be established. However, this two-step model of the mechanism of action provides an initial step toward understanding how this antibiotic gains access to and interacts with bacterial membranes. Since the other acidic lipopeptide antibiotics CDA, A54145, friulimicins, and amphomycins share key structural features with daptomycin; they might undergo similar interactions with calcium ions and bacterial membranes. Therefore, it is essential to further probe the structure-function relationship of all acidic lipopeptide antibiotics. Using this knowledge will enable the design of new and improved derivatives of this remarkable class of antibiotics. However, in order to engineer more potent variants, one has to understand the biosynthesis of these complex compounds. This will be the focus of the following section.

2.3. Production of Acidic Lipopeptides by Nonribosomal Peptide Synthetases (NRPSs)

Despite the structural diversity of the nonribosomally produced acidic lipopeptide antibiotics, these secondary metabolites share a common mode of synthesis, the so-called “multiple carrier thio-template mechanism” [6, 26, 27]. According to this model, peptide synthesis is performed by nonribosomal peptide synthetases (NRPSs). Figure 2.4 shows the NRPS assembly lines for daptomycin, A54145 and CDA. Detailed analysis of the daptomycin gene cluster revealed that the daptomycin biosynthetic system consists of three distinct NRPSs, namely DptA (684 kDa), DptBC (815 kDa), and DptD (265 kDa). In contrast, the closely related A54145 biosynthetic system comprises 4 NRPSs (LptA, LptB, LptC, and LptD). It is assumed that DptBC arises from a fusion of two NRPSs similar to LptB and LptC [28]. Finally, the nonribosomal CDA biosynthetic system is a multienzyme complex consisting of three enzymatic subunits, CDA I (799 kDa), CDA II (395 kDa), and CDA III (259 kDa) [17]. The multifunctional NRPSs of daptomycin, A54145, and CDA are organized into sets of repetitive catalytic units called modules (Figure 2.4). Each module is responsible for the specific incorporation of one residue into the peptide backbone [29]. Therefore, the number of modules within the NRPSs exactly matches the number of residues of the corresponding peptides. Moreover, the order of modules corresponds directly to the primary sequence, because nonribosomal peptide synthesis proceeds colinearly in an N- to C-terminal direction [30].

The proper coordination of communication between partner NRPSs *in trans* (i.e., last module of DptA and first module of DptBC) is facilitated by short regions at the C and N termini of the corresponding proteins [31]. These communication-mediating (COM) domains, also referred to as docking domains, comprise 15-30 amino acid residues and prevent undesired interactions between mismatching NRPSs (i.e., last module of DptA and first module of DptD), which would lead to the formation of truncated peptide products. Sequence alignments

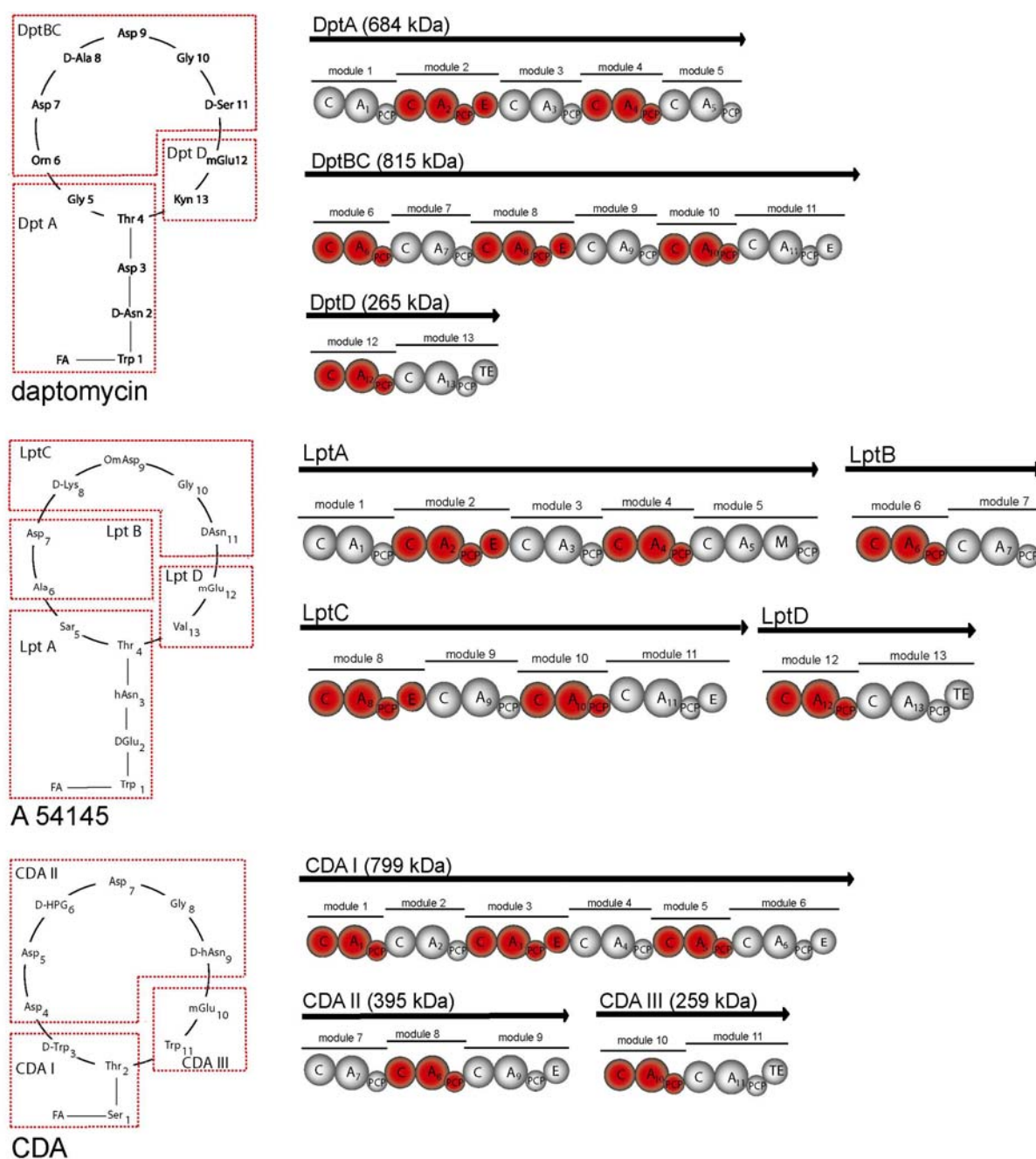


Figure 2.4: Comparison of enzymatic subunits of the daptomycin (DptA, BC and D), A54145 (LptA, B, C and D), and CDA (CDAI, II and III) NRPSs that are responsible for the synthesis of the respective peptide cores. Parts of the peptide cores that are synthesized by their dedicated enzymatic subunits are surrounded by red dotted lines. The modules indicated in red and white are subdivided into catalytically independent domains responsible for substrate recognition/activation (A, adenylation-domain), binding (PCP, peptidyl-carrier protein), elongation (C, condensation-domain), epimerization (E, epimerization-domain), N-methylation (M, N-methyltransferase) and release by cyclization (TE, thioesterase-domain). FA, fatty acid; hAsn, 3-hydroxyasparagine; HPG, 4-hydroxyphenylglycine; mGlu, 3-methylglutamate; Sar, sarcosine; omAsp, 3-methoxyaspartate; Orn, ornithine; Kyn, kynurenine.

revealed that the overall identity among COM domains is low, reflecting the high degree of specialization for their dedicated partner COM domains. First structural insights into the interaction between multimodular subunits were gained from NMR spectroscopy on related polyketide synthases (PKS) [32]. Studies of fused docking domains of the 6-deoxyerythronolide B synthase (DEBS) multienzyme subunits DEBS 2 and DEBS 3 revealed that protein-protein recognition is primarily mediated by interhelical contacts. The most important determinant of docking is a set of conserved hydrophobic interactions between four α -helices, which together form the core of a parallel four-helix bundle. In addition to the hydrophobic interface, two partially buried salt bridges between two of these α -helices may play a role in stabilizing this docking interaction. Furthermore, such ionic contacts might contribute to the destabilization of misdocked partner PKS subunits. The knowledge of the structural aspects of intersubunit communication may contribute to engineering of optimized protein-protein interfaces between NRPS, PKS, and mixed NRPS/PKS systems.

NRPS modules are further subdivided into domains that catalyze the single reaction steps such as amino acid activation, covalent binding of activated residues, amide bond formation, epimerization of covalently bound residues, and peptide release from the NRPS complex. These autonomous catalytic units will be discussed below.

2.3.1. Principles of Nonribosomal Peptide Synthesis: Dissecting the Modules into Domains

At least three domains are necessary for the nonribosomal production of peptides (Figure 2.5), the adenylation-domain (A-domain), the peptidyl-carrier protein (PCP), and the condensation-domain (C-domain). The A-domain (ca. 550 aa) controls the first step of nonribosomal peptide synthesis, namely the specific recognition and activation of the dedicated amino acid [33, 34]. This domain catalyzes two reactions. First, the A-domain selects the cognate building block from the pool of available substrates, followed by activation as an aminoacyl adenylate intermediate (Figure 2.5). The corresponding reaction in ribosomal synthesis is

2 Introduction

performed by aminoacyl-tRNA-synthetases, although these enzyme families share neither sequence nor structural relations [35]. Second, the activated aminoacyl adenylate is transferred onto the thiol-group of the ppan cofactor of the PCP, which is the only NRPS domain without autonomous catalytic activity.

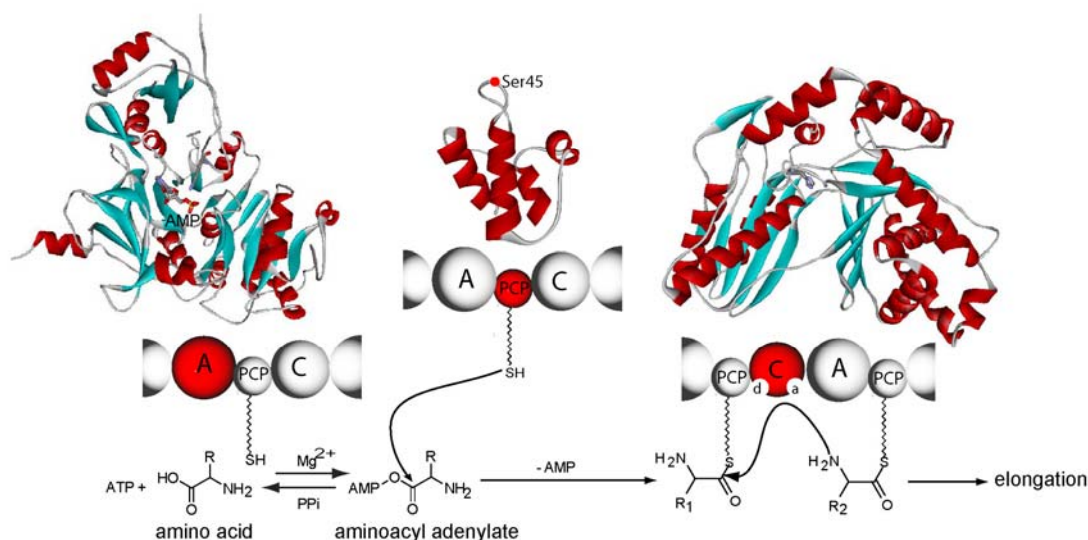


Figure 2.5: Chemical principles of nonribosomal peptide synthesis. Domains in action are indicated in red and the respective crystal structure is shown above. First, the A-domain specifically recognizes a dedicated amino acid and catalyses formation of the aminoacyl adenylate under consumption of ATP. Second, the activated aminoacyl adenylate is tethered to the free thiol group of the PCP-bound ppan cofactor. Third, the C-domain catalyzes peptide elongation. Here, the nucleophilic amine of the acceptor substrate nucleophilically attacks the electrophilic thioester of the donor substrate (a, acceptor site; d, donor site).

The crystal structure of the A-domain is derived from the phenylalanine-activating A-domain (PheA) of the first module of gramicidin S synthetase of *B. brevis* [44]. The NMR-structure of the PCP is derived from the third module of the *B. brevis* tyrocidine synthetase [45] and the C-domain is derived from the crystal structure of VibH, a stand alone C-domain of the *V. cholerae* vibriobactin synthetase [46].

The PCP (ca. 80 aa) facilitates the ordered transport of substrates and elongation intermediates to the catalytic centers with all intermediates covalently tethered to the 20 Å long 4'-phosphopantetheine (ppan) cofactor (Figure 2.5) [36, 37]. This principle facilitates substrate channeling and overcomes diffusive barriers, therefore maximizing the catalytic efficiency of the NRPS-mediated biosynthesis [5]. The ppan cofactor is post-translationally transferred from CoA to a conserved serine residue of the PCP. This apo-to-holo conversion

of the PCP is mediated by NRPS associated 4'-phosphopantetheinyl transferases (see also chapter 2.6) [38].

Formation of the peptide bond in nonribosomal peptide biosynthesis is mediated by the C-domain (ca. 450 aa) [39, 40]. This domain catalyzes the nucleophilic attack of the downstream PCP-bound amino acid with its α -amino group on the electrophilic thioester of the upstream PCP-bound amino acid or peptide (Figure 2.5). The directionality of this process is realized by donor and acceptor sites on the C-domain for electrophiles and nucleophiles, respectively [30]. According to the multiple carrier thio-template mechanism [41], the acceptor site binds the nucleophile with high affinity until the incoming electrophile completes the condensation process. Biochemical characterization of different C-domains revealed that the acceptor site discriminates against amino acids of opposite stereochemistry and with non-cognate side chains [42, 43]. In contrast, the donor site is more tolerant to the respective electrophile. Nevertheless, further investigations with the C-domain of tyrocidine elongation module 5 indicated that the donor position exhibits stereoselectivity towards the C-terminal residue for condensation reactions [42]. This shows that, in addition to A-domains, C-domains serve as a selectivity filter in nonribosomal peptide synthesis.

2.3.2. Proofreading of Nonribosomal Peptide Synthesis

The low substrate specificity of ppan transferases causes undesired misacylation of PCPs. Since the bacterial cell produces a large fraction of CoA in the form of acyl-CoAs [47], it is therefore likely that these enzymes also modify the PCPs of NRPSs with acylated ppan cofactors. Such misprimed PCPs are not recognized by later-acting domains, thereby blocking nonribosomal peptide synthesis. In order to regenerate these misprimed NRPS templates, a type II thioesterase (TEII) is assumed to catalyze hydrolysis of the undesired acyl groups [48]. Moreover, a recent study suggests, that the TEII also hydrolyzes incorrectly loaded amino acids that are not processed by the nonribosomal machinery [49]. According to this

model, TEII discriminates “correct” from “incorrect” residues based on the increased half-life of unprocessed aminoacyl-S-ppan intermediates. In contrast to this, TEII does not catalyze the hydrolysis of stalled peptide intermediates, which indicates that the release of these energy-consuming intermediates is prevented by rigorous editing of misloaded amino acids prior to incorporation into the product [49, 50].

2.3.3. Lipidation of Nonribosomally-Produced Peptides

N-terminal lipidation is a key structural feature of many nonribosomal peptides such as the acidic lipopeptide antibiotics, fengycin, surfactin, syringomycin, mycosubtilin, etc. As discussed in chapter 2.2, it is important for interaction with hydrophobic targets, e.g., cell membranes. However, in contrast to the well-studied peptide elongation, very little is known about the mechanism of this chemical transformation. In the case of daptomycin, the deduced translation products of the *dptE* and *dptF* genes are likely to have a role in N-terminal lipidation [51]. DptE exhibits conserved motifs typical of adenylate-forming enzymes and may therefore activate the long-chain fatty acid as acyl-adenylate (Figure 2.6). A similar mode of activation was previously described for the long-chain fatty acyl-AMP ligases (FAALs) of *Mycobacterium tuberculosis* [52]. According to this work, long-chain fatty acids are activated as acyl-adenylates, which are then transferred on to the ppan cofactor of the N-terminal PCP of the corresponding PKS. However, the daptomycin biosynthetic system lacks such an N-terminal PCP. Instead, DptF may serve this function due to its significant alignment to ppan-binding acyl carrier proteins (ACPs). This domain could then transfer the ppan-bound fatty acid to Trp₁ tethered to the N-terminal module of DptA. Acylation of Trp₁ is presumably catalyzed by the most upstream C-domain, the so-called starter C-domain. Specific starter C-domain-ACP docking may facilitate this acyl transfer reaction (Figure 2.6). However, further studies are needed to clarify the specificity and biochemistry of the

interaction between the ACP and the starter C-domain of the daptomycin as well as other lipopeptide-encoding biosynthetic systems.

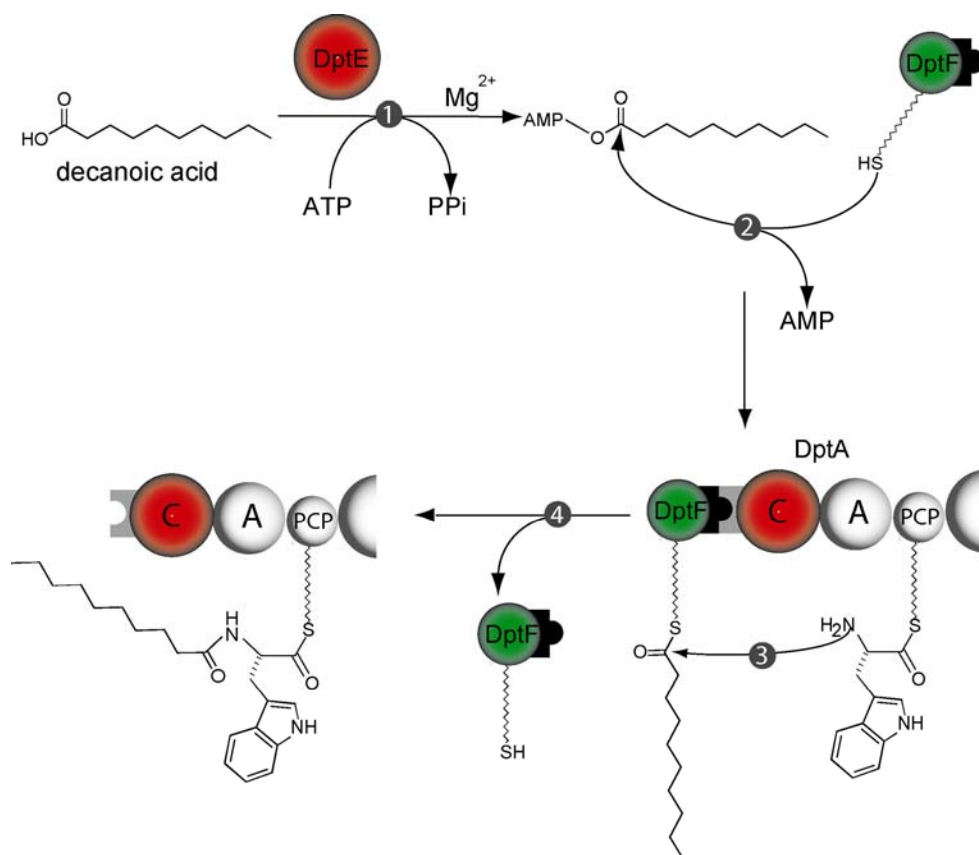


Figure 2.6: Proposed mechanism of the lipidation of daptomycin. **1.** Decanoic acid is activated as decanoyl-adenylate under the consumption of ATP. This step is catalyzed by DptE. **2.** The fatty acid is transferred on to the ppan cofactor of the putative acyl-carrier protein DptF. **3.** DptF interacts with the starter C-domain (red) of DptA, which catalyzes the subsequent acylation of Trp₁. **4.** DptF is released.

2.3.4. Generation of D-Amino Acid Residues in NRPSs

One striking feature of many NRPSs is that they incorporate D-amino acids into their peptide products. The D-configured residues may inhibit the degradation of nonribosomal peptides by naturally L-specific proteases or may serve structural functions by determining the bioactive conformation [53-55]. In most cases, incorporation of D-amino acids into the peptide sequence is mediated by an interplay between the epimerization domain (E-domain, ~ 450 aa) [55, 56] and the downstream C-domain (Figure 2.7 A). The E-domain catalyzes racemization (equilibration between L- and D-enantiomers) of the PCP-bound L-amino acid or

epimerization of the C-terminal amino acid (equilibration between L- and D-epimers) of the growing peptide chain. In order to ensure selective incorporation of the D-amino acid into the peptide backbone, the donor site (d) of the downstream C-domain is D-specific for the incoming cofactor-bound electrophile [43]. Hence, the C-domain functions as a $^D C_L$ catalyst, directing the condensation of an upstream D-amino acid with a downstream L-amino acid.

A different mechanism for the incorporation of D-amino acids is realized by the cyclosporin synthetase (Figure 2.7 B) [57]. The corresponding biosynthetic gene cluster encodes an alanine racemase to provide substrate for the D-Ala selective A-domain in the first module. This shows that besides C-domains, A-domains may also represent a stereoselective filter in nonribosomal peptide synthesis.

Recently, a third strategy of D-amino acid incorporation was observed in multiple Gram-negative *Pseudomonas* strains producing arthrofactin, syringomycin, and syringopeptin [58]. The lipopeptidolactone arthrofactin, for instance, contains seven D-amino acids, yet there are no E-domains in any of the three NRPSs, ArfA, ArfB, and ArfC. Moreover, kinetic measurements revealed that at least the three most upstream A-domains activate L-amino acids rather than D-amino acids. Interestingly, epimerization of amino acids is catalyzed by a new type of C/E-domain, which is proposed to have dual catalytic roles for epimerization and condensation (Figure 2.7 C). Remarkably, the epimerization reaction does not take place unless the PCP downstream of this C/E-domain is loaded with the dedicated amino acid. Therefore, the epimerization activity may be triggered by a conformational change of the C/E-domain which is induced by the aminoacylated downstream PCP that is primed for peptide bond formation. After epimerization of the upstream aminoacyl/peptidyl thioester, the C/E-domain finally catalyzes the elongation of the peptidyl chain with $^D C_L$ chirality.

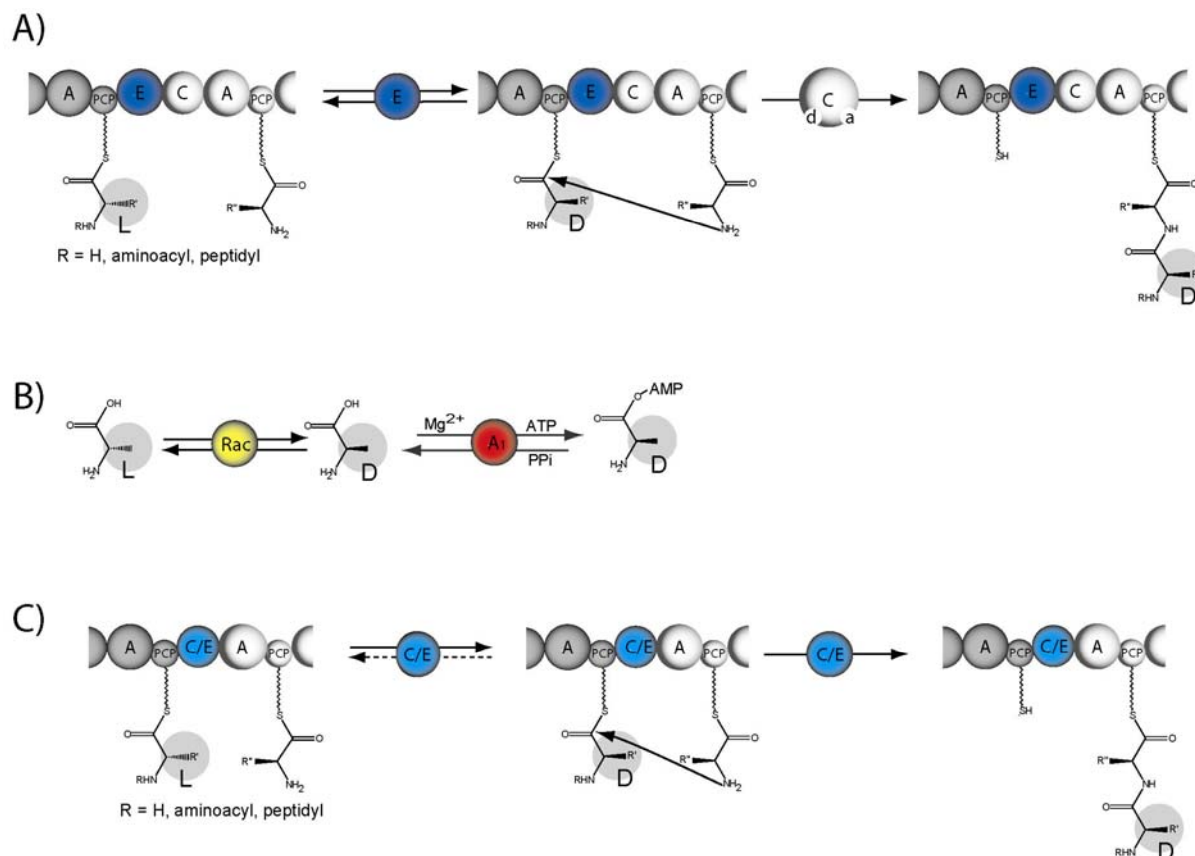


Figure 2.7: Proposed mechanisms underlying amino acid epimerization. (A) The E-domain converts the PCP-tethered aminoacyl substrate into a D/L equilibrium. The stereoselective donor site (d) of the C-domain of the downstream module uses only the D-configured amino acid for subsequent peptide elongation. (B) In some cases, an external racemase (Rac) catalyzes the racemization of a freely diffusible amino acid. Here, a stereoselective A-domain is the determinant that activates solely the corresponding D-enantiomer. (C) D-amino acid incorporation into arthrfactin, syringomycin, and syringopeptin is catalyzed by a new type of condensation-domain (C/E-domain). Epimerization does not take place unless the PCP downstream of this C/E-domain is loaded with the dedicated amino acid. It is not yet known, whether the epimerization reaction is reversible or not. After epimerization of the upstream aminoacyl/peptidyl thioester, the C/E-domain mediates the elongation of the peptidyl chain with $^D C_L$ chirality.

2.4. Macrocyclization Catalyzed by Nonribosomal Thioesterase-Domains

Nonribosomal peptides grow by consecutive addition of activated aminoacyl monomer units. The elongated chain is translocated each time from upstream to downstream PCPs during chain elongation. Once the peptide chain reaches its full length at the most downstream PCP, it has to be released in order to reactivate the NRPS machinery for the next synthesis cycle. Typically, termination of peptide synthesis is accomplished by a thioesterase-domain (TE-

domain, ca. 280 aa) fused to the C-terminal module [7]. This enzyme uses an active site serine as a nucleophilic catalyst. Peptide release is initiated by transfer of the ppan-bound peptide chain to the active site serine of the downstream TE-domain to generate an acyl-O-TE intermediate [7]. This covalent enzyme intermediate may break down either by the attack of a water molecule to yield a linear peptide (e.g., vancomycin) or by attack of an internal nucleophile, producing a cyclopeptide (e.g., daptomycin; Figure 2.8 A).

While TE-domains represent the most common solution to peptide release in nonribosomal biosynthesis, alternative strategies are known. In the synthesis of cyclosporin, for instance, the most downstream C-domain of cyclosporin synthetase is proposed to catalyze peptide release by head-to-tail condensation (Figure 2.8 B) [59]. Moreover, peptide release can occur under reduction of the carboxy group mediated by the NAD(P)H-dependent reduction-domain (R-domain) such as in the biosynthesis of the linear peptide alcohol gramicidin A in *B. brevis* [60] and in the formation of the macrocyclic imine nostocyclopeptide **12** from *Nostoc* sp. [61] (Figure 2.8 C).

However, macrocyclization catalyzed by nonribosomal TE-domains seems to be the favored mechanism for peptide release, not least because of the role this structural constraint plays in resistance to proteolytic degradation and enhanced bioactivity. For example, the conformation of daptomycin is constrained by a branched cyclic decapeptide lactone derived from TE-mediated cyclization of an L-threonine side chain onto the C-terminus [17]. Considering the diversity in cyclization strategies of nonribosomal peptides (see chapter 2.1), it is not surprising that the overall identity among TE-domains is only 10-15%, therefore reflecting the high degree of specialization for their catalyzed cyclization reactions [1]. Structural and mechanistic aspects of these versatile macrocyclization catalysts (also referred to as peptide cyclases) are discussed in the following section.

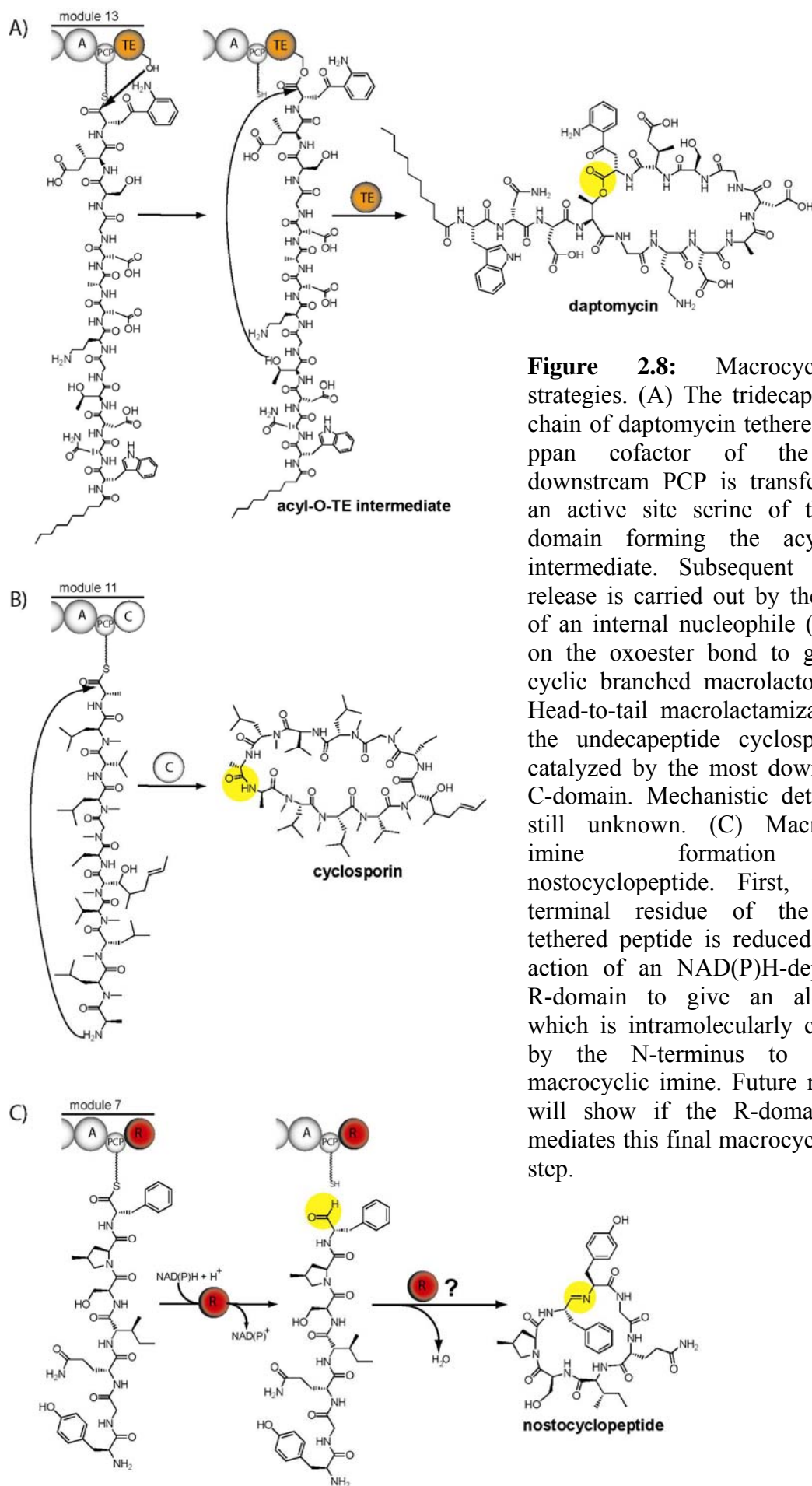


Figure 2.8: Macrocyclization strategies. (A) The tridecapeptidyl-chain of daptomycin tethered to the ppan cofactor of the most downstream PCP is transferred to an active site serine of the TE-domain forming the acyl-O-TE intermediate. Subsequent product release is carried out by the attack of an internal nucleophile (L-Thr₄) on the oxoester bond to give the cyclic branched macrolactone. (B) Head-to-tail macrolactamization of the undeca-peptide cyclosporin is catalyzed by the most downstream C-domain. Mechanistic details are still unknown. (C) Macrocylic imine formation of nostocyclopeptide. First, the C-terminal residue of the ppan-tethered peptide is reduced by the action of an NAD(P)H-dependent R-domain to give an aldehyde, which is intramolecularly captured by the N-terminus to give a macrocyclic imine. Future research will show if the R-domain also mediates this final macrocyclization step.

2.4.1. Structural and Mechanistic Aspects of Peptide Cyclases

First structural and mechanistic insights into the mode of TE-mediated peptide cyclization were gained from the crystal structure of the surfactin cyclase (Srf TE) [62]. The crystallographic studies revealed similarities to structures previously solved for α/β hydrolase family members. However, the Srf TE most significantly differed from the canonical fold of this superfamily by an extended insertion composed of three α -helices that reach over the active site. Based on alignment, this “lid” differs significantly from the corresponding regions of other TE domains, suggesting that the substrate specificity is encoded in this predominantly nonconserved region of the cyclase [7]. The nonconserved residues in the lid may direct cyclization through specific interactions with the Srf TE-bound peptide chain. Based on further studies, the two positively charged residues Lys₁₁₁ and Arg₁₂₀ in the active site may also contribute to the proper folding of the substrate by coordination of the negatively charged residues Glu₁ and Asp₅ in the surfactin sequence [63].

In NRPS assembly lines, the TE-domain acts in concert with the upstream PCP that donates the ppan-bound peptide chain. In the case of Srf TE, a putative interaction site allows docking of the C _{α} chain of PCP to the cyclase [62]. The peptide chain tethered to the 20 Å-long ppan cofactor is presumably directed via a cleft into the active site of the globular cyclase and transferred onto a conserved serine residue. This residue belongs to a catalytic triad composed of Ser₈₀, His₂₀₇, and Asp₁₀₇. CocrySTALLIZATION studies with a boronic acid inhibitor revealed distinct recognition and binding of the C-terminal residues Leu₇ and D-Leu₆ of the surfactin peptide in the active site [63]. Finally, breakdown of the generated acyl-O-TE intermediate occurs by regioselective intramolecular attack of the fatty acid β -hydroxyl group on the oxoester bond to exclusively release the macrolactone.

2.4.2. Autonomous Cyclization Activity of Excised TE Domains

The great pharmacological potential of many cyclic peptides emphasizes their role in drug discovery, as they show specific interactions with defined cellular targets and high stability against proteolytic digestion [5]. They are therefore most promising scaffolds for drug leads. So far, modern organic chemistry faces many difficulties in the reliable production of cyclopeptides. In many cases the yield is poor or the reaction lacks sufficient regio- and stereoselectivity [64, 65]. These problems could be solved by using nonribosomal cyclases, which catalyze the regio- and stereoselective cyclization of linear precursor peptides without the use of protecting groups. However, the application of nonribosomal TE-domains for cell-free synthesis of cyclic peptides requires translation between the biological and chemical languages. First, the complex NRPS multienzyme machinery required for peptide elongation is replaced by well established solid-phase peptide synthesis (SPPS), which greatly facilitates the rapid synthesis of peptides containing unnatural amino acids [64]. Second, the TE-domain is used as an isolated enzyme for *in vitro* peptide cyclization, because the large size of the whole multienzyme complex causes severe preparative problems. Third, to ensure acylation of the excised TE-domain, the natural PCP-bound phosphopantetheine prosthetic group is replaced by a cofactor mimic, which is attached to the C-terminal end of the chemically synthesized peptide.

This chemoenzymatic approach was first achieved by a cooperation between the Walsh and Marahiel laboratories, which reported on the isolation and characterization of the TE-domain of tyrocidine synthetase from *Bacillus brevis* (Figure 2.9) [66]. Incubation of a chemically synthesized tyrocidine decapeptidyl-SNAC thioester and excised tyrocidine cyclase (Tyc TE) resulted in the formation of the cyclic decapeptide antibiotic tyrocidine A. Hydrolysis of the substrate mimic could be detected to a lesser extent and might be due to the fact that the excised cyclase lacks the hydrophobic environment of the multienzyme complex. Recent results indicate that the interaction of the isolated Tyc TE with detergent micelles may serve

2 Introduction

to mimic the natural contacts of this domain with the larger synthetase [67]. In fact, the addition of nonionic detergent induced a significant shift in the product ratio of Tyc TE in favor of macrocyclization.

To explore the substrate specificity of Tyc TE, a scan through all ten positions of the peptidyl-SNAC thioester was performed [66]. Notably, it was found that only the substitution of amino acids near the end of the decapeptide, namely D-Phe₁ and L-Orn₉, significantly decreased the rate of TE-catalyzed cyclization. It was also observed that thioester substrates 6-14 residues in length could be efficiently cyclized by Tyc TE, resulting in the formation of different size macrolactams [68]. Alterations of the peptide backbone either by the replacement of three amino acid blocks with flexible spacers or by replacement of individual amide bonds with ester bonds provided evidence that product-like intramolecular hydrogen bonds facilitate peptide preorganization [69]. This preorganization was efficient enough to allow macrolactone formation by using a hydroxyl group as intramolecular nucleophile despite the lower nucleophilicity of hydroxyl versus amine. Based on these findings, a model of a minimal cyclization substrate for the Tyc TE was postulated [69].

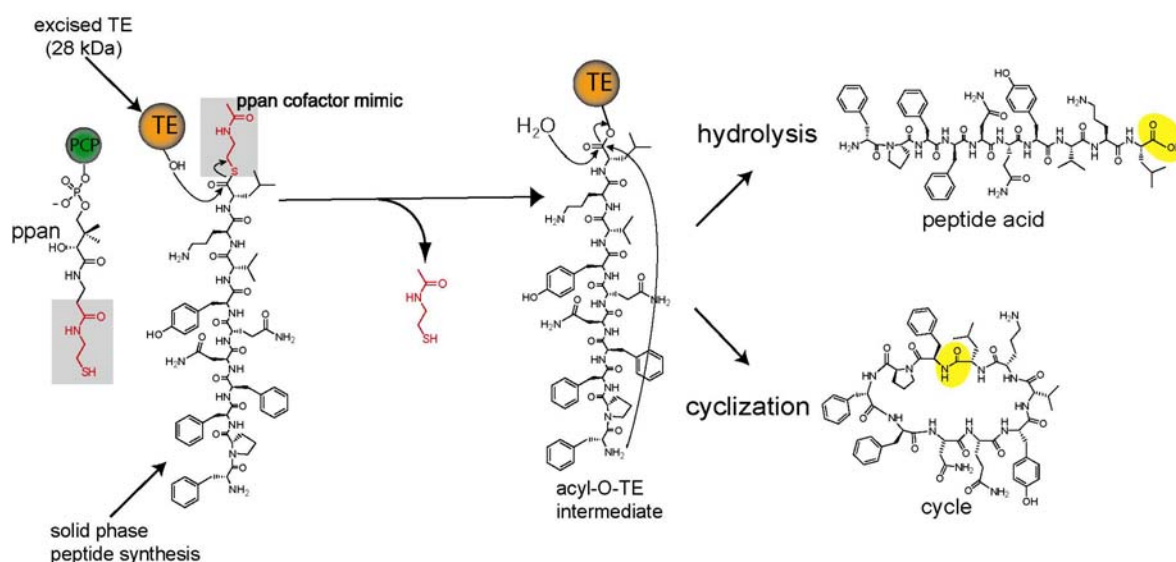


Figure 2.9: The experimental design for the study of excised cyclases exemplified for Tyc-TE. First, the NRPS multienzyme machinery for tyrocidine synthesis is replaced by solid-phase peptide synthesis. Second, the TE-domain is used as an excised enzyme for *in vitro* peptide cyclization. Third, recognition of the artificial substrate by the excised cyclase is ensured by the phosphopantetheine cofactor mimic SNAC (highlighted by shading).

2.4.3. Generality of TE-Catalyzed Peptide Cyclization

To provide evidence for the general utility of TE catalysis as a means to synthesize a wide range of macrocyclic compounds, peptide cyclases from other NRPS systems were cloned and overexpressed. The excised TE-domain of surfactin synthetase (Srf TE) retains autonomous macrocyclization activity when provided with a 3-hydroxybutyryl-heptapeptidyl-SNAC substrate [63, 68]. However, in contrast to Tyc TE, alterations in the cyclization nucleophile and insertion of residues into the peptide were not tolerated [63].

The recombinant thioesterase domain SnbDE TE of the pristinamycin I nonribosomal peptide synthetase from *S. pristinaespiralis* is a versatile cyclase for the production of streptogramin B antibiotics [70]. Although the streptogramin B (S_B) SNAC substrates with the natural phenylglycine (Phg) at the C-terminus undergo rapid C-terminal racemization under assay conditions, stereoselective SnbDE TE only incorporates L-Phg into the cyclic product (Figure 2.10). This dynamic kinetic resolution [71] simplifies challenging S_B synthesis to standard peptide chemistry and subsequent enzymatic reaction. Besides the high stereoselectivity, SnbDE TE was able to mediate both macrolactonization and macrolactamization of peptide thioester substrates. Interestingly, macrolactamic S_B derivatives are promising pharmacophores because in some cases S_B resistance arises from lyase-catalyzed cleavage of the natural lactone bond [72].

To further expand the set of cyclization catalysts the peptide cyclases Syr TE from syringomycin synthetase, Fen TE from fengycin synthetase, and Myc TE from mycosubtilin synthetase were cloned and overexpressed [73, 74]. However, the inability to recognize and bind conventional peptidyl-SNAC substrates precluded examination of these cyclases. To mimic the natural substrate presentation as close as possible, a strategy was employed which allowed Sfp-catalyzed loading of peptidyl-CoA substrates onto apo-PCP-TE didomains [74].

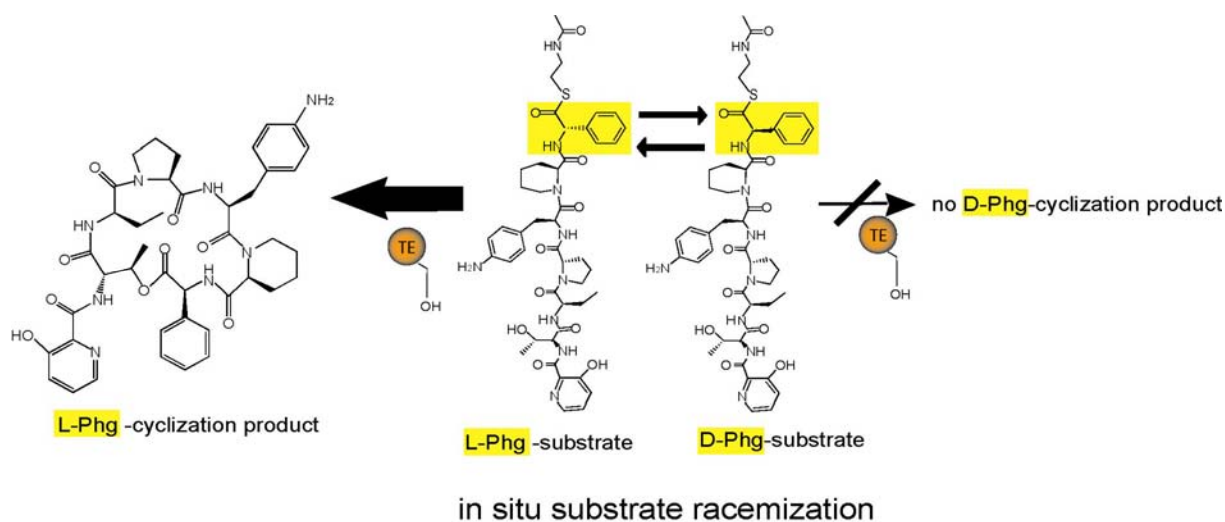


Figure 2.10: Dynamic kinetic resolution of a streptogramin B (S_B) SNAC substrate with Phg at the C-terminus, which is prone to in situ substrate racemization. The resulting two diastereomers are able to acylate the active Ser residue of SnbDE TE resulting in two different peptidyl-O-TE intermediates. However, only the peptidyl-O-TE intermediate with the L-Phg-configuration is able to undergo cyclization to the natural product with L-Phg configuration.

This strategy takes advantage of the direct interaction between the ppan-bound substrate of the PCP and the C-terminally adjacent TE-domain. Using this approach, it was possible to detect cyclization of a linear fengycin analog. However, one major drawback of this method is that the ppan cofactor remains attached to the PCP-TE didomain, thereby blocking Sfp-catalyzed transfer of additional peptidyl-CoA substrates onto PCP. To force multiple turnover catalysis, it was tried to reload the ppan-PCP-TE didomain by chemical trans-thioesterification using peptidyl-thiophenol substrates [73]. Surprisingly, instead of ppan reloading the highly electrophilic peptidyl-thiophenol substrates directly acylated the TE active site serine. Furthermore, it was possible to biochemically characterize Syr TE, Fen TE, and Myc TE, which displayed no activity with less electrophilic peptidyl-SNAC substrates. Activity-based TE acylation with various leaving groups is also subject of investigations presented in this work.

2.4.4. Chemoenzymatic approaches towards novel cyclopeptides

In order to investigate the general utility of NRPS cyclases for generating small molecules with different therapeutic potential, broad substrate tolerance would be highly desirable. Walsh and co-workers showed that Tyc TE was capable to cyclize peptide substrates, in which up to 7 of 10 cognate residues were simultaneously replaced [75]. Macrolactamization of these linear peptide precursors containing an integrated RGD sequence yielded potent inhibitors of ligand binding by integrin receptors, with cyclization and N-methylation being important contributors to nanomolar potency (Figure 2.11). Therefore, the therapeutic activity of the cyclization product was successfully moved from infectious disease (tyrocidine A) to cardiovascular pharmacology. The ability of Tyc TE to tolerate simultaneous side chain alterations was further utilized to mediate cyclization of substrates containing nonpeptidic elements. Incorporation of ϵ -amino acid building blocks into the peptide backbone led to the formation of cyclic polyketide/tyrocidine hybrids (Figure 2.11) [76], which could be used to further optimize macrocyclic peptide/polyketide natural products, such as the immunosuppressant rapamycin and the anticancer agent epothilone [77]. Furthermore, the insertion of (*E*)-alkene-dipeptide isosters allows the peptide backbone to be modified post-synthetically by chemical metathesis [78].

To evaluate the potential utility of excised TE domains for generating cyclic peptide libraries, a combinatorial approach was developed by Walsh and co-workers [7]. In a biomimetic synthetic strategy, a solid-phase PEGA (poly(ethylene glycol)acrylamide copolymer) resin functionalized with a synthetic tether substitutes for the ppan cofactor of the PCP (Figure 2.11). Subsequent SPPS was used for the preparation of more than 300 linear tyrocidine derivatives. When these solid support-bound peptides were incubated with the recombinant Tyc TE, the cyclase could productively catalyze peptide release by enzymatic on-resin cyclization. The resulting library of cyclopeptides revealed that replacement of D-Phe₄ in tyrocidine by a positively charged D-amino acid led to 30-fold selectivity for bacterial

2 Introduction

membranes, thereby minimizing the hemolysis of red blood cells. These improved tyrocidine derivatives can now be translated back into an engineered NRPS template for large scale production via fermentation.

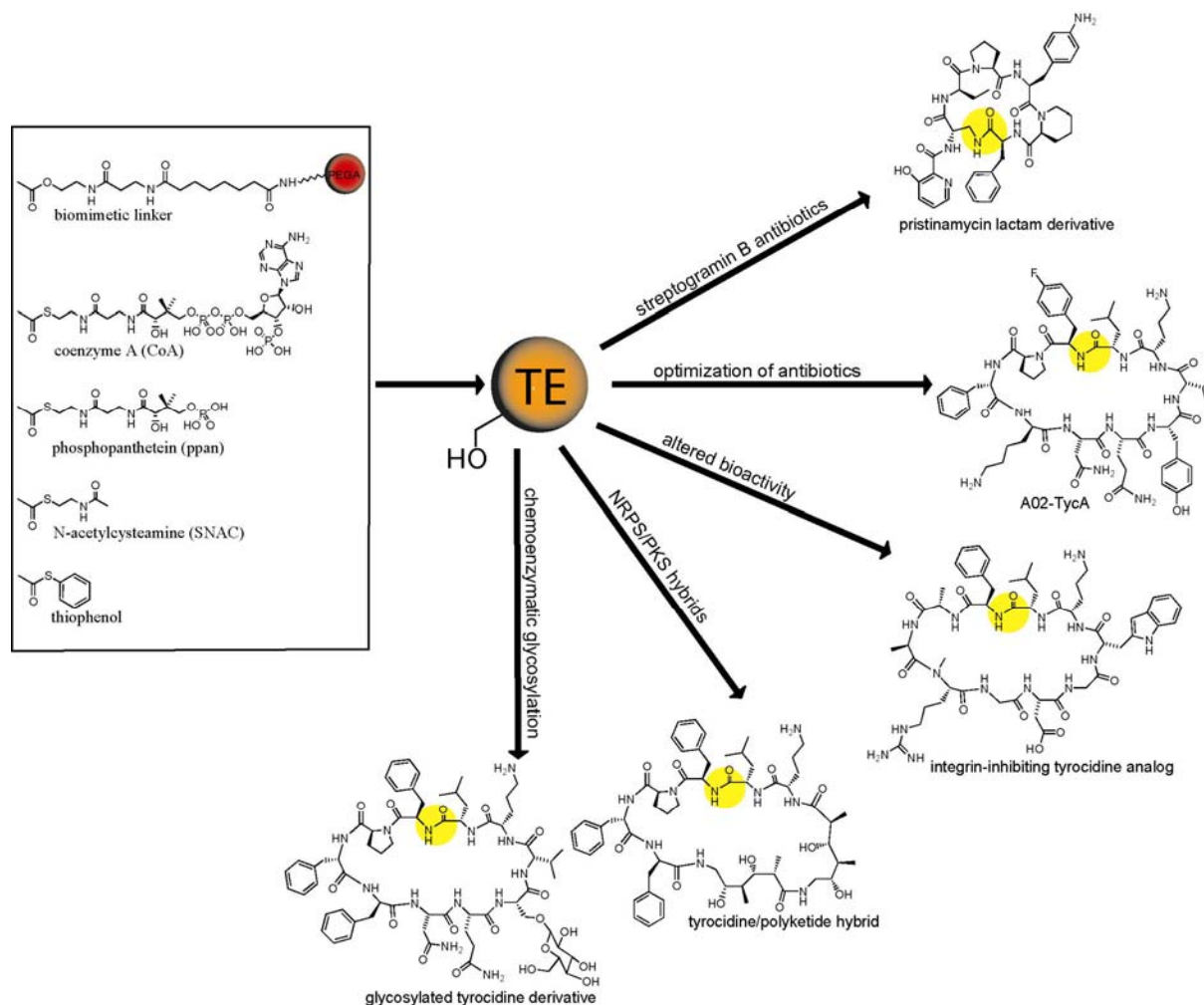


Figure 2.11: Chemoenzymatic synthesis of novel bioactive compounds by excised TE-domains. Substrates can be presented to the cyclase either bound to an artificial solid support (PEGA resin) or by soluble thioester leaving groups.

The chemoenzymatic potential of Tyc TE was also used to generate glycosylated cyclopeptides. Using this cyclase, macrocyclized tyrocidine decapeptide analogs with unnatural propargylglycine residues incorporated at positions 3 to 8 were prepared [79]. The peptide backbones containing these alkyne residues allowed subsequent postsynthetic modification to selectively introduce azido-functionalized sugar residues by copper(I)-mediated [2+3] cycloaddition reactions, also referred to as “click chemistry” (Figure 2.12 A).

Later, Walsh and co-workers developed an alternative method to prepare glycosylated cyclopeptides by incorporating glycosylated amino acids into linear peptides via SPPS followed by enzyme-catalyzed macrolactamization (Figure 2.12 B) [80]. Numerous *O*-linked glycosylated peptidolactams were prepared using glycosylated serine or tyrosine residues at positions 5-8.

While conventional chemical glycosylation of cyclic peptides suffers from little regiochemical control and enzymatic glycosylation is limited by the high substrate specificity of glycosyltransferases, these chemoenzymatic strategies combine regioselective incorporation of sugar moieties with the broad tolerance of Tyc TE for side chain replacements. Hence, these approaches allow carbohydrate complexity to be generated into macrocyclic peptides and should be generalizable to other NRPS cyclases, thereby providing a powerful tool for the production of novel drug leads by large cyclic library screens. The ability of recombinant TE-domains to synthesize and to derivatize important drug candidates is also subject of investigations in this thesis.

2.5. Diversification and Rigidification of Peptides Mediated by Tailoring Enzymes

Tailoring enzymes act in the maturation of NRPS-derived products. These supplementary enzymes can carry out modifications to the peptide backbone like C-, N-methylation, oxidation, and cross-linking, thereby enlarging the structural diversity of these natural products. Furthermore, these chemical modifications add much to the structural rigidity and stability against proteolytic digestion.

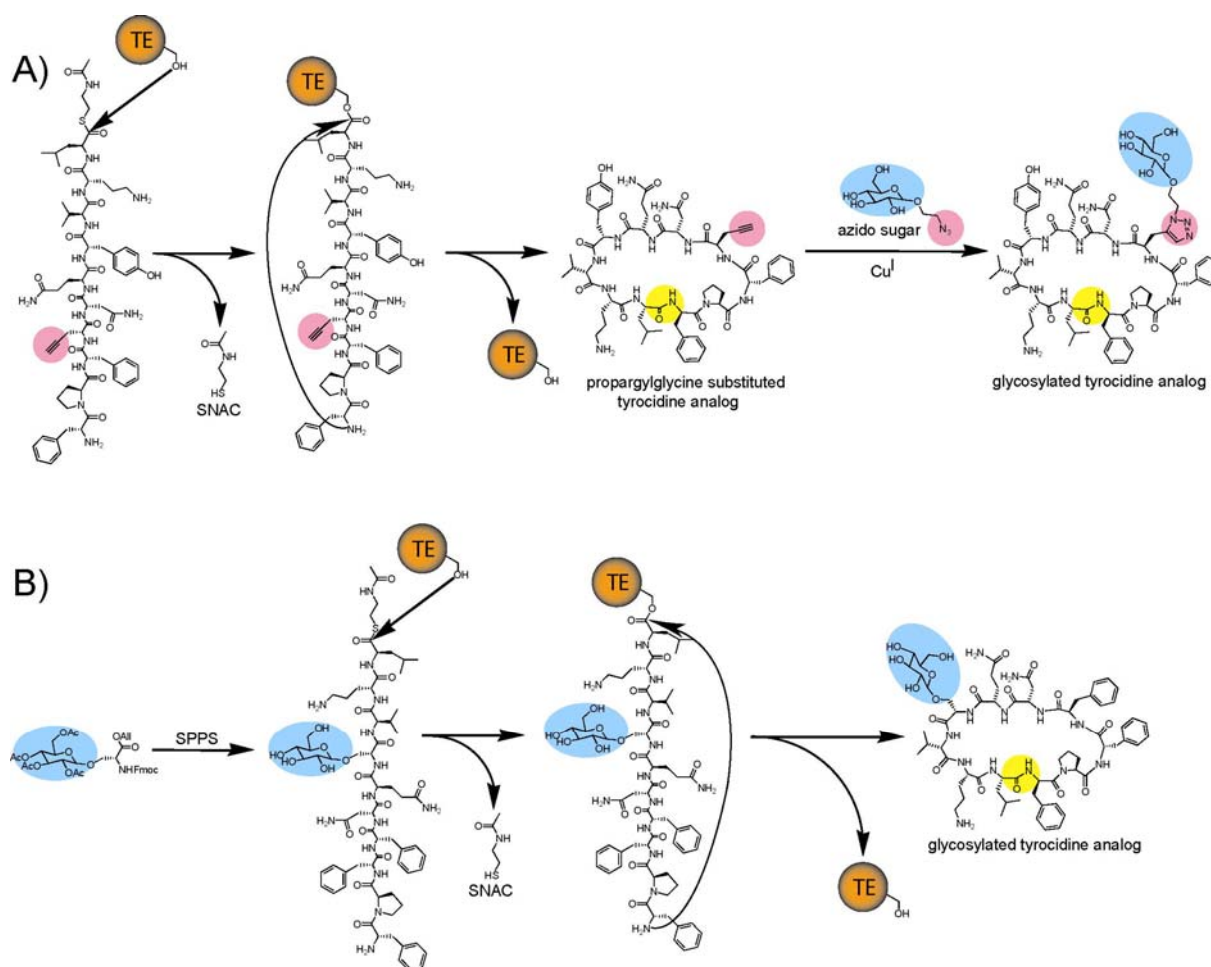


Figure 2.12: Chemoenzymatic approaches to glycopeptide antibiotics. (A) A chemically synthesized propargylglycine substituted tyrocidine SNAC substrate is cyclized by Tyc TE. The resulting alkyne-containing macrolactam is then conjugated to an azido sugar to produce a glycosylated cyclic peptide using copper(I)-catalyzed [3+2] cycloaddition. (B) A glycosylated amino acid is incorporated into a linear tyrocidine SNAC thioester via SPPS. Tyc TE-catalyzed head-to-tail-cyclization then produces a glycosyl-tyrocidine analog.

2.5.1. C-, N-Methylation of Nonribosomal Peptides

One striking feature of many acidic lipopeptide antibiotics is that they incorporate C-methylated amino acids into their peptide backbones (see chapter 2.2). For instance, in daptomycin, CDA, and A54145 the penultimate position in the cyclopeptide is nonproteinogenic 3-methylglutamate (3mGlu). However, some A54145 and CDA variants also contain nonmethylated Glu at this position. For A54145 produced by *S. fradiae*, a temporal shift toward 3mGlu-containing variants was observed during fermentation [81], whereas Glu-containing daptomycin/A21978C factors have no been reported to date. In the

2 Introduction

biosynthetic gene clusters for each of these acidic lipopeptides the deduced translation products of the *dptI* gene (daptomycin) [51], the *lptI* gene (A54145) [28], and the *glmT* gene (CDA) [17] are likely to have a role in β -methylation of Glu. These putative 3-mGlu methyltransferases contain three key S-adenosylmethionine (SAM) dependent methyltransferase motifs [82]. β -Methylation of Glu is proposed to occur prior to its activation by the cognate A-domain in the CDA biosynthetic system, because the respective A-domain differs from conventional Glu-activating domains [17]. It is further speculated that Glu is converted into a more C_{β} -H-acidic 2-oxoglutarate by a transaminase prior to deprotonation by an as yet unknown base (Figure 2.13 A) [83]. After methyltransferase-mediated stereoselective β -methylation, transamination of 2-oxo-3-methylglutarate leads to the formation of final product *L-threo*-3-mGlu.

In contrast to β -methylation of glutamate in daptomycin, CDA, and A54145, a different mechanism has been proposed to be involved in the formation of analogous 3-methylaspartate (3mAsp) found in the structures of the acidic lipopeptides amphomycin and friulimicin [84]. By a reverse genetic approach, the two overlapping genes *glmA* and *glmB* were identified in the friulimicin biosynthetic gene cluster. The deduced active enzyme GlmA-GlmB probably forms a complex of two subunits. Furthermore, a putative cofactor B_{12} binding motif in GlmA suggests a glutamate mutase mechanism, which was previously described for glutamate fermentation in *Clostridium* sp. [85] or members of the family *Enterobacteriaceae* [86] (Figure 2.13 B). Overexpression of the resulting genes in *Streptomyces lividans* verified the assumed function of GlmA-GlmB as a glutamate mutase in providing 3mAsp in friulimicin biosynthesis [84].

2 Introduction

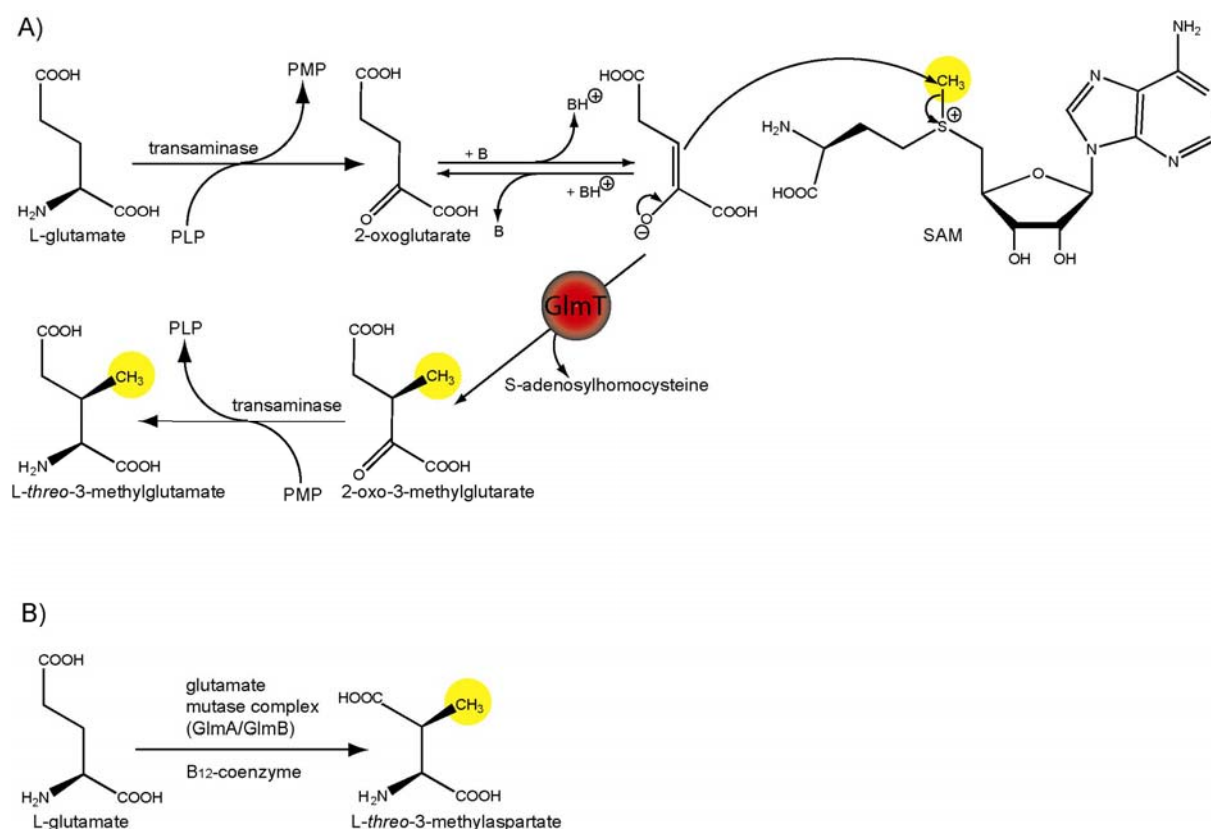


Figure 2.13: C-Methylation of nonribosomal peptides. (A) C-Methylation of L-glutamate in CDA. L-Glu is converted into 2-oxoglutarate in the presence of a transaminase, which uses pyridoxal phosphate (PLP) as a cofactor. After deprotonation by an as yet unknown base (B), GlmT catalyzes the stereoselective methylation of the resulting enolate using SAM. The methylated product 2-oxo-3-methylglutarate is finally converted to *L-threo*-3-methylglutamate under consumption of pyridoxamine phosphate (PMP). (B) β -Methylaspartate formation in friulimicin. The conversion of L-Glu into *L-threo*-3-methylaspartate is mediated by a GlmA/GlmB mutase complex, which uses cofactor B₁₂ as a cofactor.

Numerous nonribosomal peptides such as cyclosporin [87], pristnamycin [70, 88], and actinomycin [89] contain N-methylated peptide bonds. In most cases, N-methylation is introduced by an in-cis acting N-methyltransferase (N-Mt-domain, ca. 420 aa) which is inserted into the C-terminal end of the accompanying A domain. Transfer of the *S*-methyl group of SAM to the α -amino group occurs when the respective amino acid is tethered to the pp_{an} cofactor, whereupon amide bond formation can occur, generating an N-methylated peptide bond [89]. However, in contrast to in-cis acting N-methyltransferases, MtfA of the chloroeremomycin biosynthetic system catalyzes in-trans methyl transfer to the N-terminal leucine of chloroeremomycin [90].

2.5.2. Tailoring of Rigidity-Conferring Heterocyclic Elements

In some cysteine-, serine- and threonine-incorporating NRPS modules the C-domain is replaced by a cyclization-domain (Cy-domain) [5]. In addition to peptide bond formation, the Cy-domain catalyzes cyclodehydration of the peptide bond to generate rigid five-membered heterocycles, such as oxazolines derived from threonine or serine, and thiazolines derived from cysteine. In many cases, Cy-domain catalyzed heterocyclization is subsequently followed by a two-electron oxidation to form aromatic thiazoles and oxazoles. This is achieved by an oxidation-domain (Ox-domain, ca. 250 aa), which uses flavin mononucleotide (FMN) as a cofactor [91, 92]. Although Ox-domains are strictly associated with Cy-domains, they can be found in two different locations within the corresponding NRPS module: inserted into the C-terminal part of the A-domain or downstream of the PCP [93-96]. For instance, in epothilone synthase the Ox-domain is an integral part of the A-domain of EpoB whereas for bleomycin the Ox-domain is C-terminally fused to the PCP in BlmIII.

Since heterocyclic thiazoles are important determinants for bioactivity in both bleomycin and epothilone molecules, Ox-domains are interesting targets for engineering NRPSs. Entire modules containing Ox domains were swapped into bimodular model systems, resulting in the release of unnatural oxidized dipeptide products [97]. Moreover, the portability of an Ox-domain to a heterologous NRPS assembly line was reported recently [92]. Replacement of an E-domain of PchE, involved in pyochelin biosynthesis, with an Ox-domain from MtaD of the myxothiazol NRPS assembly line led to the production of a soluble FMN-containing chimeric module, which was assayed for oxidation activity *in vitro*. In fact, the chimeric module catalyzed the formation of an anticipated oxidized product, revealing the activity of the transplanted Ox-domain. Therefore, this result underscored the high portability of Ox-domains and their potential for the development of novel heterocyclic compounds.

2.5.3. Rigidification of Peptide Scaffolds by Oxidative Cross-Linking

During the biosynthesis of the glycopeptides vancomycin and balhimycin – both molecules share the same aglycone – three oxidative cross-linking reactions of the electron-rich phenol side chains are catalyzed by three cytochrome P450-like oxygenases (OxyA, OxyB, and OxyC) [98]. These cross-links convert the acyclic, floppy heptapeptides into rigid, cup-shaped scaffolds. Gene knockout experiments in the balhimycin-producing *A. mediterranei* revealed the order of the three oxidative phenol coupling reactions that sets the rigid architecture of the heptapeptide scaffold. The first coupling reaction takes place between rings C and D and is mediated by OxyB, followed by the second cross-link formation between D and E catalyzed by OxyA. The last coupling reaction occurs between rings A and B and is catalyzed by OxyC (Figure 2.14 A) [99].

Further insights into the timing of oxidative cross-linking were provided by experiments with recombinant OxyB from the vancomycin NRPS (Figure 2.14 B) [100]. The purified enzyme failed to catalyze the phenol coupling reaction of a free hexapeptide substrate. However, when the same peptide was loaded onto a PCP using the ppan transferase Sfp, incubation with OxyB resulted in 80% conversion into the desired cross-linked product. These results provide evidence that the oxidative cross-linking reaction between rings C and D takes place whilst the peptide intermediate is covalently attached as a thioester to a PCP of the glycopeptide assembly line. Although little is known about the cross-linking mechanism in detail, it was demonstrated that at least the catalytic action of OxyB is closely associated with the nonribosomal biosynthetic machinery.

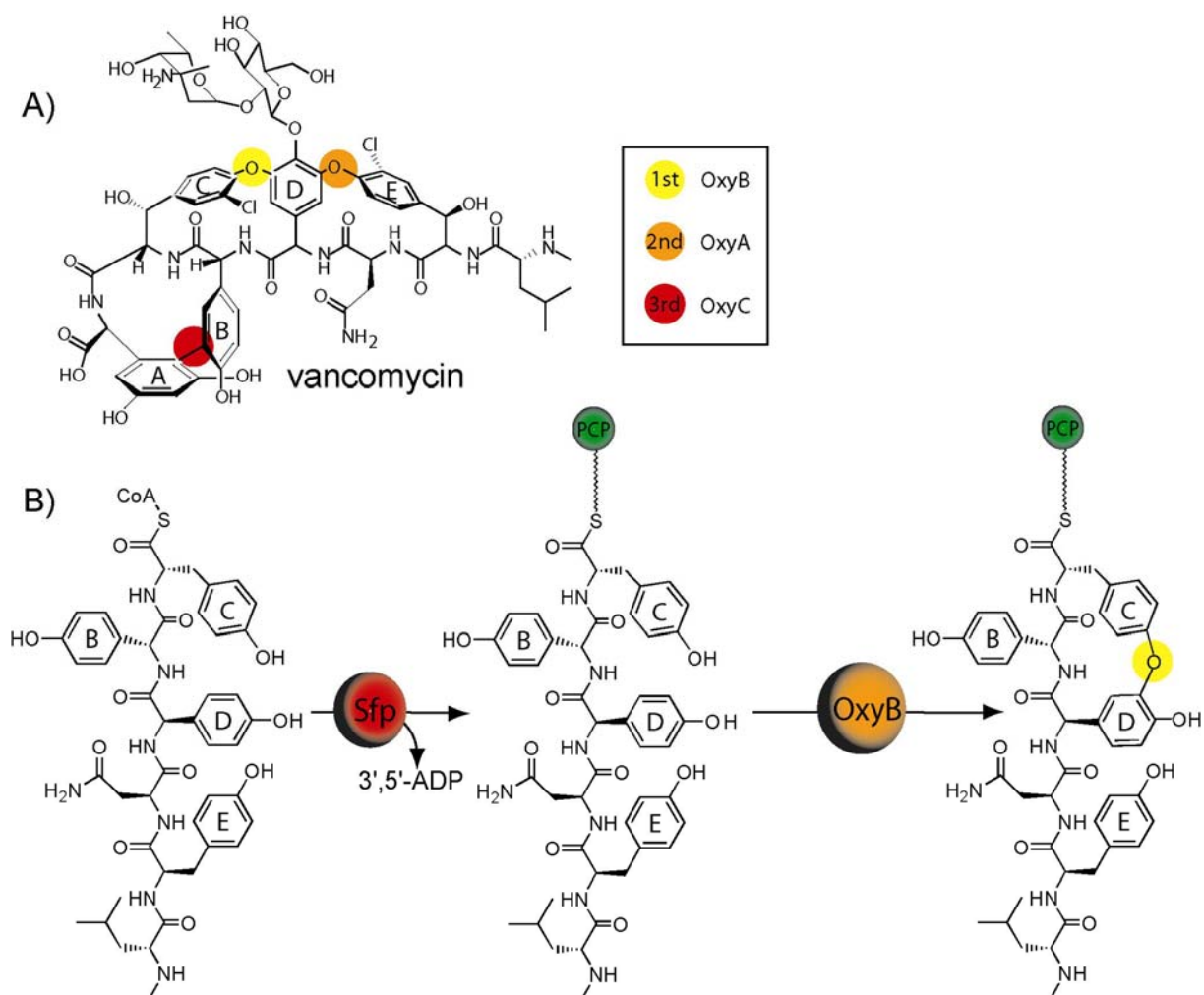


Figure 2.14: Oxidative cross-linking of phenol side chains occurs only on NRPS-bound peptide chains. (A) Chemical structure of vancomycin. The order of oxidative cross-linking mediated by OxyB, OxyA and OxyC is indicated. (B) A chemically synthesized balhimycin-like hexapeptide CoA thioester is loaded onto a PCP using Sfp. Subsequent incubation with OxyB leads to cross-linking between rings C and D.

2.6. Manipulation of Carrier Proteins by Posttranslational Modification

Nonribosomal PCPs are post-translationally modified at a conserved serine residue with a ppan moiety from coenzyme A (CoA). This modification is catalyzed by ppan transferases, such as Sfp from *B. subtilis* (Figure 2.15 A). Sfp was shown to exhibit extremely low substrate specificity and has been frequently used in metabolic engineering [101]. An interesting feature of Sfp lies in its ability to accept various functionalized CoA derivatives (Figure 2.15 B). The synthesis of these CoA conjugates can be readily achieved via Michael addition once maleimide functionalities are linked to the desired small molecule [102].

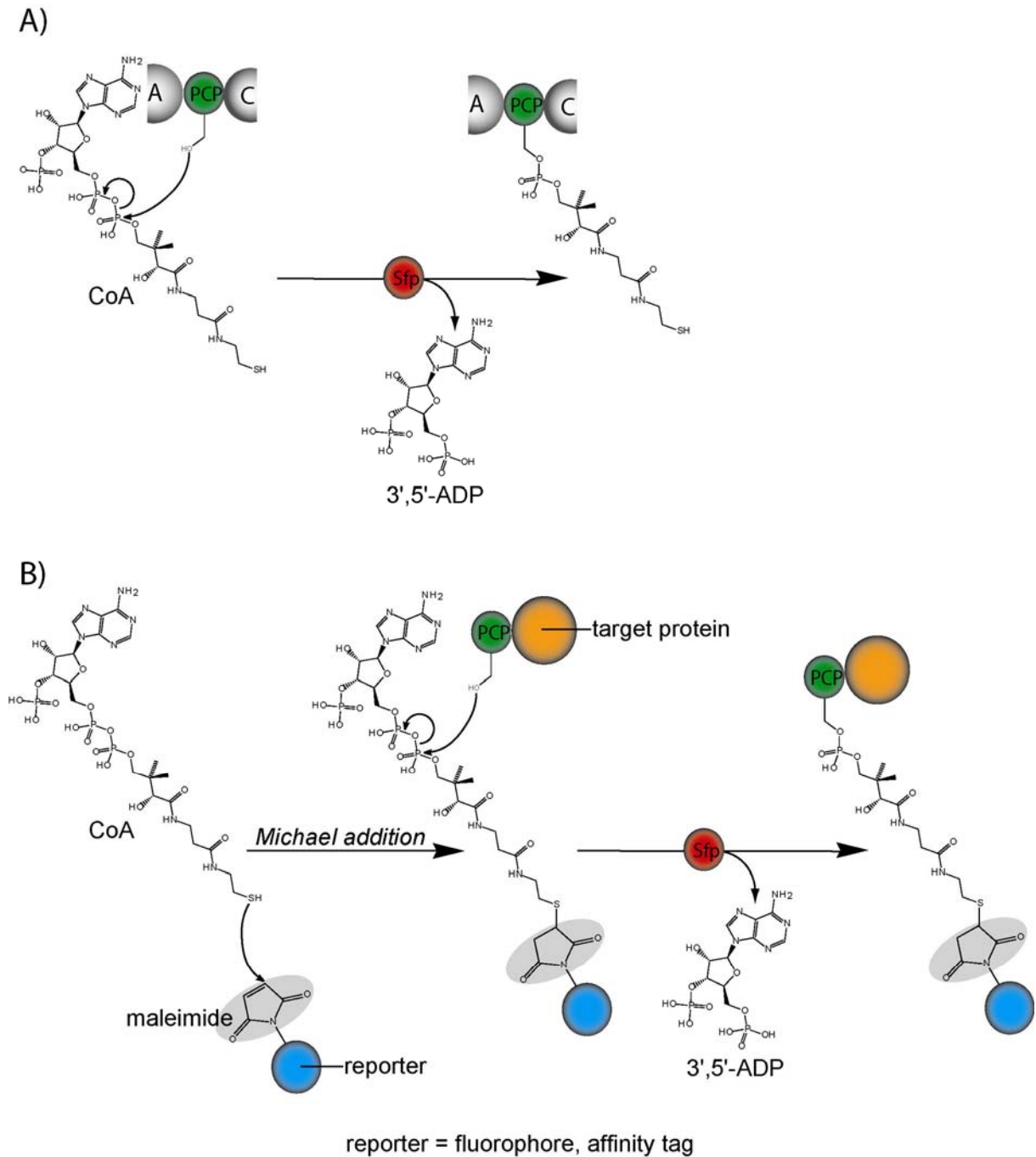


Figure 2.15: Posttranslational modification of PCPs. (A) Ppan transferases such as Sfp from *B. subtilis* transfer a 4'-phosphopantetheine residue from CoA to a strictly conserved serine residue of apo-PCP, creating the holo-PCP and 3',5'-ADP. (B) CoA-reporter analogs are created through a Michael addition of the free thiol group in CoA across the double bond of reporter-linked maleimide. Subsequent Sfp-catalyzed reporter labeling of PCP fusion proteins may be used to label the target protein with small molecules, i.e., fluorophores and affinity tags.

Researches have used the relaxed specificity of Sfp to tag carrier proteins with a variety of reporter groups, such as fluorophore- and affinity-labeled CoA [102]. The kinetics of this site-

2 Introduction

specific posttranslational modification depends on the small molecule tethered to CoA. Based on this finding, a three-color fluorescent multiplex analysis of carrier proteins was constructed by using orthogonal sets of fluorescent CoA derivatives [103]. Here, the relative population of the three fluorescent tags depends on the type of carrier protein. By using this approach carrier proteins within mixtures were convincingly identified spectrophotometrically.

The advantage of posttranslational modification of carrier proteins is that this method can be selectively carried out in a complex mixture of cellular proteins. Hence, PCP can be used as a peptide tag to direct the specific labeling of a target protein. Recently, Yin et al. reported the affinity labeling of target proteins that were expressed as artificial fusions to a PCP. These PCP-tagged target proteins were selectively labeled with biotin in the cell lysate followed by rapid immobilization on a streptavidin surface, thereby providing a high-throughput method for protein microarray fabrication and enzymatic screening [104]. In an other application, the PCP was N-terminally fused to the phage capsid protein III [105]. Subsequent Sfp catalyzed PCP modification with CoA-small molecule conjugates enabled the display of small molecules on phage surfaces. By using this method, phagemid encoded small molecule libraries could be screened for target binding.

In addition to phage surfaces, specific labeling of carrier proteins with chemically diverse compounds can be achieved on cell surfaces [106, 107]. This approach was demonstrated with the *E. coli* acyl carrier protein (ACP) fused to the α -agglutinin receptor Aga2p in yeast as well as ACP-tagged human G protein-coupled receptor neurokinin-1 (NK₁) in mammalian HEK293 cells. Instead of Sfp from *B. subtilis*, the *E. coli* ppan transferase AcpS was used to achieve specific labeling of these cell surface proteins due to its narrow substrate specificity with respect to ACP, thereby suppressing undesired side reactions.

The cell-impermeability of CoA-small molecule conjugates limits posttranslational modification of carrier proteins to cell-surface protein labeling. In order to label proteins inside of cells Clarke et al. replaced these CoA derivatives with a cell-permeable fluorophor-

2 Introduction

labeled pantetheine analog (Figure 2.16) [108]. After cellular uptake in *E. coli*, this reporter-labeled pantetheine was converted to reporter-labeled CoA via a four-step enzymatic sequence including CoAA, CoAD, and CoAE. The metabolic conversion into an active, labeled CoA derivative was followed by Sfp-mediated posttranslational modification of coexpressed VibB from *Vibriobacter cholerae*, a natural fusion between a carrier protein (CP) and isochorismate lyase (ICL). Labeling of VibB was confirmed by fluorescent SDS-PAGE of the cell lysate. These results demonstrated for the first time that one could rationally engineer a chemoenzymatic route to covalently label carrier proteins *in vivo* via metabolic delivery of cell-permeable CoA precursors.

The utility of chemoenzymatic modification of carrier proteins with synthetic CoA analogs will be part of this thesis and discussed later.

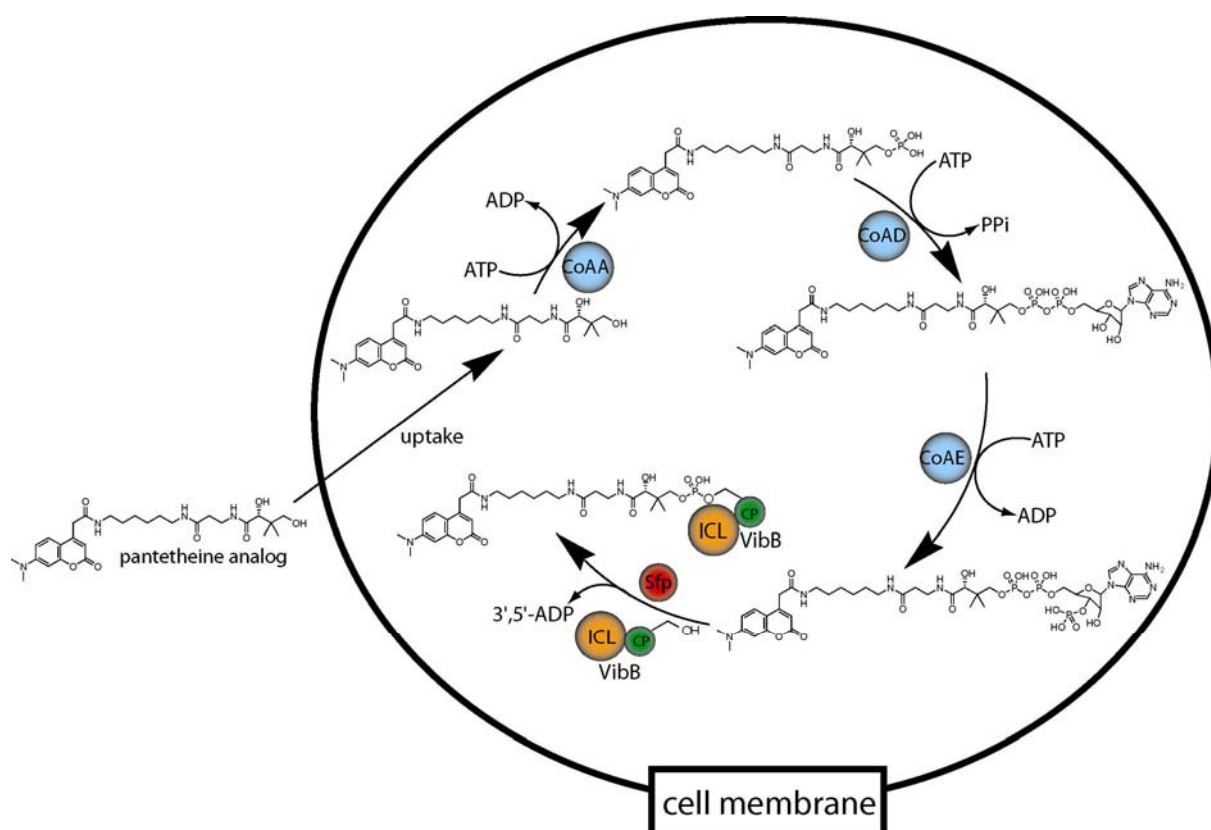


Figure 2.16: In vivo tagging of carrier protein fusion VibB within *E. coli*. To allow cellular uptake, a cell-permeable fluorophore-labeled pantetheine analog was used. This reporter-labeled pantetheine is converted to reporter-labeled CoA by CoAA, CoAD, and CoAE *in vivo*. This process is followed by reaction of coexpressed Sfp to yield fluorophore-labeled VibB. CP, carrier protein; ICL, isochorismate lyase.

2.7. Task

The main task of this work was to investigate the mechanism of peptide cyclization catalyzed by the thioesterase domain of the nonribosomal CDA synthetase (CDA TE). One aspect of this thesis was to elucidate the role of the fatty acid chain of the CDA lipopeptide for enzymatic peptide cyclization, especially its influence on the regio-, stereo-, and chemoselectivity. Moreover, systematic alterations were made to the CDA peptide backbone in order to evaluate the utility of CDA TE as a catalytic cyclization tool for the synthesis of the approved antibiotic daptomycin. Finally, investigations were made to determine the feasibility of FRET as a probe for monitoring peptide cyclization catalyzed by nonribosomal thioesterase domains. In particular, the following questions were addressed:

- To what extent is TE-mediated macrocyclization of lipopeptides controlled by the fatty acid chain length?
- What is the best leaving group for enzymatic peptide cyclization?
- How tolerant is the CDA TE to side chain alterations of the peptide substrate?
- Is it possible to monitor TE-catalyzed peptide cyclization via FRET?
- Is the immobilized CDA TE an active peptide cyclization catalyst?

3. Material

3.1. Chemicals, Enzymes and General Materials

Chemicals not listed were purchased as standard compounds from other manufacturers in p.a.-quality.

Table 3.1: Materials.

Manufacturer	Product
Agilent Technologies	DHB-matrix solution
Amersham Biosciences European GmbH	various restriction endonucleases, ampicillin, IPTG, kanamycin, yeast extract, coomassie brilliant blue G and R250, agar Nr.1, HiTrap™-desalting columns, ECL-detection reagent 1 and 2
Applied Biosystems	ABI prism™ dRhodamine terminator cycle sequencing ready reaction kit v. 3.0, HiDi Formamide
Bachem	N _α -Fmoc-protected amino acids, N _α -Boc-protected amino acids
Böhringer Mannheim	Expand™ Long Template PCR Kit, lysozyme
Eurogentech	agarose, electroporation cuvettes
Fluka	SDS, TEMED, DMF
IBA	Strep-Tactin sepharose column
Kodak	Biomax X-ray film
Macherey und Nagel	C ₁₈ -Nucleodur HPLC column, C ₁₈ -Nucleosil-HPLC column
Merck	silica gel 60 F ₂₅₄ plates
Millipore	dialysis membrane (0,025 μm)
New England Biolabs	desoxyribonucleotides (dATP, dTTP, dGTP, dCTP), prestained protein molmarker, various restriction endonucleases, 1kb-DNA-ladder
Novabiochem	N _α -Fmoc-protected amino acids, 2-chlorotritylchloride resin, HBTU, HOBt, PyBOP
Oxoid	agar Nr.1, tryptone
Pierce	biotin maleimide
Promega	SoftLink™ soft release avidin resin
Qiagen	oligonucleotides, QIAquick-spin PCR purification kit, Ni ²⁺ -NTA-agarose, QIAexpress vector kit ATG, QIAEXII extraction kit, anti-His-antibody
Roth	EtBr, β-mercaptoethanol, acrylamide for

Manufacturer	Product
Schleicher & Schüll	SDS-PAGE, piperidine
Serva	Whatmann-3MM paper
Sigma	Triton X-100, Visking dialysis tubes, APS
Stratagene	EDTA, coenzyme A, N-acetylcysteamine, thiophenol, nucleotide pyrophosphatase
Vivascience AG	QuikChange™ site-directed mutagenesis kit, PfuTurbo DNA polymerase
	Vivaspin 20 concentrators 10000 MWCO, 30000 MWCO

3.2. Equipment

Table 3.2: Equipment

Device	Manufacturer
Autoclave	Tuttnauer 5075 ELV
Bidistilled water supply	Seral Seralpur Pro90CN
Centrifugation	Heraeus Biofuge pico, Sorvall RC 26 plus, rotors SS34 und SLA3000, Sorvall RC 5B Plus, Kendro Megafuge 1.0R, Minifuge RF
DNA-gel documentation	Cybertech CS1, thermoprinter Mitsubishi Video Copy processor
DNA-sequence analyzer	Perkin-Elmer/ABI, ABI Prism 310 Genetic Analyzer
Electroporation-pulse control	Bio-Rad Gene Pulser II
fluorescence detection	Agilent Standard FLD cell; Jasco spectrofluorometer FP-6500, Jasco temperature controller ETC-273T
FPLC-system	Pharmacia FPLC-biotechnology FPLC-System 250: Gradient-programmer GP-250 Pump P-500 Uvicord optical device UV-1 (λ = 280 nm) Uvicord control element UV-1 2-channel printer REC-102 Injection valve V-7 3-way-valve PSV-100 Fraction collector FRAC-100
French Press	SLM Aminco; French-Pressure Cell-Version 5.1; 20k Rapid-fill cell (40 mL)

Device	Manufacturer
HPLC-system	Agilent series 1100 HPLC-System with DAD-detection, vacuum degasser, quaternary pump, auto sampler and HP-chemstation software columns: Macherey & Nagel Nucleosil 250/3, pore diameter 120 Å, particle size 3 µm; Nucleodur 250/3, pore diameter 100 Å, particle size 3 µm columns: Macherey & Nagel Nucleodur 250/21, pore diameter 100 Å, particle size 3 µm
MALDI-TOF	Per Septive Biosystems Voyager-DE RP BioSpectrometry, Bruker FLEX III
MS-MS sequencing	Applied Biosystems, API Qstar Pulsar I
Peptide synthesizer	Advanced ChemTech APEX 396 synthesizer
Photometer	Pharmacia Biotech Ultraspec 3000
Shaker	New Brunswick Scientific Series 25 Incubator Shaker, New Brunswick Scientific Innova 4300 Incubator Shaker
Speed-Vac	Savant Speed Vac Concentrator, Uniequip Univapo 150
Thermocycler	Perkin-Elmer Thermal Cycler 480, Perkin Elmer Gene Amp PCR System 2400, Perkin Elmer Gene Amp PCR System 9700
Water bath	Infors Aquatron Shaker

3.3. Vector systems

3.3.1. *pQE60*-vector

The pQE60 vector system was used for cloning and overexpression of Tyc TE (Figure 3.1). The vector allows purification of recombinant proteins by Ni-NTA chromatography by fusing a His₆-tag to the C-terminal end of the overexpressed protein. The pQE60-vector carries two *lac*-operators in the promoter region. In the presence of a *lac*-repressor the gene can not be transcribed. After induction with IPTG, repression is abolished and gene transcription occurs. Therefore, this system allows a defined start of protein overexpression.

gene can not be transcribed. After induction with IPTG, repression is abolished and gene transcription occurs.

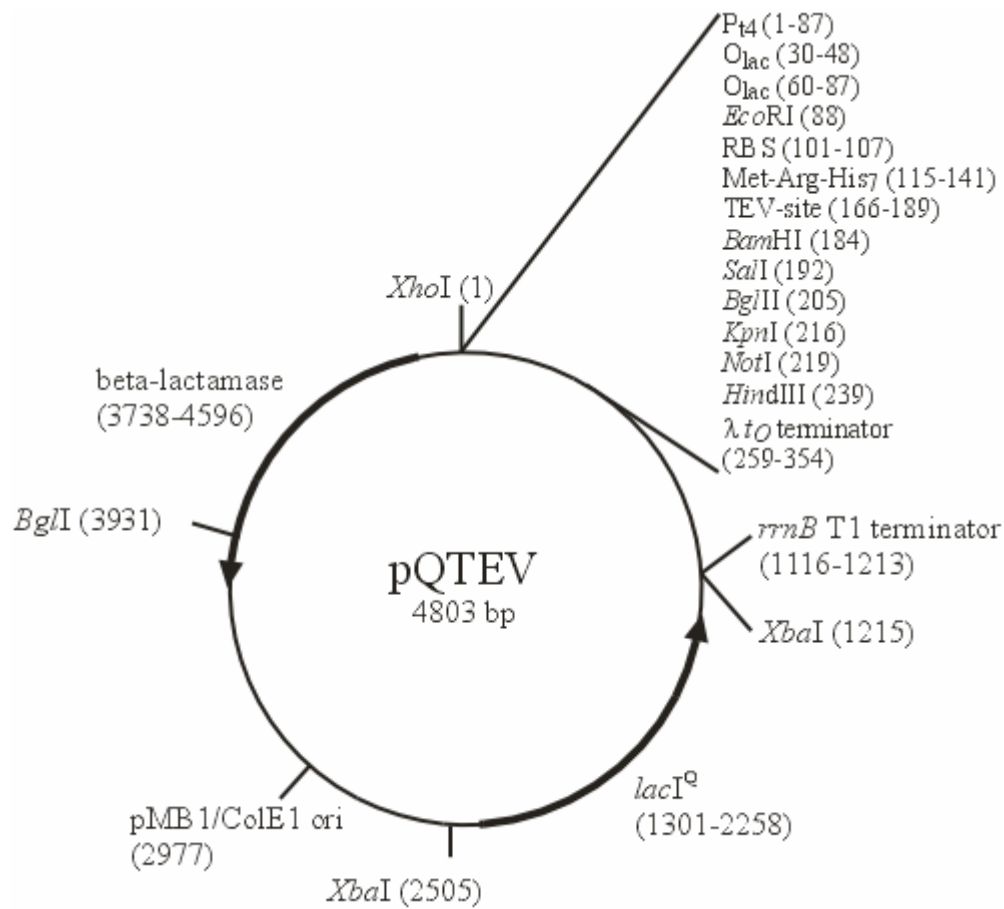


Figure 3.2: Physical map of the pQTEV-vector.

3.3.3. pBAD202/D-TOPO

The pBAD202/D-TOPO vector system (Invitrogen) was used for cloning and overexpression of CDA TE and CDA PCP-TE. The vector is regulated by the araBAD-promoter (P_{BAD}) and is induced by arabinose. The His-patch thioredoxin leader (11.7 Da) increases translation efficiency and improves protein solubility. Removal of this thioredoxin fusion can be performed using EK (enterokinase) protease, which selectively recognizes the EK cleavage site. The vector also allows Ni-NTA chromatography purification of recombinant proteins by fusion of a His₆-tag to the C-terminal end of the overexpressed protein.

The plasmid also contains the following components:

- origin of replication from pUC plasmids
- *rrnB* transcription terminator
- codon sequence coding a V5 epitope
- CAP-(cAMP binding protein) binding site for transcription enhancement by binding of the CAP-cAMP-complex
- Kanamycin resistance

3.4. Microorganisms

3.4.1. *E. coli XL1-Blue*

This strain was frequently used for cloning and sequencing purposes. The genotype is as follows: *recA1, endA11, gyrA96, thi-1, hsdR17, supE44, relA1, lac, F'(proAB⁺, lacI^q, lacZDM15, Tn10(Tet^I)).*

3.4.2. *E. coli Top 10*

E. coli Top 10 is another strain for cloning and sequencing purposes. The genotype is as follows: F- *mcrA. (mrr-hsdRMS-mcrBC) 80lacZ.M15.lacX74 deoR recA1 araD139. (ara-leu)7697 galU galK rpsL (StrR) endA1 nupG.*

3.4.3. *E. coli BL21(DE3)*

The *E. coli* strain BL21(DE3) with the genotype F⁻ *ompT*[*lon*]*r_b⁻m_b⁻* is used as a bacterial host for the expression of plasmid DNA. It is characterized by a lack of *lon* protease and by a deficiency of *OmpT* protease, thereby significantly increasing protein stability. It further contains the IPTG-inducible T7 RNA polymerase gene, which is inserted in the chromosome after *lacZ* and the promoter *lacuV5* on a λ -prophage. This is essential for the IPTG induction of genes under T7-promotor control.

3.4.4. *E. coli* BL21(M15)

This strain lacks the T7-polymerase. It has the following genotype: *nals*, *strs*, *rifs*, *lac*, *ara*, *gal*, *mtl*, *F*.

3.5. Media

E. coli strains were grown in LB-media.

LB-media	16 g/L bacto-trypton
	10 g/L yeast-extract
	5 g/L NaCl

Culture plates: 1.2% (w/v) of agar no.1 was added to the LB-media and heated at 121°C and 1,5 bar for 30 min. Antibiotics were added after cooling down to 55°C in the following standard concentrations: 100 µg/mL ampicillin, 50 µg/mL kanamycin, 34 µg/mL chloramphenicol.

4. Methods

4.1. Molecular Biology Techniques

4.1.1. Construction of Recombinant Plasmids

Amplification of all DNA gene fragments was performed by polymerase chain reaction (PCR) with Pfu Turbo DNA polymerase (Stratagene) according to the manufacturer's protocol with synthetic oligonucleotides (Qiagen). Purification of PCR-fragments was performed by the "QIAquick-spin PCR purification kit" in agreement with the manufacturer's manual (Qiagen). All constructs were analyzed by restriction digests and DNA-sequencing.

Construction of pBAD202/D-TOPO[cda TE] – The *cda TE* gene fragment was amplified using the chromosomal DNA of *S. coelicolor* A3(2) as template. The following oligonucleotides were used: 5'-C ACC ATG CGC GGC GGC CGG GAG CC-3' and 5'-GGC GAC CTC GGT CGA ATC G-3'. The PCR product of *cda TE* was directionally cloned into a pBAD202/D-TOPO vector (Invitrogen) using the pBAD directional TOPO expression kit (Invitrogen) according to the manufacturer's guidelines. The pBAD202/D-TOPO vector appends an N-terminal His-patch thioredoxin leader and a C-terminal His₆-tag to the expressed protein. Preparation of recombinant plasmids was carried out in *E. coli* TOP 10.

Construction of pBAD202/D-TOPO[cda PCP-TE] – The *cda PCP-TE* gene fragment was amplified using the chromosomal DNA of *S. coelicolor* A3(2) as template. The following oligonucleotides were used: 5'-C ACC CGC ACC GTC GAG GGC CGC-3' and 5'-GGC GAC CTC GGT CGA ATC G-3'. The PCR product was directionally cloned into a pBAD202/D-TOPO vector (Invitrogen) using the pBAD directional TOPO expression kit (Invitrogen) according to the manufacturer's protocol.

Construction of pQTEV[cda TE] – The *cda TE* gene fragment was amplified using the chromosomal DNA of *S. coelicolor* A3(2) as template. The PCR reaction was performed with Pfu Turbo DNA polymerase (Stratagene) using the following oligonucleotides: 5'-AAA AAA GGA TCC CGC GGC GGC CGG GAG CC-3' and 5'-AAA AAA AAG CTT GGC GAC CTC GGT CGA ATC GAG CG-3'. The PCR product of *cda TE* was cloned into the BamHI/HindIII site of the pQTEV vector (Qiagen). The plasmid was directly used to produce protein with an N-terminal heptahistidine tag. Preparation of recombinant plasmids was carried out in *E. coli* XL1-Blue.

Construction of pQTEV[cda PCP-TE] – The *cda PCP-TE* gene fragment was amplified using the following oligonucleotides: 5'-AAA AAA GGA TCC CGC ACC GTC GAG GGC CGC TC-3' and 5'-AAA AAA AAG CTT GGC GAC CTC GGT CGA ATC GAG CG-3'. The PCR product of *cda PCP-TE* was cloned into the BamHI/HindIII site of the pQTEV vector (Qiagen). The recombinant plasmid was directly used to produce protein with an N-terminal His₇-tag.

Construction of pQE60[Tyc TE] – The construction of *pQE60[Tyc TE]* has been described elsewhere [66].

4.1.2. DNA Sequencing

DNA sequencing of double stranded DNA was performed by the method of chain termination (147 RF) with the “ABI prismTM dRhodamine terminator cycle sequencing ready reaction kit” according to the manufacturer’s protocol. Sequencing of the GC-rich targets was performed with 500 ng DNA per kbp, 10 pmol primer, 5 % DMSO (v/v), and 4 µL sequence mix. After 30 rounds of PCR and subsequent purification the sequence analysis was performed on an

“ABI Prism 310 Genetic Analyzer” (Applied Biosystems). Alternatively, DNA sequencing was carried out by GATC Biotech.

Table 4.1: PCR protocol for DNA sequencing

Cycles	Temperature [°C]	Time [min]
1	95	1:00
30	95	1:00
	50	0:10
	60	4:00
1	60	5:00

4.2. Protein Methods

Standard methods frequently used in protein analysis like SDS-PAGE and coomassie-staining have been described elsewhere [109, 110].

4.2.1. Gene Expression

Heterologous expression of recombinant TE and PCP-TE enzymes was performed in the pQE60, pQTEV and pBAD202/D-TOPO vectors systems. For this purpose *E. coli* BL21 (DE3) were transformed with the expression plasmids, with the exception of tyc TE where *E. coli* M15 was transformed with the corresponding expression plasmid.

4.2.1.1. Expression with the pQE60- and pQTEV-Vector Systems

20 mL overnight culture of the corresponding expression strain in LB-media was inoculated in 2L of LB-media. Cells were grown to OD = 0.5 (600 nm), induced with 1 mM IPTG, and

4 Methods

again grown at 30°C, 250 rpm for 3 h. The culture was subsequently harvested by centrifugation (7000 rpm, 4°C, 15 min) and the resulting pellet was resuspended in Hepes A buffer (50 mM Hepes, 300 mM NaCl, pH 8.0). The cell suspension was stored at -20°C.

4.2.1.2. Expression with the pBAD202/D-TOPO-Vector System

20 mL overnight culture of the corresponding expression strain in LB-media was inoculated in 2L of LB-media. The transformed cells were grown to OD = 0.5 (600 nm), induced with 0.01% arabinose (w/v), and again grown at 25 °C, 250 rpm for 2.5 h. The cells were subsequently harvested by centrifugation (7000 rpm, 4°C, 15 min) and the resulting pellet was resuspended in Hepes A buffer (50 mM Hepes, 300 mM NaCl, pH 8.0). The cell suspension was stored at -20°C.

4.2.2. Protein Purification

All recombinant proteins were purified by nickel-nitrilotriacetic acid (Ni-NTA) affinity chromatography (Amersham Pharmacia Biotech).

4.2.2.1. Disruption of cell material

Disruption of cell material was carried out by using a pre-cooled 20k French Press cell (SLM Aminco). Four cycles of compression and decompression were carried out with each cell extract. Insoluble cell material was separated from the cell extract by centrifugation (17000 rpm, 30 min, 4°C). The supernatant was subsequently used for Ni²⁺-NTA affinity chromatography.

4.2.2.2. *Ni²⁺-NTA affinity chromatography*

Recombinant His₆-tagged proteins were purified by Ni²⁺-NTA affinity chromatography (Amersham Biosciences). In standard purifications cell extracts from 2L expressions were loaded onto a Ni²⁺-NTA superflow (Qiagen) column (HR 10/2, Amersham Biosciences). The column was loaded with a flow rate of 1 mL/min in 3 % buffer Hepes B (50 mM Hepes, 300 mM NaCl, 250 mM imidazole, pH 8.0) on a FPLC system (Amersham Biosciences). When the absorbance at $\lambda = 220$ nm was at baseline again, a 30 min linear gradient up to 45 % Hepes B followed by a 10 min linear gradient to 100 % Hepes B with a flow rate of 1 mL/min was applied. Proteins were identified by Bradford-assay [111] and by SDS-PAGE. Dialysis into 25 mM Hepes and 50 mM NaCl, pH 7.0, was carried out using HiTrap desalting columns (Amersham Biosciences). After being flash frozen in liquid nitrogen, the proteins were stored at -80 °C.

4.2.2.3. *Determination of Protein Concentrations*

The concentrations of the purified proteins were determined spectrophotometrically using the calculated extinction coefficient at 280 nm, which was determined by the program “Protean”.

Table 4.2: Theoretical extinction coefficients ($\lambda = 280$ nm)

Protein (vector system)	Theoretical extinction coefficient [mg/mL]
CDA TE (pBAD202/D-TOPO)	1.22
CDA PCP-TE (pBAD202/D-TOPO)	1.43
CDA TE (pQTEV)	1.24
CDA PCP-TE (pQTEV)	1.54
Tyc TE (pQE60)	1.34

4.3. Biochemical Methods

4.3.1. Cyclization Assays

Reactions were performed in 25 mM Hepes and 50 mM NaCl, pH 7.0, in a total volume of 50 μ L. Dissolution of peptidyl thiophenols was facilitated by the addition of 5% DMSO (v/v). In standard reactions the substrate concentration was 250 μ M. Kinetic characterization of the cyclization reactions was performed by determining initial rates at varying substrate concentrations. All cyclization reactions were initiated by addition of enzyme to a final concentration of 5 μ M for CDA TE, 5 μ M for CDA PCP-TE, and 0.5 μ M for Tyc TE. Reactions were quenched by addition of 35 μ L of 4% TFA/H₂O. All assays were analyzed by LC/MS on a reversed phase C₁₈ Nucleodur column (Macherey and Nagel, 250/3, pore diameter 100 Å, particle size 3 μ m) except for assays with CDA SNAC substrate, which were analyzed on a C₁₈ Nucleosil column (Macherey and Nagel, 250/3, pore diameter 120 Å, particle size 3 μ m) with the following gradients: all CDA thiophenol substrates (except hex-CDA thiophenol), CDA CoA, and CDA SNAC, 0-40 min, 15-45% acetonitrile/0.1% TFA in water/0.1% TFA, 0.4 mL/min, 45 °C; CDA ppan, 0-40 min, 5-60% acetonitrile/0.1% TFA in water/0.1% TFA, 0.4 mL/min, 45 °C; hex-CDA thiophenol, hybrid CDA-daptomycin thiophenol substrates, and daptomycin-like thiophenol substrates 0-40 min, 15-60% acetonitrile/0.1% TFA in water/0.1% TFA, 0.4 mL/min, 45 °C. Identities of the products were verified by ESI-MS and MALDI-TOF. Connection regiospecificity of cyclic products was determined by MS-MS analysis on an API Qstar Pulsar i Q-q-TOF mass spectrometer (Applied Biosystems).

Concentrations of various peptidyl thioesters were calculated using experimentally determined extinction coefficients at a wavelength of 220 nm. The extinction coefficients of peptidyl thioesters were assumed to be identical to the corresponding cyclized and hydrolyzed products.

4.3.2. Preparation of Linear and Cyclic Peptides for Bioassays and Fluorescence Measurements

Semipreparative scale production of linear and cyclic peptide products was performed to obtain enough material for bioactivity and fluorescence studies. For the semipreparative scale generation of cyclic products, the reactions were carried out in a total volume of 3-12 mL with 5 μ M CDA TE, 250 μ M peptidyl thiophenol, 25 mM Hepes, 50 mM NaCl, and 5% DMSO (v/v), at pH 7.0 and room temperature. Substrate turnover into cyclic product and linear peptide acid was monitored by analytical HPLC and thin-layer chromatography (TLC) on silica gel 60 F₂₅₄ plates (Merck) and visualized under UV (365 nm). After a time period of 2-5 h the semipreparative scale assays were quenched by adding TFA to a final concentration of 1.6% (v/v). After flash freezing in liquid nitrogen the samples were lyophilized overnight. The resulting solid was redissolved in 1 mL of 35-50% acetonitrile/water. Purification of the cyclic products was achieved on a 250/10 Nucleodur 100-7 C18 reversed-phase column (Macherey and Nagel) by applying a gradient from 35% to 45% acetonitrile in 0.1%TFA/water over 30 min at a flow rate of 8 mL min⁻¹. The purity of the products was more than 95% as determined by analytical HPLC.

The concentrations were determined by comparing the area of absorption at 215 nm with that of a known concentration of linear peptide thioester or daptomycin.

Semipreparative scale generation of the linear peptide acid was performed by treatment of the peptide loaded 2-chlorotrityl resin with a mixture containing trifluoroacetic acid (TFA), triisopropylsilane (TIPS), and water in a ratio of 95:2.5:2.5 (v/v). The peptide acid was precipitated in ice cold diethyl ether and purified by semipreparative HPLC as described for the cyclic products.

4.3.3. Peptide Cyclization by the Immobilized CDA PCP-TE Didomain

Sfp phosphopantetheine transferase catalyzed biotin CoA labeling of the purified CDA PCP-TE (pQTEV) protein was performed according to Clugston et al. [42]. In a total volume of 100 μ L, 5 μ M Sfp, 5 μ M biotin CoA, 10 mM $MgCl_2$, and 1 mM TCEP in 50 mM Hepes (pH 7.5) were incubated with 20 μ M CDA PCP-TE didomain for 90 minutes at 30°C. The labeling reaction mixture was then run over a column loaded with SoftLink™ soft release avidin resin (Promega) (bed volume 1 mL). Incubation was carried out at 4°C prior to washing with a solution containing 5 mL 0.1 M $NaPO_4$ (pH 7.0). 5 mM peptidyl thiophenol **InDap-U₁W₁₃** (see appendix) dissolved in 100 μ L DMSO was then added to the column. After incubation at 25°C for 3h, the reaction products were eluted with 1 mL phosphate buffer. After lyophilizing to dryness, the eluate was extracted with methanol:DMSO 9:1. Product analysis was conducted by analytical HPLC on a C₁₈ Nucleodur column (Macherey and Nagel, 125/3, pore diameter 100 Å, particle size 3 μ m) by applying a gradient from 30% to 90% acetonitrile in 0.1% TFA/water over 10 min at a flow rate of 0.8 mL min⁻¹ and by fluorescence detection without HPLC column (Standard FLD cell (Agilent), emission wavelength 452 nm, excitation wavelength 280 nm, PMT gain 10, injection volume 10 μ L, 100% methanol over 2 min, 0.5 mL min⁻¹). The CDA PCP-TE didomain was eluted with 5 mM biotin in the phosphate buffer. The eluate was resolved by SDS-PAGE (12.5%) and visualized by Coomassie stain.

4.4. Analytical Methods

4.4.1. Biological Activity Assays

Two-fold serial dilutions of peptide acids and peptidolactones including authentic daptomycin as reference compound were prepared in sterile microtitre plates as described elsewhere [112]. All tests were performed with *B. subtilis* PY79. Incubation was carried out at 37 °C for 18 h

prior to visual determination of MICs. The bactericidal activity was examined in LB media as well as in LB media supplemented with 50 mg of Ca²⁺/L. The calcium content of LB media was determined by elementary analysis to be 23.6 mg/L. For determination of hemolytic activity sheep blood agar plates were used. Sterile disks (6 mm diameter) were soaked with 2.5-10 µL of solutions of cyclic peptides in methanol varying in their concentrations from 0.64 µg/mL to 640 µg/mL. Plates were incubated at 37 °C for 16 h. Surfactin was used as a positive control. The hemolytic zone diameters were determined by visual assay.

4.4.2. Mass Spectrometry

All substrates and products were analyzed by LC-MS or MALDI-TOF MS.

Matrix assisted laser desorption ionization – time of flight mass spectrometry (MALDI-TOF MS) is an analytical method to determine the molecular mass of peptides and proteins in high vacuum. Samples were prepared by mixing 1 µL peptide/protein solution with 1 µL DHB-matrix solution (Agilent Technologies). 1 µL of this mixture was pipetted onto a metallic 384-well plate. After evaporation to dryness, the cocrystallized samples were investigated with a “Bruker FLEX III” (Bruker Daltonics).

High performance liquid chromatography – mass spectrometry (HPLC-MS) was used to separate and to analyze complex peptide/protein mixtures. Separation is achieved by reversed phase chromatography, which is based on hydrophobic interactions with the unpolar stationary phase (C₁₈ or C₈ coated silica gel). Elution is mediated by a gradual increase of the acetonitrile-to-water ratio. The characteristic retention times of the separated peptides/proteins are monitored by UV-detection. The ESI interface allows the mass analysis of samples at atmospheric pressure. Ionization of the analytical compounds is facilitated by the addition of 0.1 % TFA. Experiments were performed on an Agilent series 1100 HPLC-System.

Table 4.3: Characterization of CDA-like thioester substrates by MS

Compound	Species	Ionization method	Observed mass (calculated mass) (Da)	Cy/Hy ratio
CDA-CoA	[M+H] ⁺	ESI	2176.4 (2176.6)	8 : 1
CDA-ppan	[M+H] ⁺	ESI	1767.3 (1767.6)	2 : 1
CDA-SNAC	[M+H] ⁺	ESI	1528.4 (1528.6)	9 : 1
CDA-thiophenol	[M+H] ⁺	ESI	1519.3 (1519.5)	5 : 1
Hex-CDA-thiophenol	[M+H] ⁺	ESI	1575.4 (1575.6)	10 : 1
CDA-A1A2	[M+H] ⁺	ESI	1473.4 (1473.5)	
CDA-A1	[M+H] ⁺	ESI	1503.2 (1503.5)	3 : 1
CDA-A2	[M+H] ⁺	ESI	1489.3 (1489.5)	1 : 3
CDA-DS1A2	[M+H] ⁺	ESI	1489.3 (1489.5)	
CDA-A1DT2	[M+H] ⁺	ESI	1503.4 (1503.5)	
CDA-DS1	[M+H] ⁺	ESI	1519.4 (1519.5)	2 : 1
CDA-DT2	[M+H] ⁺	ESI	1519.3 (1519.5)	1 : 5
CDA-DS1DT2	[M+H] ⁺	ESI	1519.4 (1519.5)	

Table 4.4: Characterization of CDA-like products by MS

Compound	Species	Ionization method	Observed mass (calculated mass) (Da)		Cy/Hy ratio
			cyclized product	hydrolyzed product	
CDA-CoA	[M+H] ⁺	ESI	1409.4 (1409.5)	1427.4 (1427.5)	8 : 1
CDA-ppan	[M+H] ⁺	ESI	1409.3 (1409.5)	1427.3 (1427.5)	2 : 1
CDA-SNAC	[M+H] ⁺	ESI	1409.3 (1409.5)	1427.4 (1427.5)	9 : 1
CDA-thiophenol	[M+H] ⁺	ESI	1409.4 (1409.5)	1427.3 (1427.5)	5 : 1
Hex-CDA	[M+H] ⁺	ESI	1465.4 (1465.6)	1483.4 (1483.6)	10 : 1
CDA-A1A2	[M+H] ⁺	ESI	n. d. (1363.5)	1381.4 (1381.5)	
CDA-A1	[M+H] ⁺	ESI	1393.4 (1393.5)	1411.4 (1411.5)	3 : 1
CDA-A2	[M+H] ⁺	ESI	1379.4 (1379.5)	1397.3 (1397.5)	1 : 3
CDA-DS1A2	[M+H] ⁺	ESI	n. d. (1379.5)	1397.3 (1397.5)	
CDA-A1DT2	[M+H] ⁺	ESI	n. d. (1393.5)	1411.4 (1411.5)	
CDA-DS1	[M+H] ⁺	ESI	1409.4 (1409.5)	1427.4 (1427.5)	2 : 1
CDA-DT2	[M+H] ⁺	ESI	1409.4 (1409.5)	1427.2 (1427.5)	1 : 5
CDA-DS1DT2	[M+H] ⁺	ESI	n. d. (1409.5)	1427.4 (1427.5)	

Table 4.5: Characterization of hybrid CDA-daptomycin and daptomycin-like substrates and products by MS

*cyclization via L-Orn; †cyclization via L-Kyn

compound	species	ionization method	observed mass (calculated mass) (Da)		
			substrate	cyclized product	hydrolysis
AcCDA-G3	[M+H] ⁺	ESI	1390.3 (1390.5)	1280.2 (1280.5)	1298.3 (1298.5)
AcCDA-O4	[M+H] ⁺	ESI	1518.2 (1518.6)	1408.4 (1408.6) 1408.7 (1408.6)*	1426.3 (1426.6)
AcCDA-DA6	[M+H] ⁺	ESI	1443.2 (1443.5)	1333.2 (1333.5)	1351.2 (1351.5)
AcCDA-DS9	[M+H] ⁺	ESI	1492.3 (1492.5)	1382.2 (1382.5)	1400.3 (1400.5)
HexCDA-G3	[M+H] ⁺	MALDI-TOF	1446.6 (1446.5)	1336.5 (1336.5)	1354.5 (1354.5)
HexCDA-O4	[M+H] ⁺	MALDI-TOF	1574.6 (1574.7)	1464.4 (1464.7) 1465.2 (1464.7)*	1482.4 (1482.7)
HexCDA-DA6	[M+H] ⁺	MALDI-TOF	1499.4 (1499.6)	1389.4 (1389.6)	1407.3 (1407.6)
HexCDA-DS9	[M+H] ⁺	MALDI-TOF	1548.5 (1548.6)	1438.5 (1438.6)	1456.4 (1456.6)
HexCDA-D1	[M+H] ⁺	ESI	1603.4 (1603.6)	1493.4 (1493.6)	1511.3 (1511.6)
HexCDA-U11	[M+H] ⁺	ESI	1579.3 (1579.6)	1469.4 (1469.6) 1469.3 (1469.6) [†]	1487.3 (1487.6)
Dap	[M+H] ⁺	ESI	1716.6 (1716.7)	1606.6 (1606.7) 1606.7 (1606.7)* 1606.6 (1606.7) [†]	1624.4 (1624.7)

Table 4.6: Characterization of semi-preparative scale generated cyclic and linear daptomycin-like peptides by MALDI-TOF MS.

Compound	Species	observed mass (calculated mass) (Da)
Dap	[M+H] ⁺	1606.7 (1606.7)
Dap-Hyd	[M+H] ⁺	1624.7 (1624.7)
Dap-N3	[M+H] ⁺	1606.0 (1605.7)
Dap-N7	[M+H] ⁺	1606.0 (1605.7)
Dap-N9	[M+H] ⁺	1605.9 (1605.7)
Dap-Q12	[M+H] ⁺	1605.9 (1605.7)
Dap-DD11	[M+H] ⁺	1634.9 (1634.7)
Dap-Aloc	[M+H] ⁺	1691.0 (1690.7)
Dap-W13	[M+H] ⁺	1603.0 (1602.7)
Dap-W13K6	[M+H] ⁺	1617.0 (1616.7)

Table 4.7: Characterization of cyclic and linear daptomycin-like peptides and the fluorescent Tyc SNAC substrate by MS

Compound	Species	Observed mass (Da)	Calculated mass (Da)
lnDap-U₁W₁₃	[M+H] ⁺	1717.2	1716.7
lnDap-U₂W₁₃	[M+H] ⁺	1716.3	1716.7
lnDap-U₃W₁₃	[M+H] ⁺	1717.0	1716.7
lnDap-U₅W₁₃	[M+H] ⁺	1716.6	1716.7
lnDap-U₇W₁₃	[M+H] ⁺	1717.0	1716.7
lnDap-U₁W₁₄	[M+H] ⁺	1773.9	1773.7
lnDap-U₁W₁₅	[M+H] ⁺	1830.3	1830.8
lnTyc-U₂W₈	[M+H] ⁺	1569.9	1569.7
cyDap-U₁W₁₃	[M+H] ⁺	1607.1	1606.7
cyDap-U₂W₁₃	[M+H] ⁺	1606.9	1606.7
cyDap-U₃W₁₃	[M+H] ⁺	1607.0	1606.7
cyDap-U₅W₁₃	[M+H] ⁺	1606.8	1606.7
cyDap-U₇W₁₃	[M+H] ⁺	1606.9	1606.7
cyDap-U₁W₁₄	[M+H] ⁺	1663.8	1663.7
cyDap-U₁W₁₅	[M+H] ⁺	1721.0	1720.8
cyTyc-U₂W₈	[M+H] ⁺	1450.6	1450.7

4.5. Fluorescence Techniques

Fluorescence measurements were performed on a spectrofluorometer (FP-6500, Jasco) with slits set to 10 nm (excitation) and 5 nm (emission) at an excitation wavelength of 280 nm. The detector was set to low sensitivity. Constant temperature was achieved by circulating water through the cell holder in which the temperature was measured by a temperature controller (ETC-273T, Jasco). The fluorescence results are expressed as the relative quantum yield (ϕ) calculated as the integrated fluorescence emission between 300 and 390 nm (Trp) and between 400 and 550 nm (Kyn). All experiments were performed in 10 mm path length cuvettes containing 300 μ L of linear peptide thioester or cyclic peptide dissolved in methanol:DMSO 9:1 to a final concentration of 200 μ M. Fluorescence measurements were also carried out using a fluorescence detector (Standard FLD cell, Agilent) without HPLC column (emission wavelength 452 nm, excitation wavelength 280 nm, PMT gain 10, injection volume 10 μ L, 100% methanol over 2 min, 0.5 mL min⁻¹). To determine $k_{\text{cat}}/K_{\text{M}}$ values, the integrated fluorescence emission at 452 nm was compared with the area of known concentrations of the corresponding cyclic peptides.

Absorptions measurements were performed on an Ultraspec 3000 UV/Visible Spectrophotometer (Pharmacia Biotech).

4.5.1. Real-time fluorescence measurements

Reactions were carried out in 10 mm path length cuvettes in a total volume of 300 μ L with 25 mM HEPES, 50 mM NaCl, and 5% DMSO (v/v) at pH 7.0 and 25 °C. The enzyme concentrations were 0.5 μ M for Tyc TE and 5 μ M for CDA cyclase. The negative controls were conducted in the presence of the corresponding heat denatured enzymes. Reactions were initiated by addition of 50 μ M peptidyl SNAC **lnTyc-U₂W₈** or 75 μ M peptidyl thiophenol **lnDap-U₃W₁₃** (see appendix). Real-time measurements were performed using various time

points with slits set to 5 nm (excitation) and 5 nm (emission) at an excitation wavelength of 280 nm and an emission wavelength of 452 nm. The detector was set to medium sensitivity. All assays were quenched by the addition of 1.6% TFA (v/v) and analyzed by analytical HPLC.

4.6. Solid Phase Peptide Synthesis (SPPS)

Solid Phase Peptide Synthesis can be defined as the process in which a peptide is constructed by the successive addition of the protected amino acids constituting its sequence. The growing peptide chain anchored via its C-terminus to an insoluble solid support makes it possible to eliminate the excess of reagents and by-products by simple filtration with savings in time and labor. However, there are also limitations in this approach: By-products from incomplete reactions, side reactions, or impure reagents will accumulate on the solid support during chain assembly. In this work Fmoc/tBu chemistry was performed on a fully automated peptide synthesizer (APEX 396 synthesizer, Advanced ChemTech) for batchwise SPPS [1/121]. 2-chlorotrityl resin was used as solid support, which allows the cleavage of fully protected sequences. Protecting groups included: tert-butyl (tBu), trityl (Trt), allyloxycarbonyl (Aloc), and tert-butyloxycarbonyl (Boc).

4.6.1. Initiation: Loading of 2-chlorotritylchloride resin

Loading of 2-chlorotritylchloride resin is achieved by treatment with the triethylammonium salt of the desired Fmoc amino acid, thus, concomitant racemization is minimized. The loading step is very important because the extent of this reaction will determine the yield of the final product. To ensure efficient loading, the resin was swelled in dry DCM, followed by incubation with 2 equivalents of Fmoc-protected amino acid supplemented with 8 equivalents of DIPEA. This sterically hindered base ensures complete deprotonation of the carboxyl-

group. The carboxyl-group then nucleophilically attacks the carbon-chlorine bond of the 2-chlorotritylchloride resin, covalently attaching the C-terminal residue to the solid phase (Figure 4.1). After 2h vigorous stirring the solvent was removed by filtration and the resin was washed several times with dry DCM. Unreacted sites on the resin were capped by using methanol, which prevents the formation of truncated peptidic products.

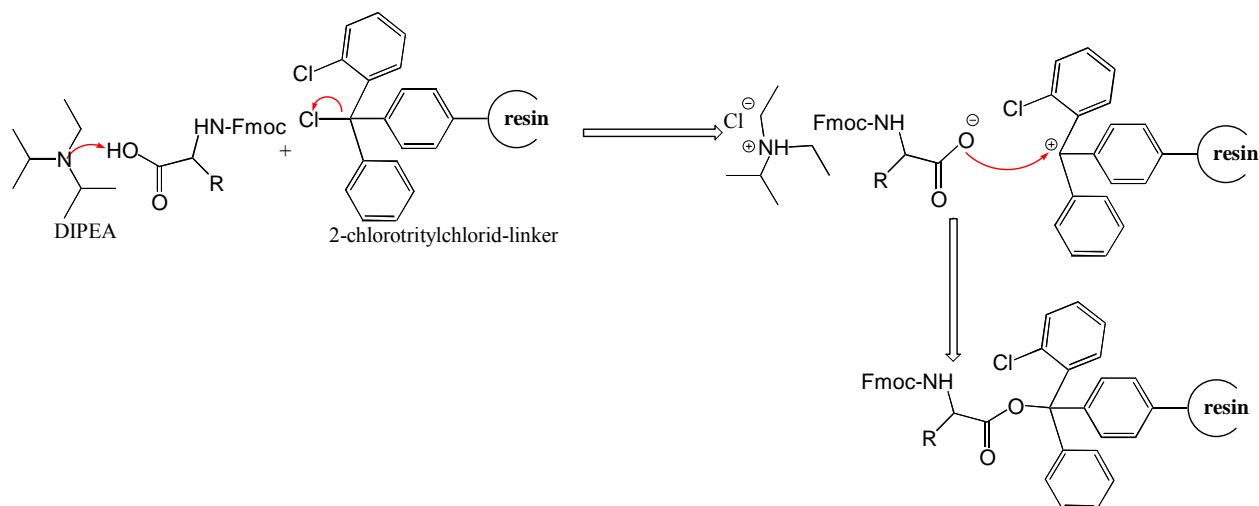


Figure 4.1: Loading of 2-chlorotritylchloride resin.

4.6.2. Elongation: Coupling of Fmoc amino acids

Elongation of the peptide chain requires deprotection of the N-terminally attached Fmoc group of the resin bound amino acid/peptide. This protecting group is removed via base-induced-elimination by treatment with 15 % piperidine in DMF for 20 min. The key step is initial deprotection of the fluorene ring to generate the aromatic cyclopentadiene-type intermediate. As a result dibenzofulvene and carbon dioxide are split off (Figure 4.2).

Chemical approaches to form peptide bonds require activation of the carboxyl-group of the Fmoc-protected amino acid. The acyluronium salt HBTU with its additive HOBT was used for the *in situ* coupling of peptide bonds as shown in Figure 4.3. After deprotonation by a ten fold excess of DIPEA, the carboxyl-group attacks the electrophilic carbenium ion of HBTU. A

highly reactive tetramethylurea intermediate is generated which is subsequently converted into the reactive benzotriazole ester in the presence of the nucleophile HOBT. The free N-terminus of the resin bound amino acid/peptide then nucleophilically attacks this intermediate giving rise to an elongated peptide chain. To ensure quantitative reactions, a 3-fold excess of Fmoc-protected amino acid is used.

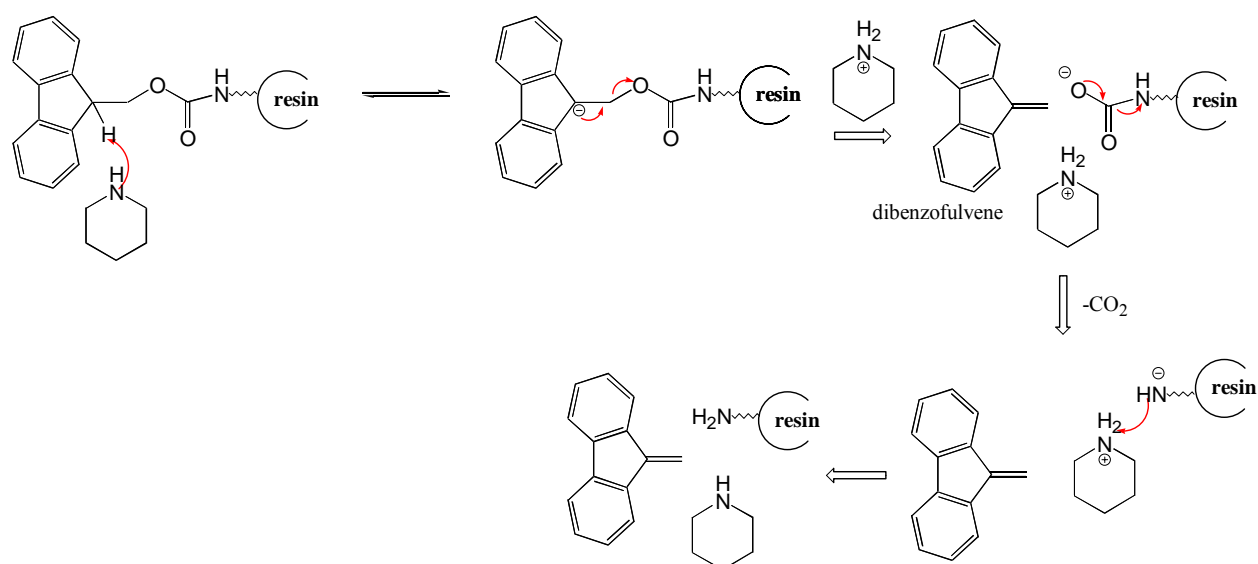


Figure 4.2: Deprotection of the N-terminally attached Fmoc group.

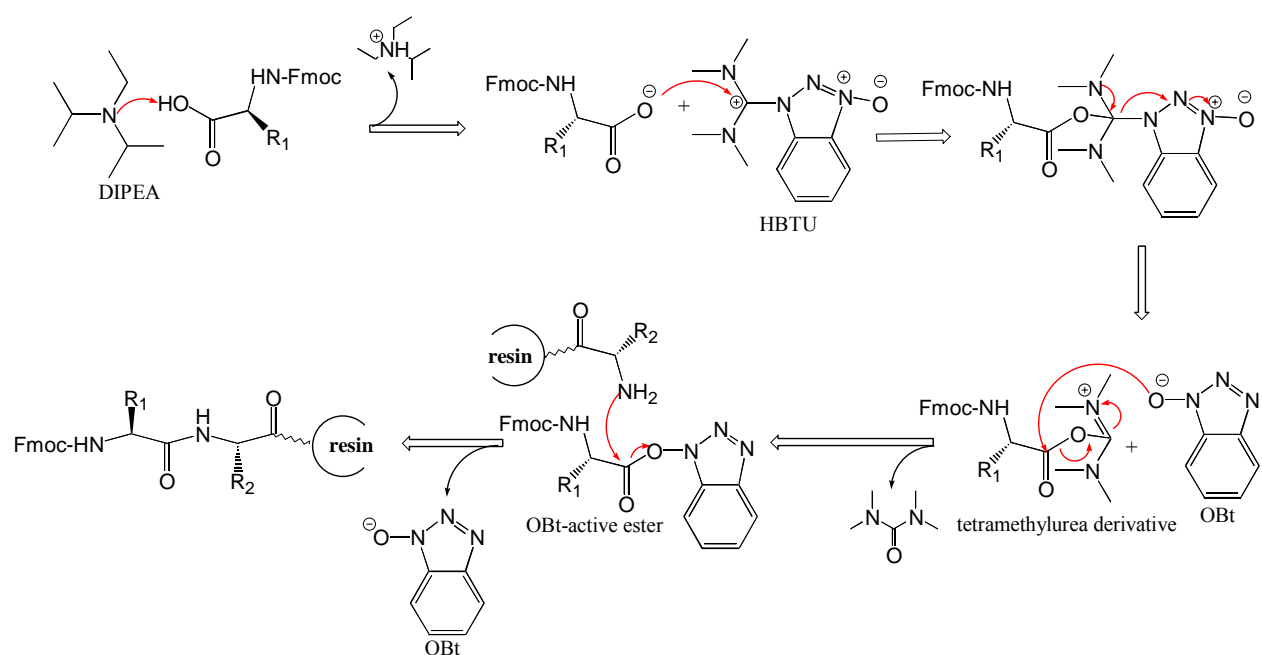


Figure 4.3: Chemical peptide bond formation.

4.6.3. Termination: Cleavage from the Resin

Protected peptide fragments can be obtained from 2-chlorotrityl resin with TFE/AcOH/DCM (2:1:7). After stirring the peptide-resin for 2 h in this cleavage mix, the reaction mixture is filtered and the resin rinsed with TFE/AcOH/DCM (2:1:7). The filtrates are pooled, the protected peptide is precipitated with hexane, and the solvent was removed by rotary evaporation.

4.7. Organic Synthesis

Linear peptides were synthesized on an Advanced ChemTech APEX 396 peptide synthesizer (0.1 mmol scale, HBTU/HOBt activation) by using 2-chlorotrityl resin derivatized with the appropriate C-terminal amino acid using Fmoc-protected monomers except for the N-terminal monomer of the linear tyrocidine derivative, which was Boc-protected. The following side chain protection groups were employed: *t*-Bu for Asp, Glu, Ser, Thr, and Tyr; Boc for Lys, Orn and Trp; Alloc for Orn; and Trt for Asn and Gln.

4.7.1. Synthesis of Peptidyl-SNAC and Peptidyl-Thiophenol Substrates

Side-chain protected peptides (1 eq.) were dissolved in DCM, followed by the addition of DCC (2 eq.), HOBt (2 eq.), thiophenol or N-acetylcysteamine (10 eq.), and potassium carbonate (2 eq.). The reaction was stirred at ambient temperature for 3 hr. After removal of the DCM, the protected peptide thioesters were treated with 95:2.5:2.5 TFA:H₂O:TIPS (2 mL) at room temperature for 2 h. Precipitation of the deprotected peptide thioesters was carried out with ice cold ether (30 mL). After centrifugation the peptide thioesters were dissolved in 50% acetonitrile/water and purified on a semipreparative 250/21 Nucleodur 100-5 C₁₈ reverse-phase column (Macherey and Nagel) by applying a gradient from 20% to 60% acetonitrile in 0.1% TFA/water over 30 min at a flow rate of 20 mL min⁻¹. The identities of

peptidyl-SNAC and peptidyl-thiophenol substrates were determined by LC-MS and MALDI-TOF MS (Tables 4.3, 4.4, and 4.5).

4.7.2. Synthesis of 4'-Phosphopantetheine (ppan)

One eq. of coenzyme A, 0.2 eq. of TCEP·HCl, and 0.5 unit/μmol nucleotide pyrophosphatase (Sigma) were dissolved in Hepes buffer (50 mM, pH 7.5). The mixture was incubated at 30 °C for 18 h and then lyophilized to dryness. The product was verified by LC-MS [113].

4.7.3. Synthesis of Peptidyl-CoA and Peptidyl-ppan Substrates

The preparation of peptidyl-ppan is based on the synthesis of peptidyl-CoA substrates described elsewhere [43]. To 1 eq. of protected peptide was added 1.5 eq. of ppan/CoA, 1.5 eq. of PyBOP, and 4 eq. of potassium carbonate, dissolved in a 1:1 THF/water mixture. The mixture was stirred for 2 h at room temperature which was followed by the removal of the solvent. Subsequent cleavage of the side-chain protecting groups was carried out using a mixture containing TFA, TIPS, and H₂O in a ratio of 95:2.5:2.5. The deprotected peptidyl-ppan/peptidyl-CoA substrate was precipitated in ice-cold diethyl ether and purified by preparative high-performance liquid chromatography (HPLC) on an Äkta purifier (Pharmacia) HPLC system with a reverse-phase C18 Nucleodur (Macherey and Nagel) column. Identification of the peptidyl-CoA and peptidyl-ppan substrates was verified by LC-MS (Table 4.4).

4.7.4. Synthesis of N-(9-Fluorenylmethoxycarbonyl)-L-kynurenine

Kynurenine sulfate (306 mg, 1 mmol) and sodium bicarbonate (252 mg, 3 mmol) were dissolved in a mixture of acetone (2.5 mL) and water (2.5 mL). After addition of Fmoc-OSu

(Novabiochem) (337.3 mg, 1 mmol), the solution was stirred overnight. The mixture was acidified to pH 2 with concentrated hydrochloric acid, and the acetone was removed by rotary evaporation. The product was extracted with chloroform and washed with 0.1 N HCl and water. After drying over anhydrous sodium sulfate, the combined organic phases were evaporated and the product was confirmed by ESI-MS and NMR: Fmoc-L-Kyn m/z 431.1 $[M + H]^+$ (431.2 calc.); δ_H (300 MHz, CD_3OD) 3.46 [dd, 1 H, J 4.6 and 17.6, $CH\beta_a$], 3.59 [dd, 1 H, J 6.5 and 17.4, $CH\beta_b$], 4.22 [t, 1 H, J 7.0, Fmoc-CH], 4.34 [d, 2 H, J 7.3, Fmoc- CH_2], 4.71 [dd, 1 H, J 4.6 and 6.3, $CH\alpha$], 6.60 [t, 1 H, J 7.5, Ph], 6.75 [d, 1 H, J 8.6, Ph], 7.27 [m, 3 H, Ph], 7.36 [m, 2 H, Ph], 7.64 [d, 2 H, J 7.3, Ph], 7.76 [m, 3 H, Ph].

4.7.5. Synthesis of Biotin CoA

A solution of biotin maleimide (Pierce) (10 mg, 19 μ mol) in 300 μ L DMSO was added to coenzyme A lithium salt (Sigma) (18.2 mg, 23 μ mol) in 2 mL MES acetate 50 mM at pH 6.0. After stirring overnight, the reaction mixture was purified on a semipreparative 250/21 Nucleodur 100-5 C_{18} reverse-phase column (Macherey and Nagel) by applying a gradient from 0% to 60% acetonitrile in 0.1% TFA/water over 35 min at a flow rate of 18 mL min^{-1} . The purified product was characterized by MALDI-MS: Biotin CoA m/z 1293.2 ($[M+H]^+$), calcd. 1293.3.

5. Results

5.1. Peptide Cyclization Catalyzed by the Recombinant Thioesterase Domain of the Calcium-Dependent Antibiotic

A key determinant of many nonribosomally synthesized microbial peptides is a rigid cyclic structure which ensures stabilization of the bioactive conformation. The generation of this structural feature is mostly catalyzed by the C-terminal TE domain of NRPS synthetases.

The following section will focus on the TE domain of the calcium-dependent antibiotic (CDA). This cyclase was excised as a free standing enzyme and the NRPS machinery for peptide elongation was replaced by solid phase peptide chemistry. Therefore, this chemoenzymatic approach allows the investigation of the principles of enzymatic peptide cyclization on the example of this lactone forming cyclase. In the course of these studies enzymatic recognition elements of CDA TE were investigated by systematic alteration of the fatty acyl group and the decapeptide backbone. In particular, these studies focused on elucidating the regio-, stereo-, and chemoselectivity of the CDA cyclase mediated macrolactonization. The last part of this section concentrates on the ability of this cyclase in producing derivatives of the approved antibiotic daptomycin, which are not accessible by the chemical modification of the parental compound. This makes possible the exploration of the calcium-dependence of this acidic lipopeptide by subsequent deletion of its four acidic residues, which are likely to be important for the interaction with calcium ions.

5.1.1. Overexpression of CDA TE as a Thioredoxin-Fusion Protein

CDA TE is a recombinant cyclase of the model actinomycete *S. coelicolor* A3(2). The corresponding *cda TE* gene fragment was cloned into a pBAD202/D-TOPO vector (Invitrogen) using a one-step cloning strategy without ligase and restriction enzymes. This expression system appends an N-terminal His-patch Thioredoxin domain (11.7 kDa) to the

recombinant cyclase, which facilitates solubility and translation efficiency of the expressed protein (49.4 kDa) [114] (Figure 5.1).

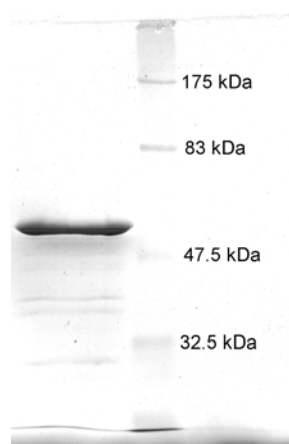


Figure 5.1: Purified recombinant CDA cyclase examined in this study. CDA cyclase (49.4 kDa) was overproduced in *E. coli* BL21 and purified by Ni-NTA affinity chromatography. The concentrated protein was resolved by SDS-PAGE (12.5%) and visualized by Coomassie stain.

5.1.2. CDA Cyclase Catalyzes Ring Formation of a Synthetic CDA Analogue

In order to examine the ability of CDA cyclase to catalyze macrolactonization, a peptidyl-thioester analogue of the natural CDA substrate was synthesized. So far seven CDA variants have been isolated, which differ in their incorporation of nonproteinogenic amino acids [17]. For synthetic reasons these nonproteinogenic amino acids were substituted by similar proteinogenic amino acids. D-4-Hydroxyphenylglycine/D-phenylglycine at position 6 was substituted by D-phenylalanine, and D-3-phosphohydroxyasparagine/D-3-hydroxyasparagine at position 9 was replaced by D-asparagine (Figure 5.2). At positions 10 and 11 the proteinogenic amino acids L-glutamate and L-tryptophan were incorporated

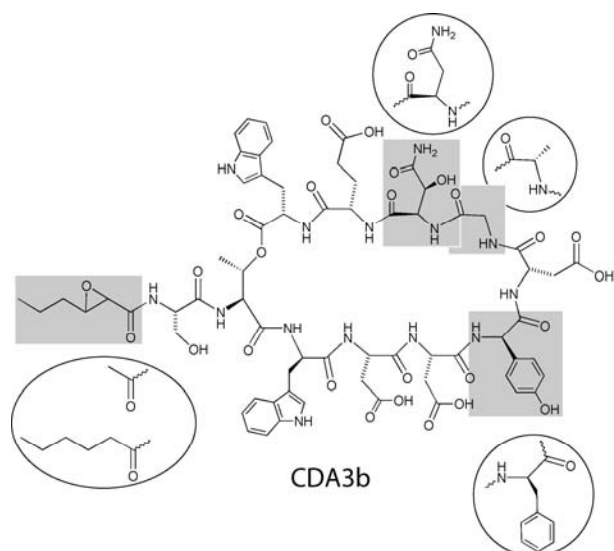


Figure 5.2: Comparison between peptide analogues used in this work and wild-type CDA3b. Regions highlighted by shading represent the molecular parts of CDA3b, which were replaced in the CDA analogues **CDA** and **Hex-CDA**. The deviating parts of these analogues are indicated by circles.

into the peptide backbone as in the case of the CDA variants CDA1b and CDA3b. The N-terminus of the synthetic CDA analogue was acetylated instead of attaching the 2,3-epoxyhexanoyl fatty acid of the natural occurring CDA. Hence the sequence of the synthesized **CDA** (see also appendix) was chosen as follows: acetyl-Ser₁-Thr₂-DTrp₃-Asp₄-Asp₅-DPh₆-Asp₇-Ala₈-DAsn₉-Glu₁₀-Trp₁₁ (Figure 5.3). The C-terminus of **CDA** was attached to the SNAC leaving group (Figure 5.4), which mimics the last part of the ppan arm of the natural cofactor. Assaying for CDA TE mediated cyclization revealed that the peptidyl-SNAC is cyclized. Remarkably, two products with the expected mass for cyclization were observed (Figure 5.5). Taking into account that **CDA** possesses two adjacent nucleophiles, L-Ser₁ and L-Thr₂, it was assumed that both nucleophiles are involved in ring formation. To ensure that no other nucleophiles except L-Ser₁ and L-Thr₂ contribute to cyclization, a thioester substrate **CDA-A1A2** (Figure 5.3) was synthesized, where both nucleophiles of **CDA** are replaced by alanine. As expected, upon incubation with CDA cyclase no cyclization product was detected. Instead, the substrate was fully hydrolyzed (data not shown).

The identities of both cyclic products were confirmed by MS-MS sequencing (Table 5.1). For the peak with the lower retention time ($t_R = 28.0$ min) four fragments were detected, which did not appear in the MS-MS-spectrum of the peak with $t_R = 28.6$ min. These fragments were characteristic for an undecapeptide lactone, where Ser₁ contributes as internal nucleophile. In these cases simultaneous fragmentation occurred between Ser₁ and Thr₂ as well as between Glu₁₀ and Trp₁₁, leading to fragments, where the former lactone bond was still maintained. If cyclization would occur via Thr₂, no such fragments would have been obtained with the apparent masses of Ser₁ cyclization. Therefore, the peak with $t_R = 28.6$ min can be assigned to the lactone cyclizing via Thr₂, because this is the only remaining nucleophile in the CDA analogue as evidenced with **CDA-A1A2**. The ratio between these two regioisomeric macrolactones was determined as 1:4 (undecapeptide lactone:decapeptide lactone), indicating

5 Results

that the natural Thr₂-nucleophile of CDA is still preferred. The flux toward hydrolysis was very low, revealing a cyclization-to-hydrolysis ratio of 9:1.

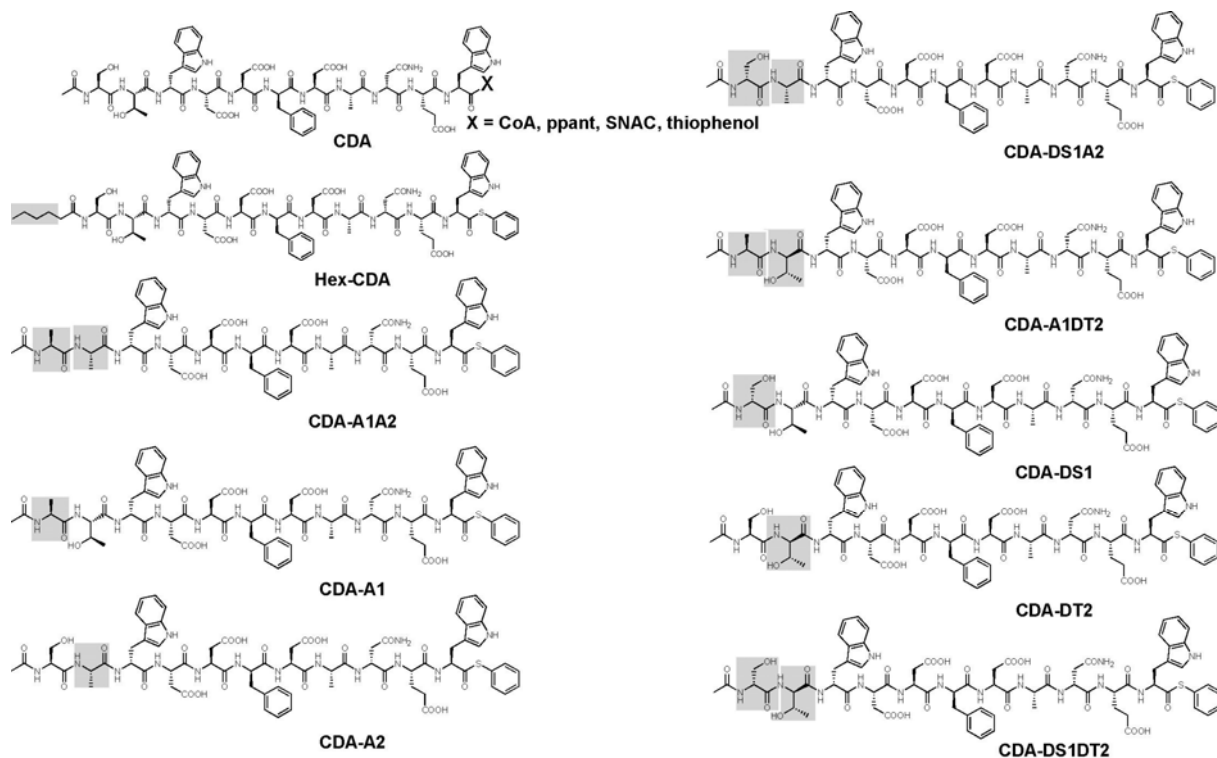


Figure 5.3: Peptides synthesized for study of the regio-, stereo-, and chemoselectivity of the CDA cyclase mediated macrolactonization. Regions highlighted by shading represent differences in substrates with respect to **CDA**. Compound **Hex-CDA** is a linear CDA thioester analogue, where the C-terminal acyl chain is elongated to its natural length. Compounds **CDA-A1A2**, **CDA-A1**, and **CDA-A2** are characterized by the replacement of the nucleophilic residues Ser1 and/or Thr2 with L-alanine. Compounds **CDA-DS1A2** and **CDA-A1DT2** each contain only one internal nucleophile, Ser1 or Thr2, with a stereochemistry opposite of the natural configuration. Compounds **CDA-DS1**, **CDA-DT2**, and **CDA-DS1DT2** possess both internal nucleophiles, Ser1 and Thr2, where either one or both are changed in their configuration. CoA = coenzyme A, ppant = phosphopantetheine, and SNAC = *N*-acetylcysteamine.

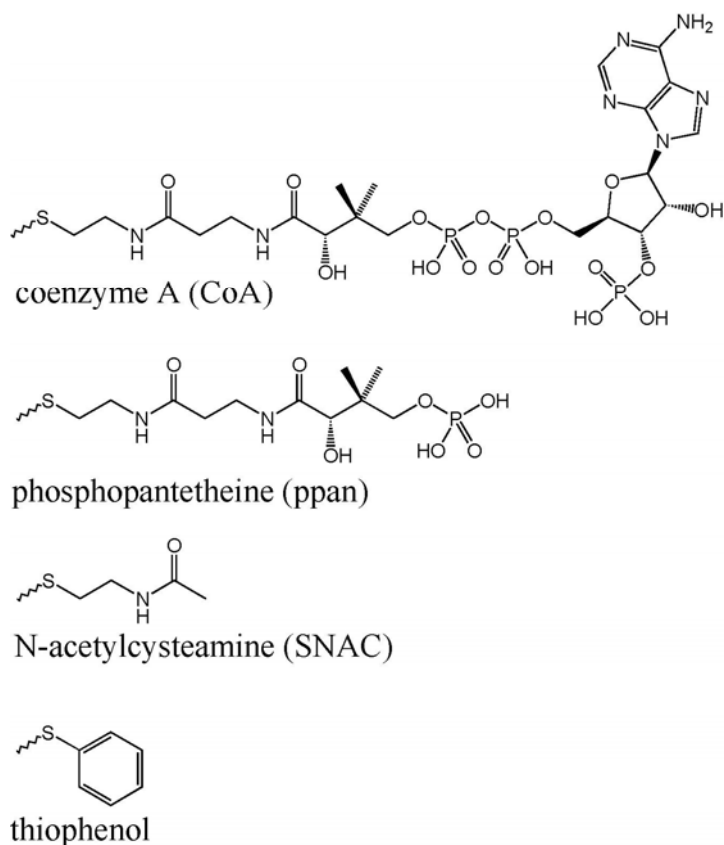


Figure 5.4: Structures of the leaving groups appended to the C-terminus of **CDA** are shown. Coenzyme A (CoA), phosphopantetheine (ppan), and *N*-acetylcysteamine (SNAC) are mimics of the phosphopantetheine cofactor covalently bound to a conserved Ser residue of the peptidyl-carrier protein (PCP). In contrast to that, thiophenol has no structural similarity to this prosthetic group.

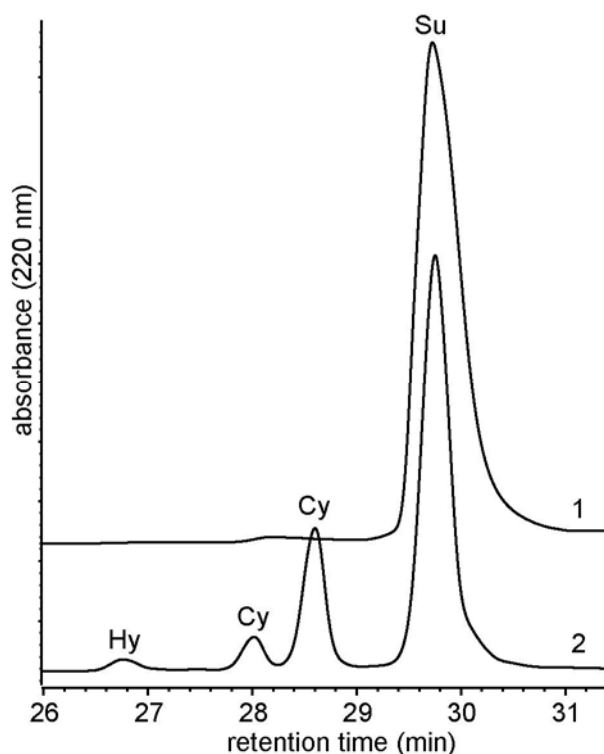
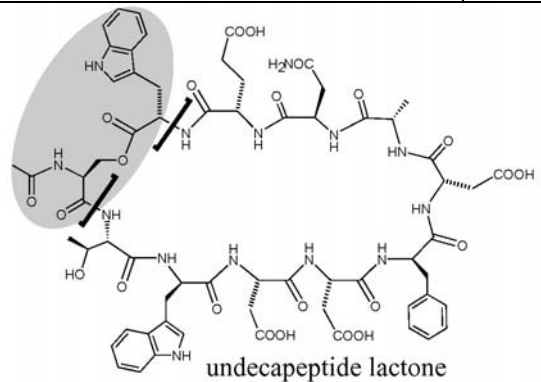


Figure 5.5: Exploring the role of the leaving group for CDA cyclase catalyzed ring formation. CDA cyclase incubated with **CDA-SNAC** for 3 h at 20 °C (trace 2). Trace 1 shows substrate incubation in the absence of enzyme. Su = substrate, Hy = hydrolyzed product, and Cy = cyclized product.

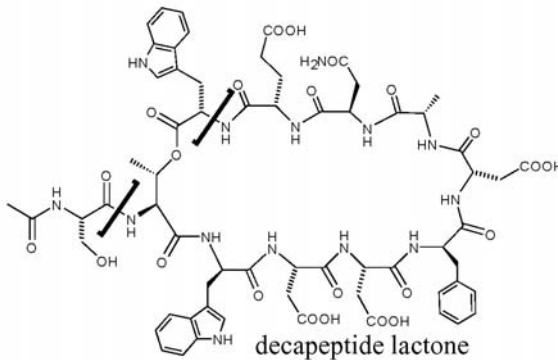
Table 5.1: MS-MS-Sequencing of Macrolactones Derived from CDA Analogues **CDA** and **Hex-CDA**.

The molecular part highlighted by shading represents a fragment (301.119 Da) characteristic for the undeca-peptide lactone, where Ser₁ contributed as internal nucleophile. If cyclization would occur via Thr₂, no such fragment would have been obtained, because simultaneous fragmentation of the same two bonds would only result in an opening of the corresponding lactone ring. Fragmentation of C-C-bonds in the fatty acyl chain of **Hex-CDA** is not possible under experimental conditions.

Compound	Mol. formula	Species	Observed mass of fragments (calculated mass) (Da)
			cyclization via Ser 1
undeca-peptide lactone	$C_{15}H_{18}N_3O_3^+$	$[M+H]^+$	288.118 (288.135)
	$C_{16}H_{17}N_2O_4^+$		301.126 (301.119)
	$C_{17}H_{19}N_4O_5^+$		359.138 (359.136)
	$C_{17}H_{21}N_4O_5^+$		361.172 (361.151)
			cyclization via Ser 1
deca-peptide lactone	$C_{15}H_{18}N_3O_3^+$	$[M+H]^+$	n. d. (288.135)
	$C_{16}H_{17}N_2O_4^+$		n. d. (301.119)
	$C_{17}H_{19}N_4O_5^+$		n. d. (359.136)
	$C_{17}H_{21}N_4O_5^+$		n. d. (361.151)
			cyclization via Ser 1
deca-peptide lactone with hexanoic acid	$C_{15}H_{18}N_3O_3^+$	$[M+H]^+$	n. d. (344.197)
	$C_{16}H_{17}N_2O_4^+$		n. d. (357.181)
	$C_{17}H_{19}N_4O_5^+$		n. d. (415.198)
	$C_{17}H_{21}N_4O_5^+$		n. d. (417.214)



undeca-peptide lactone



deca-peptide lactone

n. d. = not detected

5.1.3. Selecting the Best Leaving Group for Macrolactonization Mediated by the CDA Cyclase

In order to determine which leaving group is best suited to support CDA TE catalyzed macrolactonization, four different leaving groups were attached to the C-terminus of **CDA** (Figure 5.4). Besides the SNAC leaving group, which was successfully employed for *in vitro* cyclization of tyrocidine A, gramicidin S, and surfactin [63, 66, 68], the following three other leaving groups were tested for their ability to support ring formation of **CDA**: Coenzyme A (CoA), phosphopantetheine (ppan), and thiophenol. Ppan is structurally identical to the prosthetic group of the peptidyl-carrier protein, which is derived from coenzyme A. In contrast, the thiophenol leaving group possesses no structural analogy to the phosphopantetheine arm of the PCP. Nevertheless peptidyl-thiophenol thioesters allowed biochemical characterization of fengycin, mycosubtilin, and syringomycin, which did not show any activity with SNAC substrates [73].

Examination of CDA cyclase catalyzed product formation with **CDA-CoA** (Figure 5.6), **CDA-ppan**, and **CDA-thiophenol** revealed that the observed products were identical to that observed for **CDA-SNAC**. To determine the best leaving group for CDA TE mediated cyclization of **CDA**, the kinetics of cyclization for all four peptidyl-thioesters were measured. The cyclization reaction follows Michaelis-Menten kinetics with the K_M and k_{cat} values reported in Table 5.2. Although **CDA-ppan** is structurally identical to the ppan arm of the PCP, its K_M value is at least 10-fold higher than those measured for **CDA-thiophenol** or **CDA-SNAC**. It was also discovered that the k_{cat} value for cyclization of the **CDA-thiophenol** substrate [$k_{cat}(\text{undecapeptide lactone}) = 0.097 \text{ min}^{-1}$; $k_{cat}(\text{decapeptide lactone}) = 0.323 \text{ min}^{-1}$] was approximately 3-fold higher than observed for the other three CDA thioesters. Its catalytic efficiency for cyclization [$k_{cat}/K_M(\text{undecapeptide lactone}) = 2.44 \text{ mM}^{-1}\text{min}^{-1}$; $k_{cat}/K_M(\text{decapeptide lactone}) = 8.13 \text{ mM}^{-1}\text{min}^{-1}$] was approximately 10-16-fold the value of the SNAC substrate [$k_{cat}/K_M(\text{undecapeptide lactone}) = 0.156 \text{ mM}^{-1}\text{min}^{-1}$; $k_{cat}/K_M(\text{decapeptide$

lactone) = 0.799 mM⁻¹min⁻¹]. Surprisingly, the $k_{\text{cat}}/K_{\text{M}}$ value for CDA TE mediated cyclization was the second lowest for **CDA-ppan** [$k_{\text{cat}}/K_{\text{M}}$ (undecapeptide lactone) = 0.023 mM⁻¹ min⁻¹; $k_{\text{cat}}/K_{\text{M}}$ (decapeptide lactone) = 0.115 mM⁻¹ min⁻¹]. This result clearly indicates that the structural identity to the ppan arm of the PCP is not important for recognition by the dissected enzyme.

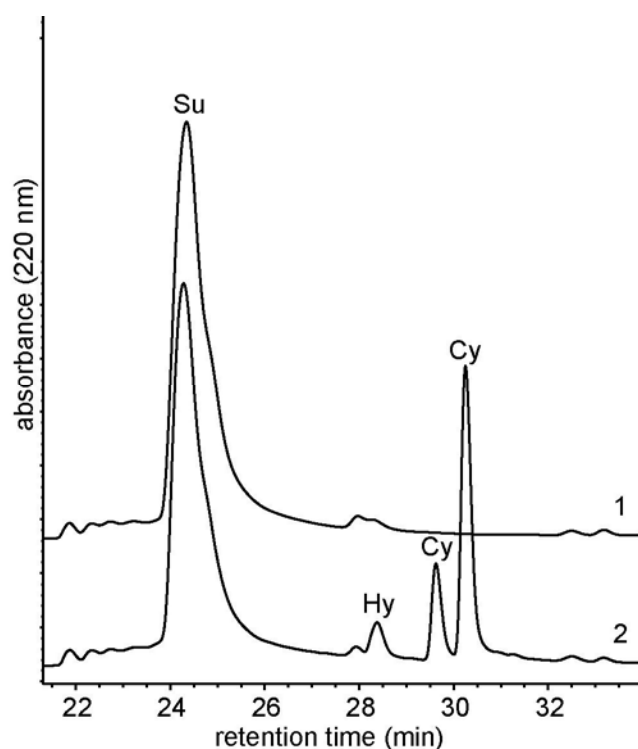


Figure 5.6: HPLC trace of CDA cyclase incubated with **CDA-CoA** for 5h at 20°C (trace 2). Trace 1 shows incubation of substrate without enzyme. Su = substrate, Hy = hydrolyzed product, and Cy = cyclized product.

Table 5.2: Kinetic constants of **CDA** (four different leaving groups attached to the C-terminus) and **Hex-CDA** are shown.

Substrate	K_{M} (μM)	k_{cat} (min ⁻¹)		$k_{\text{cat}}/K_{\text{M}}$ (min ⁻¹ mM ⁻¹)	
		undecapeptide lactone	decapeptide lactone	undecapeptide lactone	decapeptide lactone
CDA-CoA	8150	0.030	0.178	0.004	0.022
CDA-ppan	1440	0.023	0.115	0.016	0.080
CDA-SNAC	147	0.023	0.117	0.156	0.799
CDA-thiophenol	40	0.097	0.323	2.44	8.13
Hex-CDA	65	n. d.	1.92	n. d.	29.8

n. d. = not detected

The cyclization-to-hydrolysis ratios for **CDA-SNAC** and **CDA-CoA** in the presence of CDA TE were determined to be 9:1 and 8:1, respectively (Table 4.3, right column). Those values confirm the extraordinarily high chemoselectivity of this cyclase, which catalyzes almost exclusively macrolactonization of **CDA**. The lower cyclization-to-hydrolysis ratio of 5:1 for **CDA-thiophenol** indicates the higher background hydrolysis of this substrate due to the high chemical reactivity of the attached thiophenol leaving group. Surprisingly, the cyclization-to-hydrolysis ratio of **CDA-ppan** was even lower than for **CDA-thiophenol**.

5.1.4. Regioselectivity of CDA Cyclase

The results with the thioester substrates of **CDA** showed that the recombinant CDA cyclase catalyzes the simultaneous formation of two regioisomeric cyclic products. To determine whether this cyclase can be employed for the regioselective formation of peptidolactones with defined ring sizes, two additional thiophenol substrates, **CDA-A1** and **CDA-A2**, were synthesized (Figure 5.3). Compound **CDA-A1** lacks Ser₁ as a cyclization nucleophile, whereas **CDA-A2** lacks Thr₂, which was described to be the only cyclization nucleophile in naturally occurring CDA [115]. Probing CDA cyclase with these two CDA analogues revealed the formation of only one cyclization product in each case (Figure 5.7). Reaction profiles showed that **CDA-A2** was primarily converted into the peptide acid with a cyclization-to-hydrolysis ratio of 1:3 (Table 4.4). Conversely, **CDA-A1** led primarily to the formation of the peptidolactone, yielding a cyclization-to-hydrolysis ratio of 3:1, which indicates that Thr₂ is the preferred nucleophile for cyclization.

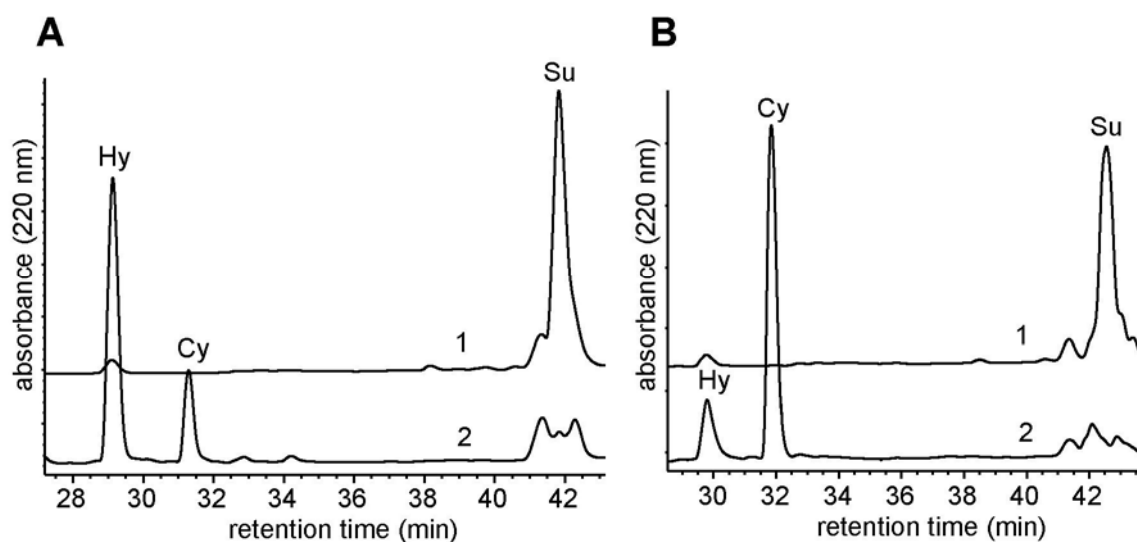


Figure 5.7: Regioselective formation of decapeptide lactone or undecapeptide lactone catalyzed by CDA cyclase. HPLC traces of CDA cyclase incubated with peptidyl-thiophenol substrates. (A) CDA cyclase incubated with **CDA-A2** for 3 h at 20 °C (trace 2). Trace 1 shows incubation of substrate in the absence of enzyme. (B) CDA cyclase incubated with **CDA-A1** for 3 h at 20 °C (trace 2). Trace 1 shows substrate incubation without enzyme. No uncatalyzed cyclization is observed. Su = substrate, Hy = hydrolyzed product, and Cy = cyclized product.

5.1.5. Stereoselectivity of CDA Cyclase

It was previously reported that syringomycin cyclase does not tolerate a change in stereochemistry of the cyclization nucleophile Ser₁ [73]. To test if CDA cyclase retains its stereoselectivity as well, two thiophenol CDA derivatives were synthesized: **CDA-DS1A2** and **CDA-A1DT2** (Figure 5.3). These peptidyl thioesters allow the selective examination of the stereochemistry of only one nucleophilic amino acid due to the replacement of the second one by alanine. Incubation of these CDA derivatives with CDA cyclase resulted only in the formation of hydrolysis product, indicating the importance of L-configured serine and threonine in positions 1 and 2 for the enzyme-mediated macrolactonization (data not shown). Additionally, the substrates **CDA-DS1** and **CDA-DT2** (Figure 5.3) were prepared, in which either serine or threonine is replaced by its corresponding D-isomer. It was found that **CDA-DS1** and **CDA-DT2** generated only one cyclization peak on the HPLC trace in the presence of CDA cyclase (Figure 5.8). Remarkably, cyclization was observed to be the main product

for **CDA-DS1** (cyclization-to-hydrolysis ratio = 2:1), while, on the other hand, **CDA-DT2** was converted primarily into the peptide acid (cyclization-to-hydrolysis ratio = 1:5) (Table 4.4). These results show that cyclization selectively occurs via the L-configured amino acids serine and threonine, while the latter is the preferred cyclization nucleophile of the CDA cyclase. The role of CDA cyclase as a stereoselective macrolactonization catalyst could be further emphasized by the thiophenol substrate **CDA-DS1DT2** (Figure 5.3), which possesses only D-configured nucleophiles. Incubation of this substrate with CDA cyclase revealed only hydrolysis (data not shown), thereby emphasizing the need for a correct stereochemistry for the enzyme-mediated cyclization at positions 1 and 2, respectively.

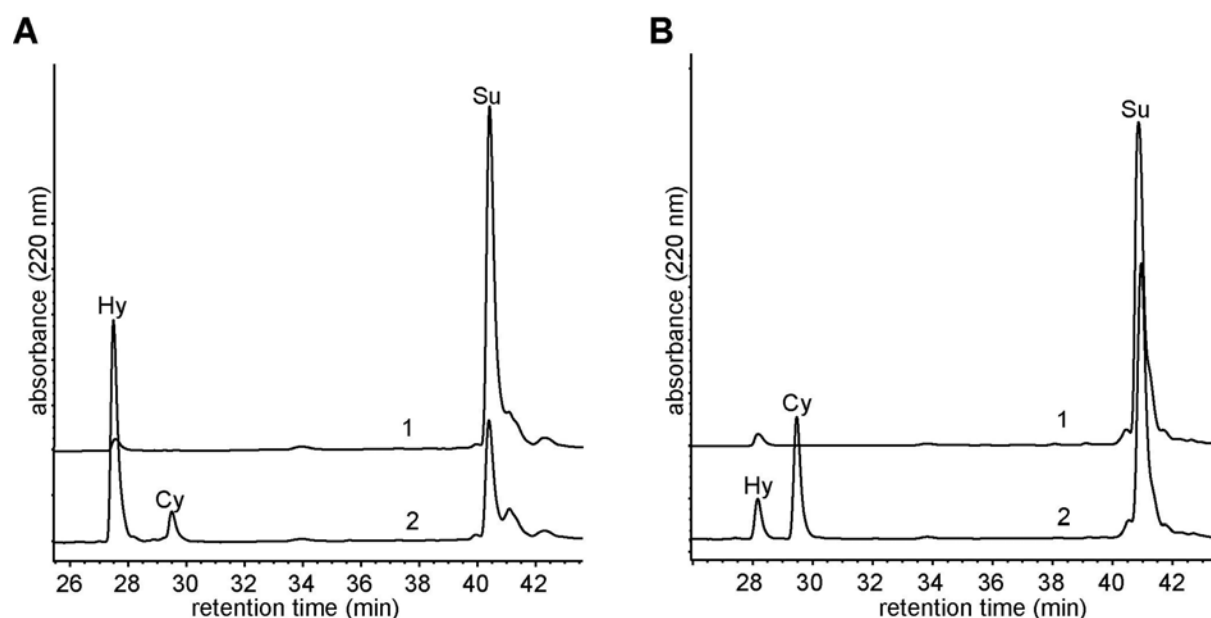


Figure 5.8: Probing the stereoselectivity of CDA cyclase mediated macrolactonization. HPLC traces of CDA cyclase incubated with peptidyl-thiophenol substrates, where either Ser1 or Thr2 is replaced by its D-configured isomer. (A) Incubation of CDA cyclase with **CDA-DT2** for 3 h at 20 °C (trace 2). Trace 1 shows incubation of substrate without enzyme. (B) CDA cyclase incubated with **CDA-DS1** for 3 h at 20 °C (trace 2). Trace 1 shows substrate incubation in the absence of enzyme. Su = substrate, Hy = hydrolyzed product, and Cy = cyclized product.

5.1.6. Extending the N-Terminal Acyl Chain of the CDA Thioester Substrate

The observation that CDA cyclase catalyzes the generation of two regioisomeric macrolactones on incubation with **CDA** (Figures 5.5 and 5.6) contradicts the findings of

Kempton et al., who characterized naturally occurring CDA to be cyclized over Thr₂ [115]. Therefore, it was tried to better approximate the natural interaction between the linear peptide precursor and the CDA cyclase. **Hex-CDA** as a new CDA analogue (Figure 5.3) was synthesized, which was structurally closer to its natural counterpart. The N-terminal acetyl residue of **CDA** was replaced by a hexanoyl fatty acid. The 2,3-epoxy group of natural CDA was omitted for synthetic reasons. Surprisingly, the reaction profile of **Hex-CDA** revealed that this compound was efficiently transformed into only one macrocycle (Figure 5.9). MS-

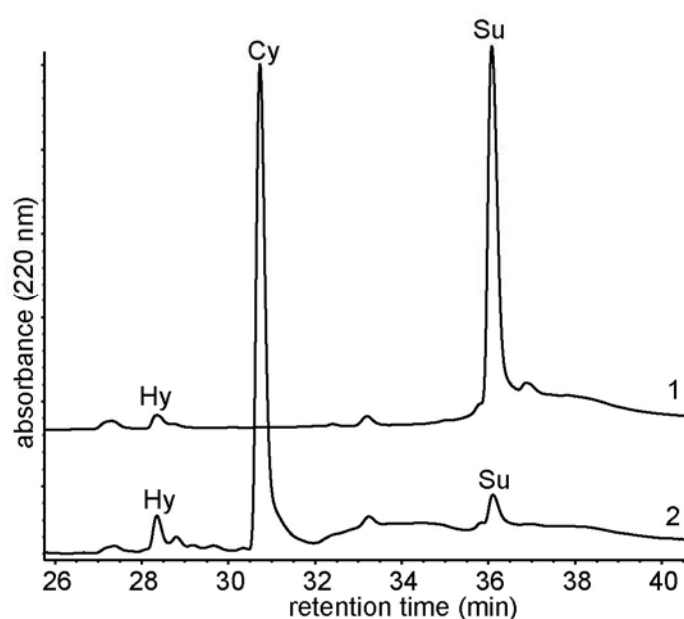


Figure 5.9: The N-terminal hexanoyl fatty acid residue ensures regioselective cyclization of the CDA thioester analogue. HPLC trace of CDA cyclase incubated with **Hex-CDA** for 3 h at 20°C (trace 2). Trace 1 shows incubation of substrate in the absence of CDA TE.

MS sequencing revealed that solely the decapeptide lactone was formed (Table 5.1), because none of the four fragments characteristic for the macrolactone cyclizing via Ser₁ were detected. This result indicates that the N-terminal hexanoyl fatty acid appears to be important for regioselective cyclization of **Hex-CDA**. The kinetic parameters for the CDA TE catalyzed cyclization were determined as $K_M = 65 \mu\text{M}$ and $k_{\text{cat}} = 1.92 \text{ min}^{-1}$ (Table 5.2). In fact, the cyclization-to-hydrolysis ratio of 10:1 (Table 4.3, right column) was significantly higher than for the corresponding **CDA-thiophenol** with the N-terminal acetyl residue (cyclization-to-hydrolysis ratio of 5:1). This result provides evidence for the substantial contribution of the

hexanoyl fatty acid in shifting the chemoselectivity of the CDA-catalyzed reaction toward cyclization.

5.2. Exploring the Substrate Tolerance of CDA Cyclase to Produce Daptomycin

5.2.1. Single Amino Acid Substitutions

To explore the ability of CDA TE to catalyze cyclization of a linear daptomycin precursor peptide in principle, four peptidyl-thioester substrates were synthesized that differ from a CDA sequence analogue by only one single amino acid substitution. Specifically, daptomycin-specific residues were incorporated into the peptide backbone of the CDA lactone ring. Therefore, the following changes were made: D-Trp₃ to Gly₃ (**AcCDAG3**), L-Asp₄ to L-Orn₄ (**AcCDA-O4**), D-Phe₆ to D-Ala₆ (**AcCDADA6**), and D-Asn₉ to D-Ser₉ (**AcCDA-DS9**) (Figure 5.10, see also appendix). Additionally, the 2,3-epoxyhexanoyl fatty acid moiety of native CDA was replaced with a shorter acetyl chain for synthetic reason.

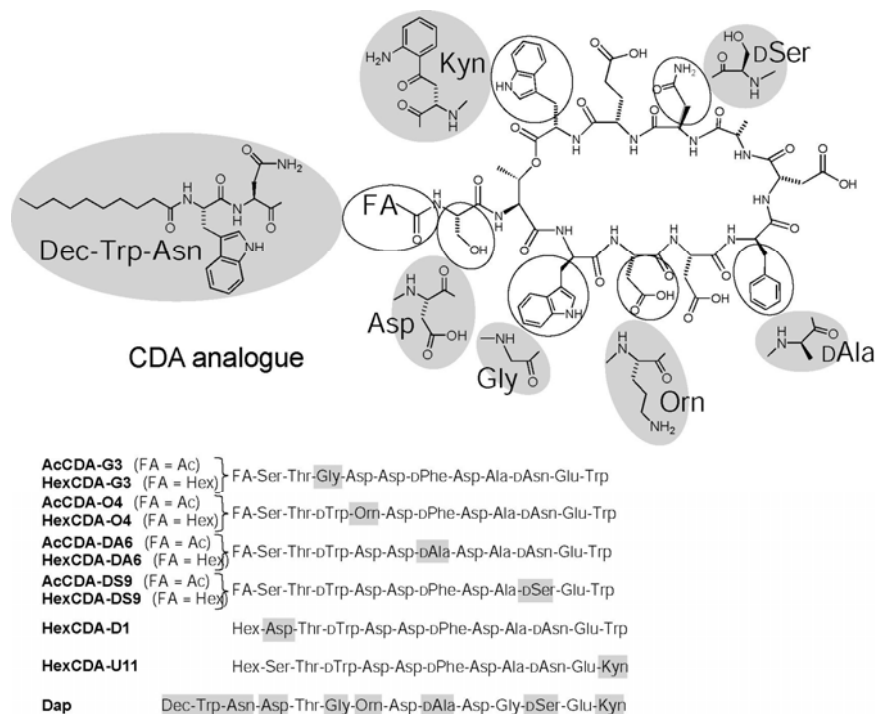


Figure 5.10: Structure of a CDA analogue is shown. Single amino acid substitution experiments were carried out to probe the ability of CDA TE to generate branched cyclic daptomycin. The incorporation of daptomycin-specific residues into the peptide backbone is indicated by shading. In **Dap** all substitutions were performed simultaneously and the N-terminus was extended by two additional amino acids fused to a decanoyl fatty acid moiety.

Assaying for CDA TE mediated cyclization revealed that three of four substrates were completely converted to macrocycles after 3 h. The only exception was **AcCDA-G3**, where only traces of cyclized product were detected within this period of time (data not shown). In all cases, the CDA cyclase catalyzed the formation of two regioisomeric macrolactones, which arise from simultaneous nucleophilic attack of the two adjacent Thr₂ and Ser₁ residues onto the C-terminus of the acyl enzyme intermediate as described earlier [113]. In order to better approximate natural CDA, the N-terminal acetyl chains of **AcCDA-G3**, **AcCDA-O4**, **AcCDADA6**, and **AcCDA-DS9** were elongated by four methylene groups through replacement by hexanoic side chains (**HexCDA-G3**, **HexCDAO4**, **HexCDA-DA6**, and **HexCDA-DS9**) (Figure 5.10, see also appendix). The poor water solubility of the peptidyl-thioester substrates was improved by the addition of 5% DMSO (v/v). In accordance with previous results, the elongated acyl side chain dramatically increased the regioselectivity of the enzyme mediated macrocyclization yielding exclusively the decapeptide lactone ring derived from nucleophilic attack of L-threonine onto the C-terminus [113] (Figure 5.11). Remarkably, the conversion to cyclic product was substantial for all substrates. This includes also **HexCDA-G3**, which is significantly converted to the macrocyclic product. In addition, the two peptidyl-thioester substrates **HexCDA-U11** and **HexCDA-D1** were prepared in which the C-terminal nonproteinogenic amino acid L-Kyn (U) and the exocyclic residue L-Asp of daptomycin were introduced to the CDA backbone (Figure 5.10). Incubation of CDA TE with the corresponding peptidyl-thiophenol substrates displays substantial formation of the corresponding peptidolactones (Figure 5.11). In conclusion, all single residue exchanges of the CDA backbone were tolerated by CDA cyclase, when hexanoic acid was fused to the N-terminus.

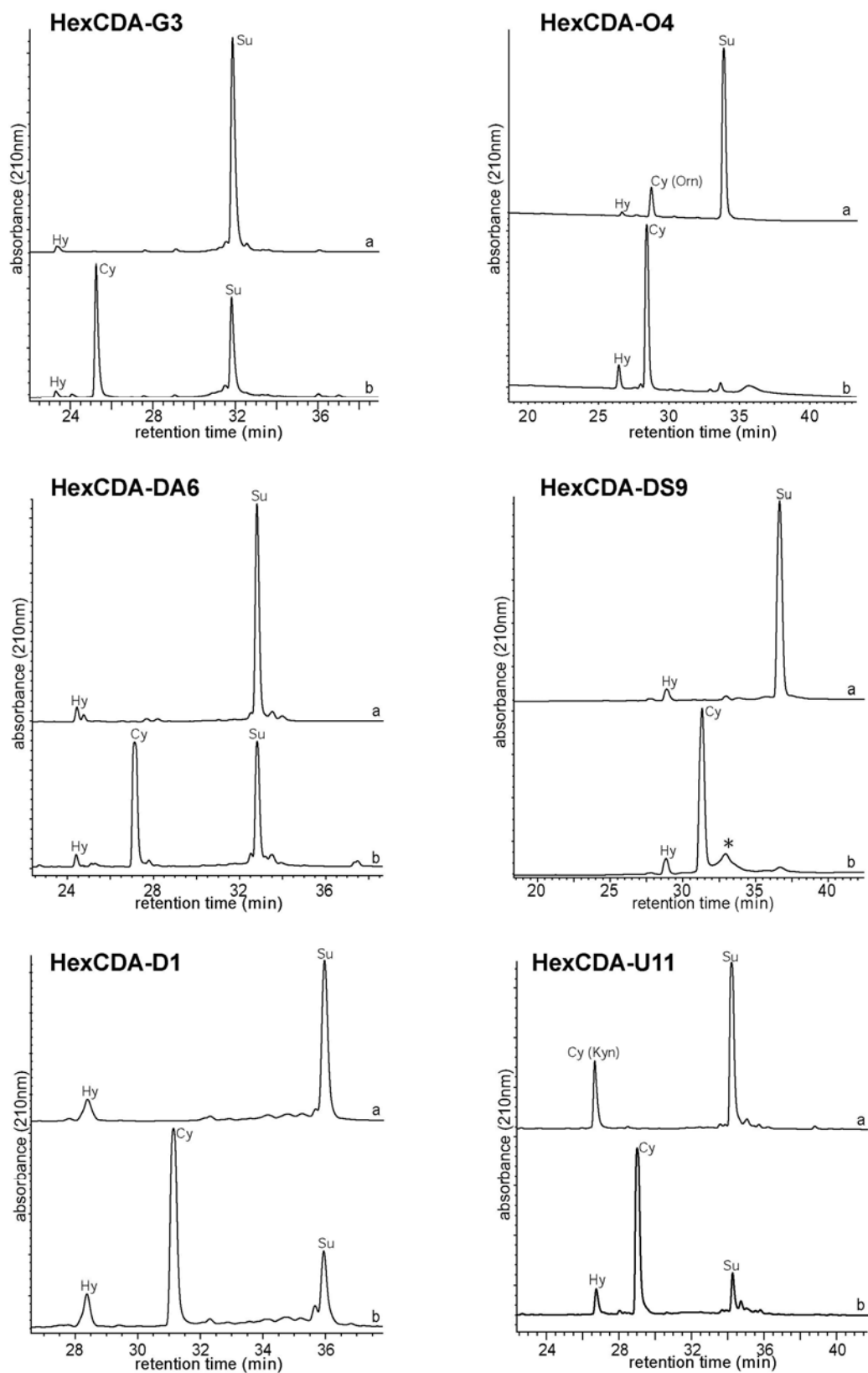


Figure 5.11: HPLC traces of CDA cyclase incubated with linear peptide thioesters comprising daptomycin-specific residues. Assays were performed with 250 μ M substrate, 25 mM HEPES, 50 mM NaCl, pH 7.0 at 25°C for 2 h in the absence (trace a) and presence of 5 μ M CDA cyclase (trace b). Identities of substrates and products were verified by ESI-MS and MALDI-TOF MS (Table 4.5). Su = substrate, Hy = hydrolyzed product, Cy = cyclized product. Enzyme is indicated with an asterisk.

5.2.2. Simultaneous Amino Acid Changes and Branch Point Movement

The single residue scan described above suggests that CDA TE is a permissive cyclization catalyst and raises the question of the effect on cyclization of simultaneous changes in the linear peptide precursor. Therefore, a peptidyl-thioester substrate (**Dap**) which was based on a sequence analogous to daptomycin was synthesized [116]. L-3-Methylglutamic acid in position twelve was replaced by L-glutamic acid for synthetic reason (Figure 5.10). In contrast to the substrates derived from CDA, **Dap** incorporates a longer N-terminal extension including two additional amino acids fused to a decanoyl fatty acid moiety moving the branch point of the peptidolactone from position 2 to position 4. Incubation of **Dap** with CDA cyclase revealed the formation of two products that were identified by ESI-MS as linear peptide acid ($t_R = 30.2$ min) and decapeptide lactone ($t_R = 30.8$ min) (Figure 5.12). MS-MS

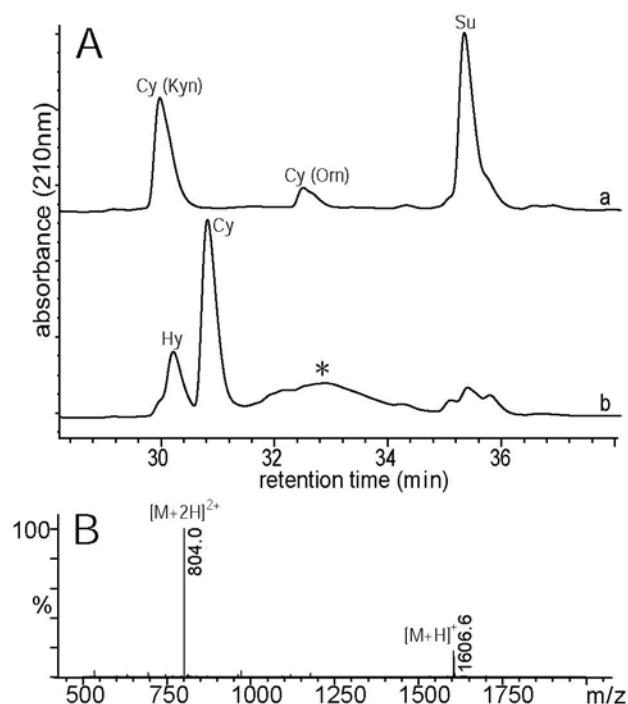


Figure 5.12: Cyclization of a daptomycin analog mediated by CDA TE. (A) Reactions of the linear precursor peptide **Dap** followed by HPLC. Trace a displays the negative control without enzyme (250 μM substrate, 25 mM Hepes, 50 mM NaCl, pH 7.0 at 25°C for 2h). Trace b shows the same reaction in the presence of 5 μM CDA cyclase. Enzyme is indicated with an asterisk. (B) Shown is the ESI mass spectrum of the decapeptide lactone ($t_R = 30.9$ min) produced by CDA TE.

sequencing of the cyclic species confirmed that cyclization is mediated through nucleophilic attack of L-Thr at position 4 as fragment ions containing the predicted linkage from Thr₄ to

(A)

compound	molecular formula	species	observed mass of fragments (calculated mass) (Da)
decapeptide lactone of Dap	$C_{20}H_{32}N_7O_{10}^+$	[M+H] ⁺	(1) 530.29 (530.22)
	$C_{53}H_{72}N_{11}O_{17}^+$		(2) 1134.62 (1134.51)
	$C_{55}H_{75}N_{12}O_{18}^+$		1191.56 (1191.53)
	$C_{57}H_{77}N_{12}O_{20}^+$		1249.55 (1249.54)
	$C_{64}H_{87}N_{14}O_{24}^+$		(3) 1435.74 (1435.60)
	$C_{66}H_{90}N_{15}O_{25}^+$		1492.77 (1492.62)

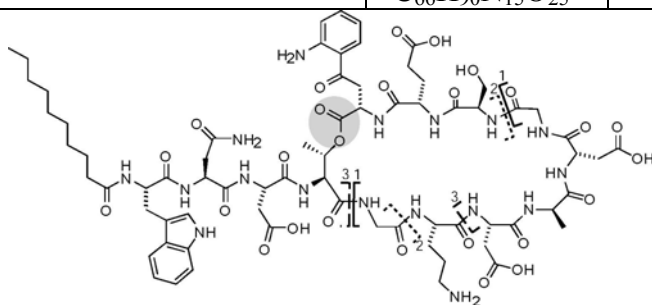


Figure 5.13: Structure of the decapeptide lactone derived from **Dap**. The detected fragments **1** (solid line), **2** (dotted line), and **3** (dashed line) are indicated. The molecular part highlighted by shading represents the lactone linkage.

(B)

x	hydrolysis observed mass of fragments (calculated mass) (Da)		cyclization via L-Kyn ₁₃ observed mass of fragments (calculated mass) (Da)
	y_x	$y_x - H_2O$ [$y_x - NH_3$]	y_x
1	209.09 (209.09)	191.08 (191.08) [192.06 (192.07)]	191.08 (191.08)
2	n. d.	n. d.	n. d.
3	425.20 (425.17)	407.18 (407.16)	407.18 (407.16)
4	482.24 (482.19)	464.23 (464.18)	464.23 (464.18)
5	n. d.	n. d.	n. d.
6	668.29 (668.25)	650.27 (650.24)	650.27 (650.24)
7	783.35 (783.28)	765.33 (765.27)	765.33 (765.27)
8	897.48 (897.36)	879.45 (879.35)	879.45 (879.35)
9	954.51 (954.38)	936.53 (936.37)	936.53 (936.37)
10	1055.57 (1055.43)	1037.59 (1037.42)	1037.59 (1037.42)
11	n. d.	n. d.	n. d.
12	1284.56 (1284.50)	1266.57 (1266.49)	1266.57 (1266.49)

n. d. = not detected

Table 5.3: MS-MS sequencing of the products derived from **Dap**. (A) MS-MS fragmentation of the decapeptide lactone (cyclization via L-Thr₄). Shown are fragments arising from simultaneous breaking of two bonds. The corresponding fragment ions were not detected for the octapeptide lactam (cyclization via L-Orn₆) and the 7-membered lactam (cyclization via L-Kyn₁₃). The pattern giving rise to the fragments **1**, **2**, and **3** is illustrated below. (B) The y series of the hydrolyzed product and the 7-membered lactam (cyclization via L-Kyn₁₃) derived from product ion MS-MS spectra. The table also indicates the loss of water or ammonia of the fragment ions. The fragmentation pattern of the y_1 series is depicted in Figure 5.14 (A).

Kyn₁₃ can be identified (Table 5.3 (A)). Cyclization occurred with a k_{cat}/K_M value of 22.2 $\text{mM}^{-1}\text{min}^{-1}$ and a ratio of cyclization to hydrolysis of 3:1. A control reaction without enzyme showed that the formation of this macrolactone was abolished. Instead, two new cyclic products were observed at retention times of 30.0 and 32.5 min, respectively. The identity of the former species ($t_R = 30.0$ min) was also investigated by MS-MS fragmentation (Table 5.3 (B), Figure 5.14 (A)). Cyclization was shown to occur through the L-Kyn residue at position 13 leading to a seven-membered lactam (Figure 5.14 (B)). In the other case nonenzymatic cyclization yielded an octapeptide lactam ring derived from nucleophilic attack of L-Orn₆ onto the C-terminal carboxyl group, because the formation of this macrolactam was abolished by orthogonal Aloc-protection of the L-Orn residue (**Dap-Aloc**) (Figure 5.15).

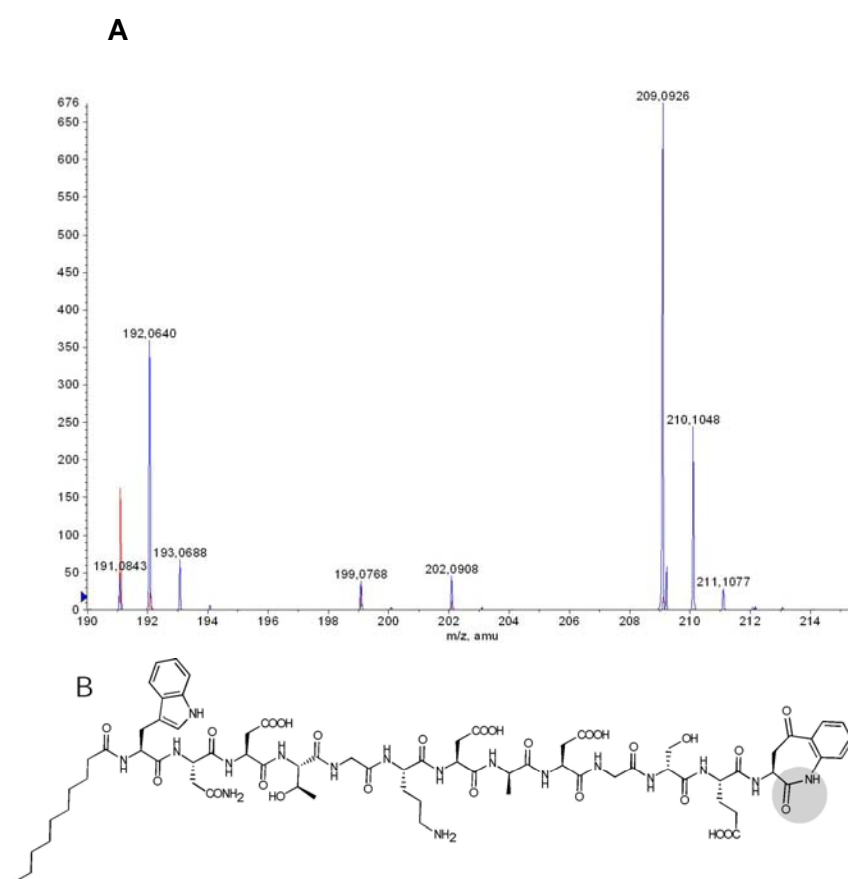


Figure 5.14: MS-MS fragmentation

(A) Overlaid MS-MS spectra of the 7-membered lactam (red) and the hydrolyzed product (blue). The assignment of the fragments is shown in Table 5.3B. The y_1 fragment ion of the 7-membered lactam does not correspond to the $y_1 - \text{H}_2\text{O}$ fragment ion of the hydrolyzed product, because the MS-MS spectrum of the 7-membered lactam lacks a peak at $m/z = 209.09$. This signal is only detected for the hydrolyzed product (y_1 fragment ion).

(B) Structure of the 7-membered lactam (cyclization via L-Kyn₁₃) derived from **Dap**.

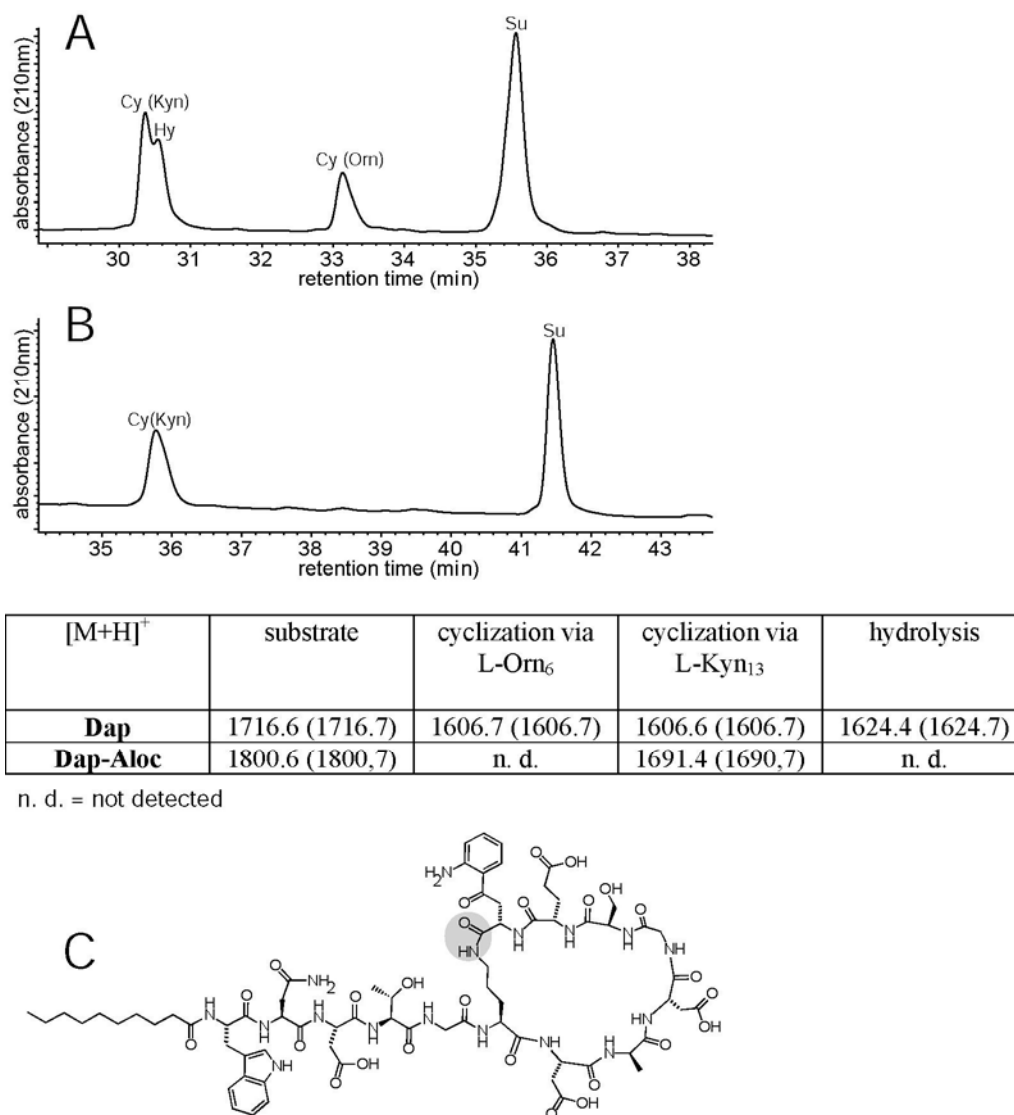


Figure 5.15: Identification of non-enzymatic macrolactam formation

(A) HPLC trace showing the incubation of **Dap** without enzyme. The assay was performed with 250 μ M substrate, 25 mM HEPES, 50 mM NaCl, pH 7.0 for 2h at 25°C. The corresponding masses are shown in the table below.

(B) HPLC trace displaying the assay of **Dap-Aloc** under the same conditions as described above. Side chain protection of L-Orn₆ by the Aloc-group abolishes macrolactam formation. The shift to higher retention times is caused by the loss of the positive charge of the ornithine side chain. The corresponding masses are shown in the table below. Su = substrate, Hy = hydrolyzed product, Cy = cyclized product.

(C) Structure of the octapeptide lactam derived from **Dap**.

5.2.3. Derivatization of Daptomycin and Bioactivity Studies

To explore the significance of selected amino acid side chains for the bioactivity of the antibiotic daptomycin, eight peptidyl-thioesters (**Dap-N3**, **Dap-N7**, **Dap-N9**, **Dap-Q12**, **Dap-**

DD11, **Dap-Aloc**, **Dap-W13**, and **Dap-W13K6**) in addition to the already mentioned linear precursor peptide **Dap** (Figure 5.16, see also appendix) were prepared.

All compounds were tested as substrates for enzymatic transformation by CDA cyclase. In each case the conversion to cyclic product was sufficient to allow semipreparative-scale reactions. The purified cyclic products were then tested for their bactericidal activity against *Bacillus subtilis* PY79 (Table 5.4).

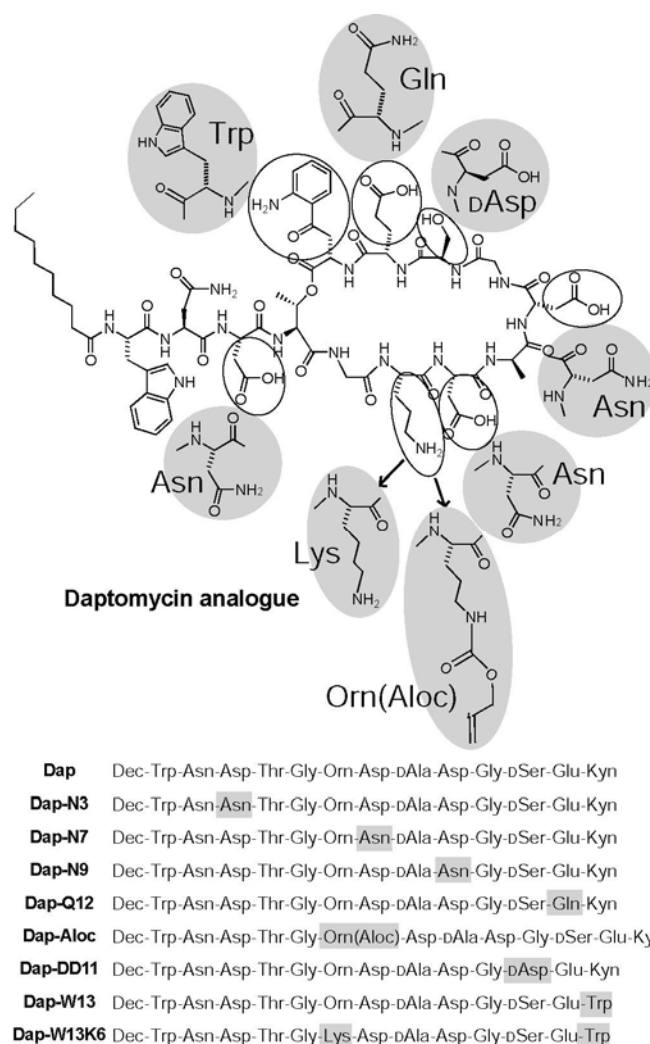


Figure 5.16:

Chemoenzymatic derivatization of daptomycin. The daptomycin analogue **Dap** cyclized by CDA TE only lacks the β -methyl group of L-3-methylglutamate (position 12) of authentic daptomycin. The residues that were incorporated into the backbone of **Dap** are indicated by shading. The corresponding sequences of the daptomycin derivatives are shown below. The differences to **Dap** are highlighted by gray boxes.

At first the bioactivity of the cyclic peptide product of **Dap** was compared to authentic daptomycin. Both compounds differ only by the β -methyl group of glutamic acid in position twelve. The macrolactone of **Dap** has a MIC of 20 $\mu\text{g/mL}$, whereas the reference compound has an MIC of 3 $\mu\text{g/mL}$ (Table 5.4). This result indicates that the β -methyl group of glutamic

acid is crucial for bioactivity. Further, when L-Kyn₁₃ was replaced by L-Trp₁₃ (**Dap-W13**), the MIC increased 5-fold to 100 µg/mL, displaying the importance of this nonproteinogenic amino acid for the bactericidal activity of daptomycin. In contrast to that, successive

Compound	MIC ₉₀ (µg/mL) at 73.6 mg/L Ca ²⁺ [at 23.6 mg/L Ca ²⁺]
Dap	20 [> 240]
authentic daptomycin	3 [20]
Dap-Hyd	> 960
Dap-N3	80
Dap-N7	> 960
Dap-N9	> 960
Dap-Q12	30
Dap-DD11	> 320
Dap-Aloc	80
Dap-W13	100
Dap-W13K6	100

Table 5.4: MIC determination of daptomycin derivatives against *B. subtilis* PY 79

substitution of the third nonproteinogenic residue L-Orn₆ by L-Lys₆ in **Dap-W13K6** did not cause a further increase of the MIC (Table 5.4).

In accordance to authentic daptomycin, the antimicrobial behavior of **Dap** strongly depends on the presence of physiological concentrations of calcium ions [117]. The MIC increased at least 12-fold, when the concentration of free calcium ions was reduced from 73.6 mg/L to 23.6 mg/L (Table 5.4). Calcium ions presumably interact with the acidic residues of daptomycin, resulting in oligomerization of daptomycin molecules to form ion channels [118]. Recent results with the closely related CDA suggest that these acidic residues are crucial for antimicrobial potency [50]. Hence, the cyclic peptides **Dap-N3**, **Dap-N7**, **Dap-N9**, and **Dap-Q12** were tested for antibiotic activity. In each peptidolactone one acidic residue of daptomycin is deleted by substitution with either L-Asn or L-Gln (Figure 5.16). Single deletion of the aspartic acid residues in the lactone ring (**Dap-N7** and **Dap-N9**) resulted in a

total loss of bioactivity (Table 5.4). Surprisingly, replacement of the two remaining acidic residues (**Dap-N3** and **Dap-Q12**) did not abolish bactericidal potency, indicating that these residues are not essential for calcium binding. Interestingly, the bioactivity of **Dap** was also abolished, when an additional acidic residue was incorporated into the peptide backbone of the lactone ring (**Dap-DD11**).

The biological function of the positively charged Orn₆ remains unclear [119]. Nevertheless, masking of the side chain by Alloc-protection (**Dap-Alloc**) significantly increased the MIC 4-fold in comparison to **Dap**, indicating the importance of this residue for antibiotic activity. In addition, the lactone ring of **Dap** was shown to be important for bioactivity as the corresponding linear peptide acid (**Dap-Hyd**) did not show antimicrobial properties. Finally, the cyclic peptide **Dap** completely lacked hemolytic activity up to a concentration 4-fold above the MIC even after the addition of 50 mg/L Ca²⁺ (data not shown). This demonstrates its specific interaction with prokaryotic membranes.

5.3. FRET-Assisted Detection of Peptide Cyclization

The following section focuses on a system for specifically detecting macrocyclic peptides by fluorescence resonance energy transfer (FRET). In this approach, peptide cyclization catalyzed by CDA TE brings the donor tryptophan (Trp) and the acceptor kynurenine (Kyn) in close spatial proximity to enable efficient FRET. To evaluate the utility and potential of FRET-assisted detection of peptide cyclization, a library of daptomycin-like peptides with variable positioning of the two fluorophores in the N- and C-terminal parts of the peptide sequence was created. Moreover, it was investigated whether this technique can be extended to TE domains of other nonribosomal peptide synthetases. The last part of this section then concentrates on initial results of such a fluorescence-based method to serve as a rapid and sensitive detection tool in high-throughput enzymatic screening.

5.3.1. Synthesis and Fluorescence Characteristics of Linear and Cyclic Daptomycin Peptides

The cyclic lipopeptide antibiotic daptomycin is a tridecapeptide that contains two fluorophores: tryptophan (Trp, W) at the N-terminus and kynurenine (Kyn, U) at the C-terminus (Figure 5.17 A). The poor fluorescence yield of the Trp residue situated between the C₁₀-fatty acid and the peptide headgroup was reported earlier [119]. It was assumed that this poor Trp emission is due to fluorescence resonance energy transfer (FRET), which results from the combination of the proximity of the two fluorophores and the overlap of the Trp emission spectrum ($\lambda_{Em} \approx 330$ nm) and Kyn absorption spectrum ($\lambda_{Ex} \approx 350$ nm). The proximity of these fluorophores mainly arises from the lactone bond, which connects threonine at position 4 with the C-terminal Kyn₁₃ residue. It was thus reasoned that the energy

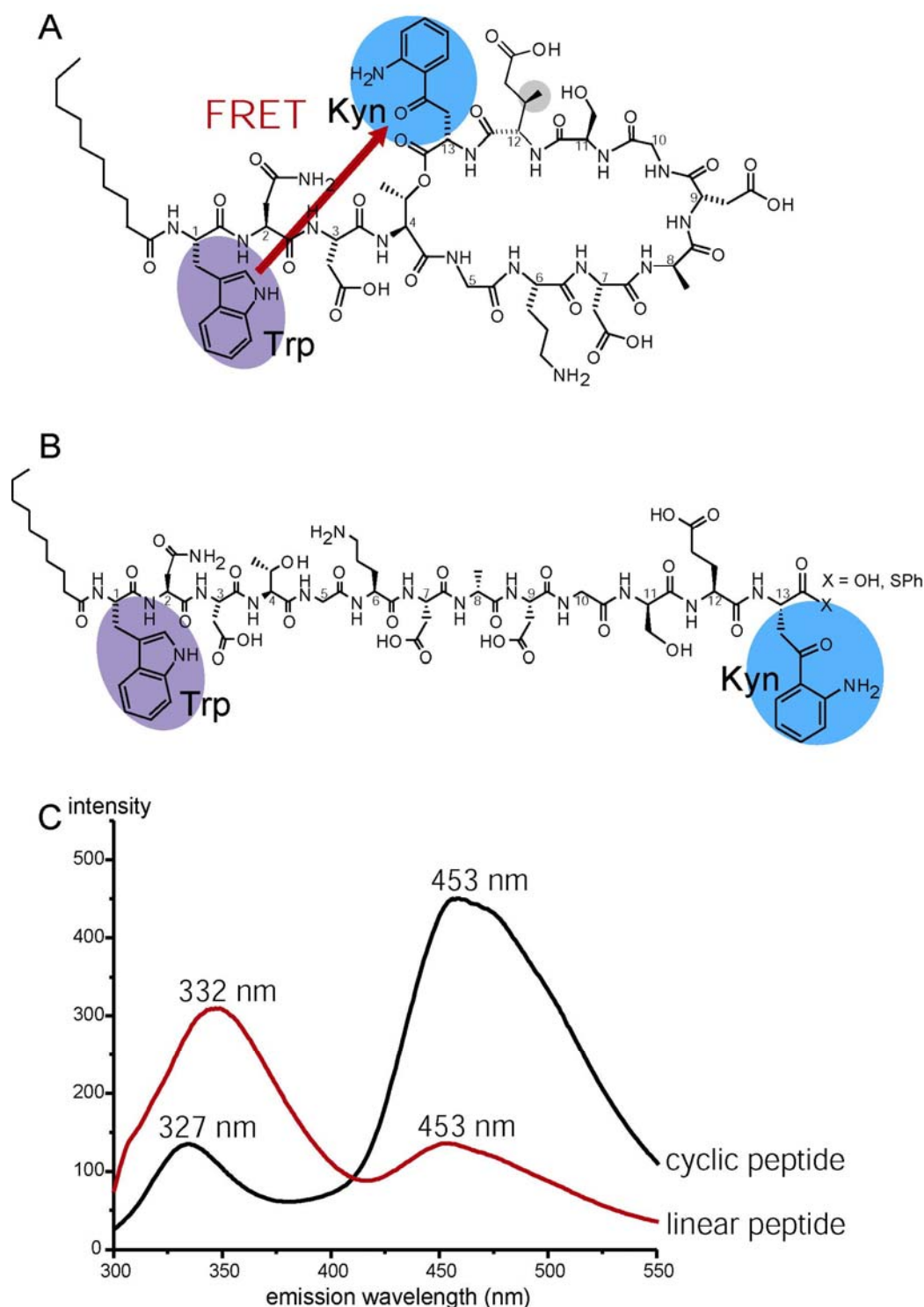


Figure 5.17: Fluorescence resonance energy transfer (FRET) in daptomycin
(A) Daptomycin adopts a conformation in which the kynurenine (Kyn) fluorophore is in close spatial proximity to the tryptophan (Trp) residue allowing FRET to occur. The methyl group of nonproteinogenic L-3-methylglutamate is indicated by shading. (B) The structure of a linear daptomycin derivative is shown. The fluorescent residues Kyn and Trp are highlighted. (C) Emission spectra of the linear and cyclic daptomycin derivatives in methanol and DMSO 9:1 (v/v): red line, linear daptomycin derivative; black line, cyclic daptomycin derivative; excitation wavelength = 280 nm.

transfer might be less efficient in the linear peptide derived from daptomycin by opening of the decapeptide lactone ring (Figure 5.17 B). Given this assumption, it was chosen to compare the fluorescence characteristics of cyclic to linear daptomycin. The latter was prepared by solid phase peptide synthesis, followed by treatment with trifluoroacetic acid (TFA), triisopropylsilane (TIPS), and water in a ratio of 95:2.5:2.5 (v/v) to yield the linear peptide acid. For the generation of cyclic daptomycin (Figure 5.17 A), linear peptidyl-thiophenol was converted to the macrolactone in the presence of CDA cyclase. In the linear and cyclic daptomycin sequence, L-3-methylglutamate at position 12 was replaced by glutamate for synthetic reason. In order to investigate the assumed distance-dependent energy transfer between the two fluorophores Trp and Kyn, the linear and cyclic daptomycin analogues were excited at 280 nm, followed by measurement of the emission spectra. Fluorescence measurements were carried out in methanol and dimethylsulfoxide (DMSO) in a ratio of 9:1 (v/v) due to 2.1-fold Kyn-fluorescence enhancement compared to 10% DMSO in water (data not shown). Interestingly, the Kyn emission at 453 nm of the linear daptomycin analogue is minimal resulting in a 4-fold difference between linear and cyclic peptide (Figure 5.17 C). Excitation at 280 nm produces preferentially UV light ($\lambda_{Em} \approx 330$ nm). Conversely, excitation of Trp in the cyclic peptide generates a strong Kyn emission in the visible region of light ($\lambda_{Em} \approx 455$ nm) due to FRET. Further proof was obtained by analytical HPLC in combination with fluorescence studies (Figure 5.18). An assay with 200 μ M linear (ln) daptomycin-like peptide precursor **lnDap-U₁W₁₃** (comprising Kyn at position 1 and Trp at position 13, Figure 5.19 shows the corresponding cyclic peptide **cyDap-U₁W₁₃**, see also appendix) and 5 μ M CDA cyclase was quenched after a time period of 30 min by the addition of aqueous trifluoroacetic acid (TFA). Analytical HPLC with monitoring at 215 nm revealed identical concentrations of peptidyl-thiophenol substrate and its macrolactone product (Figure 5.18). Remarkably, determination of the emission at 452 nm using a fluorescence detector at an excitation wavelength of 280 nm significantly enhanced signal intensity of the decapeptide lactone. Peak

area integration exhibited a 5.5-fold amplification of visible fluorescence in comparison to the linear precursor, indicating a greatly improved energy transfer between Trp and Kyn in the cyclopeptide.

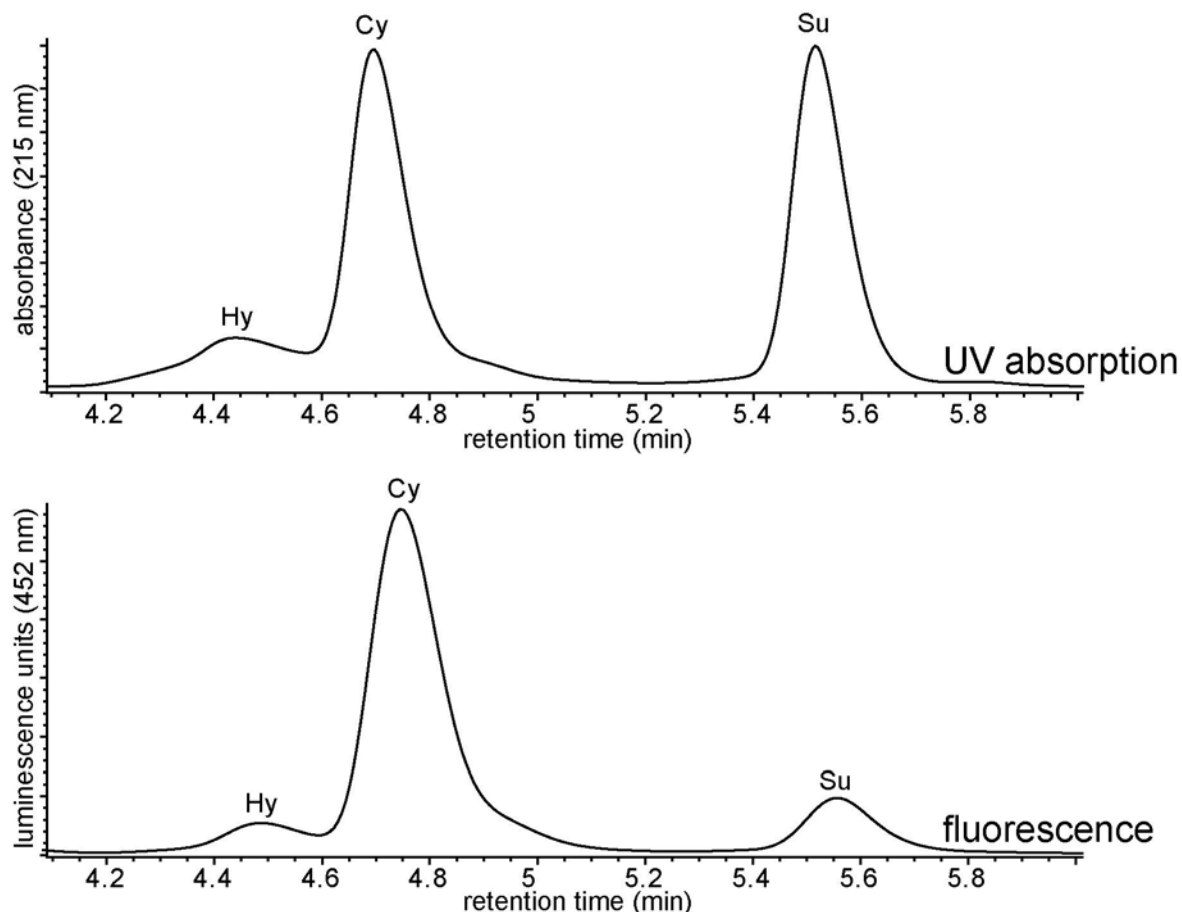


Figure 5.18: Fluorescence enhancement by TE-mediated peptide cyclization is shown. An assay containing 200 μM linear peptidyl thioester (**InDap-U1W13**) and 5 μM CDA TE was quenched by aqueous TFA and analyzed by HPLC: Upper HPLC trace, absorbance at 215 nm; lower HPLC trace, fluorescence at 452 nm (excitation wavelength = 280 nm). The fluorescence signal is slightly shifted to higher retention times, because the solvent reaches the fluorescence detector after passing the UV-detection cell. Su = substrate, Hy = hydrolyzed product, and Cy = cyclized product.

5.3.2. Examination of Distance-Dependent Interactions between Donor and Acceptor

It was reasoned that the above FRET experiments could be transferred to a variety of peptides with varying spatial proximity of donor and acceptor. To investigate the feasibility of FRET detected peptide cyclization, it was chosen to create a small library of linear and cyclic

daptomycin-like peptides (Figure 5.19). In contrast to authentic daptomycin, the positions of the fluorophores Trp and Kyn in the peptide backbone were exchanged. This strategy maximizes the yield of cyclic peptide generated by CDA TE because Trp is the C-terminal amino acid of cognate CDA [17]. Therefore, in all cases the conversion to cyclic product was sufficient to allow fluorescence studies (data not shown). To vary the distance between both fluorophores, Trp was kept at the C-terminus, whereas the position of Kyn was systematically altered. All of the HPLC purified linear and cyclic peptides were dissolved in a mixture of methanol and DMSO 9:1 to a final concentration of 200 μ M, followed by fluorescence measurements.

Since the distances between the fluorophores were systematically altered in the above-mentioned library of linear and cyclic (cy) daptomycin derivatives (Figure 5.19), a distance-dependent relationship of integrated acceptor fluorescence to integrated donor fluorescence ($E_{m_{Kyn}}/E_{m_{Trp}}$ ratio) was expected. As shown in Figure 5.20, the $E_{m_{Kyn}}/E_{m_{Trp}}$ ratio changes in the order **cyDap-U₁W₁₅** < **cyDap-U₁W₁₄** < **cyDap-U₁W₁₃** < **cyDap-U₂W₁₃** < **cyDap-U₃W₁₃** < **cyDap-U₅W₁₃** > **cyDap-U₇W₁₃** (see also appendix). Therefore, decreasing distance between both fluorophores clearly correlates with more effective energy transfer. Indeed, the compounds **cyDap-U₃W₁₃** and **cyDap-U₅W₁₃**, the latter one with the fluorescent Kyn moved to a ring position, show the highest $E_{m_{Kyn}}/E_{m_{Trp}}$ ratios of this study because the FRET pair is only separated by the cyclization nucleophile threonine.

In general, excitation at 280 nm revealed 3 to 5-fold increased $E_{m_{Kyn}}/E_{m_{Trp}}$ ratios, when the linear peptide precursors were converted into the corresponding macrolactones by CDA cyclase. The only exceptions were **lnDap-U₁W₁₅** and **lnDap-U₁W₁₄**, where peptide cyclization yielded less than 2-fold increases of the $E_{m_{Kyn}}/E_{m_{Trp}}$ ratios (Figure 5.20), indicating that more than 3 amino acid residues in between Trp and Kyn significantly limits the energy transfer.

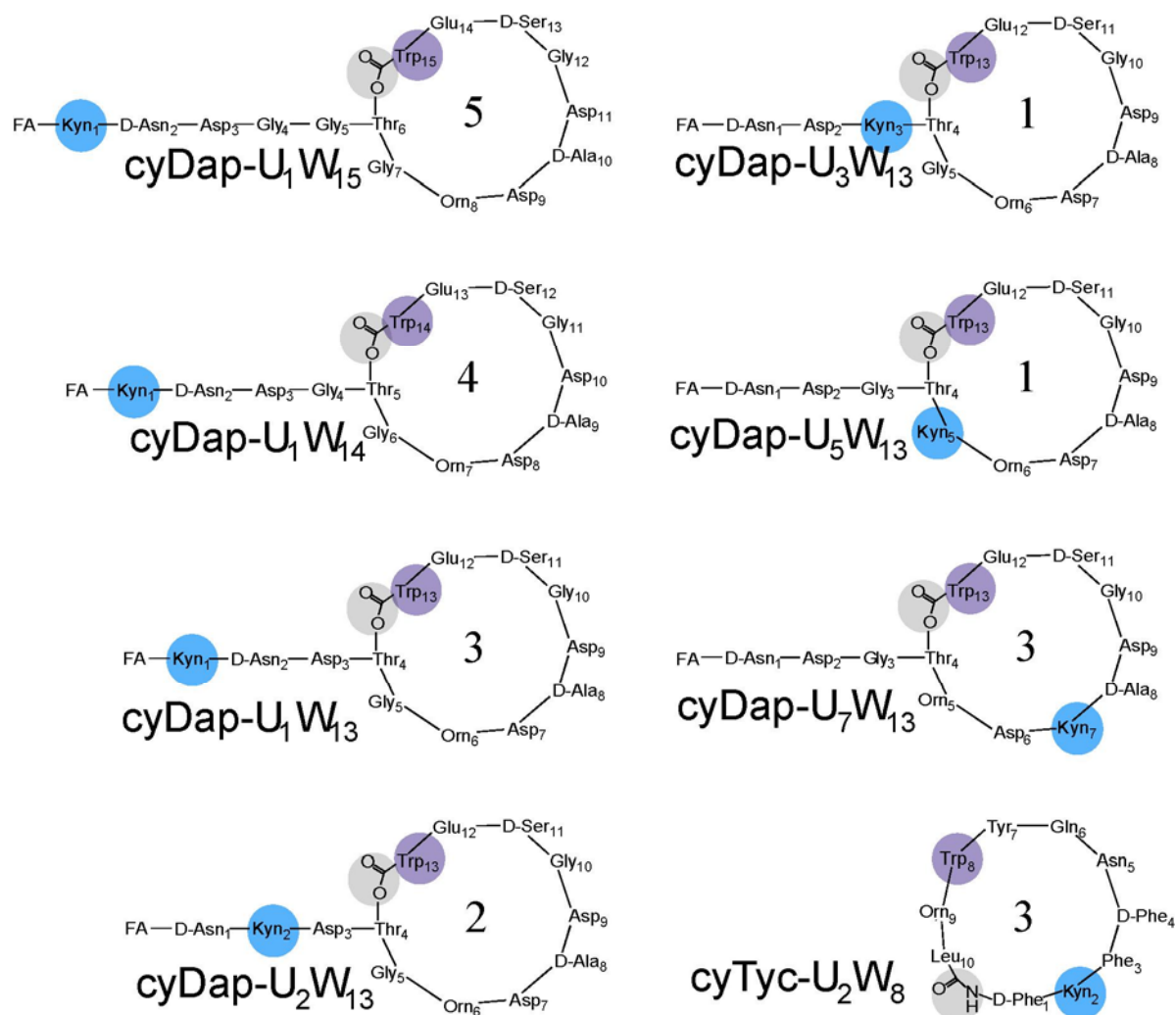


Figure 5.19: Macrocyclic peptides used in this study (see also appendix). All fluorophore-tagged cyclopeptides are shown using three letter amino acid codes. The FRET pair in each compound is highlighted. The figures in the middle of the macrocycles denote the number of amino acid residues in between Trp and Kyn. Macrolactonization/macrolactamization is indicated by grey shading. Kyn = kynurenine, Orn = ornithine, and FA = fatty acid.

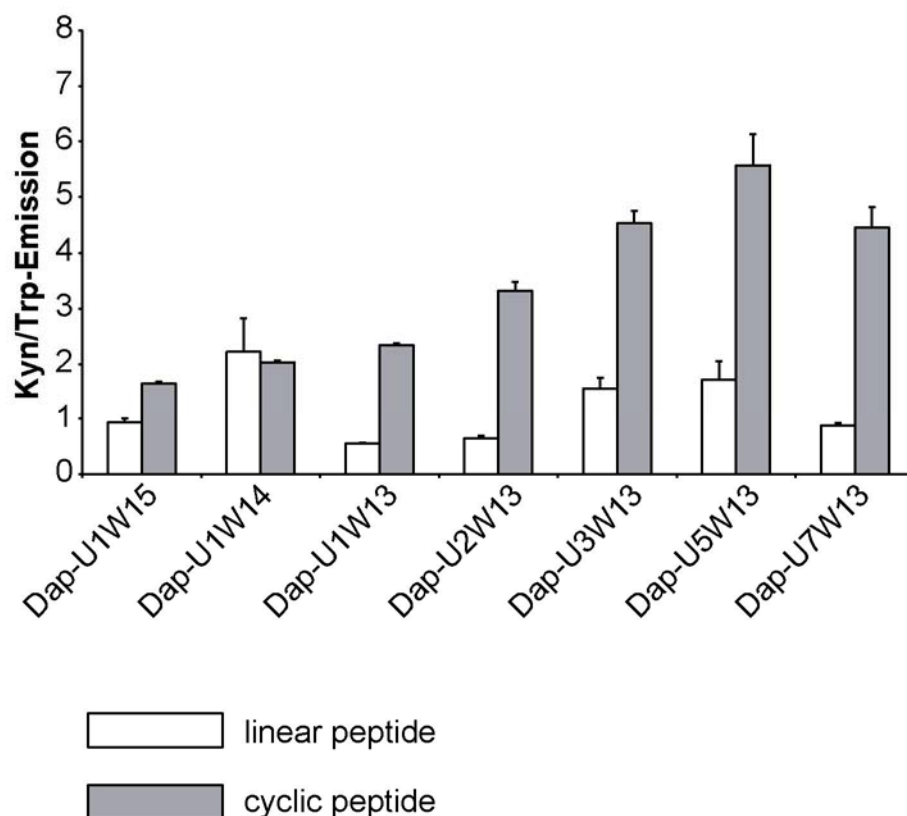


Figure 5.20: Fluorescence studies of linear and cyclic daptomycin derivatives. Determination of Em_{Kyn}/Em_{Trp} ratios of linear and cyclic daptomycin derivatives with systematically altered distance between Trp and Kyn: linear daptomycin derivatives = white bars; cyclic daptomycin derivatives = grey bars. All bars represent mean values of three measurements. The error bars indicate the standard error of the mean. Excitation wavelength = 280 nm. U = kynurenine, and W = tryptophan.

5.3.3. Real-Time Monitoring of Peptide Cyclization

FRET-assisted detection of peptide cyclization provides a useful means to follow reactions in real-time without disrupting enzymatic integrity. By incorporating fluorescent amino acids into linear peptide precursors, adding the respective recombinant cyclization enzyme, and measuring the visible fluorescence intensity ($\lambda_{Ex} = 280$ nm; $\lambda_{Em} = 452$ nm) at defined time intervals, one can easily estimate the progression of the peptide cyclization reaction. This technique was demonstrated with the daptomycin derivative **InDap-U₃W₁₃** in which the fluorescent residues Trp and Kyn were placed at positions 13 and 3, respectively (Figure 5.19, see also appendix). After addition of 5 μ M CDA cyclase, fluorescence intensity at 452 nm followed a time-dependent hyperbolic function, reaching a maximum after approximately 50

minutes (Figure 5.21 A). HPLC studies revealed total conversion to cyclic product within this period of time (Figure 5.22). Also, a control reaction in the presence of the corresponding heat denatured enzyme indicated no significant change in fluorescence emission.

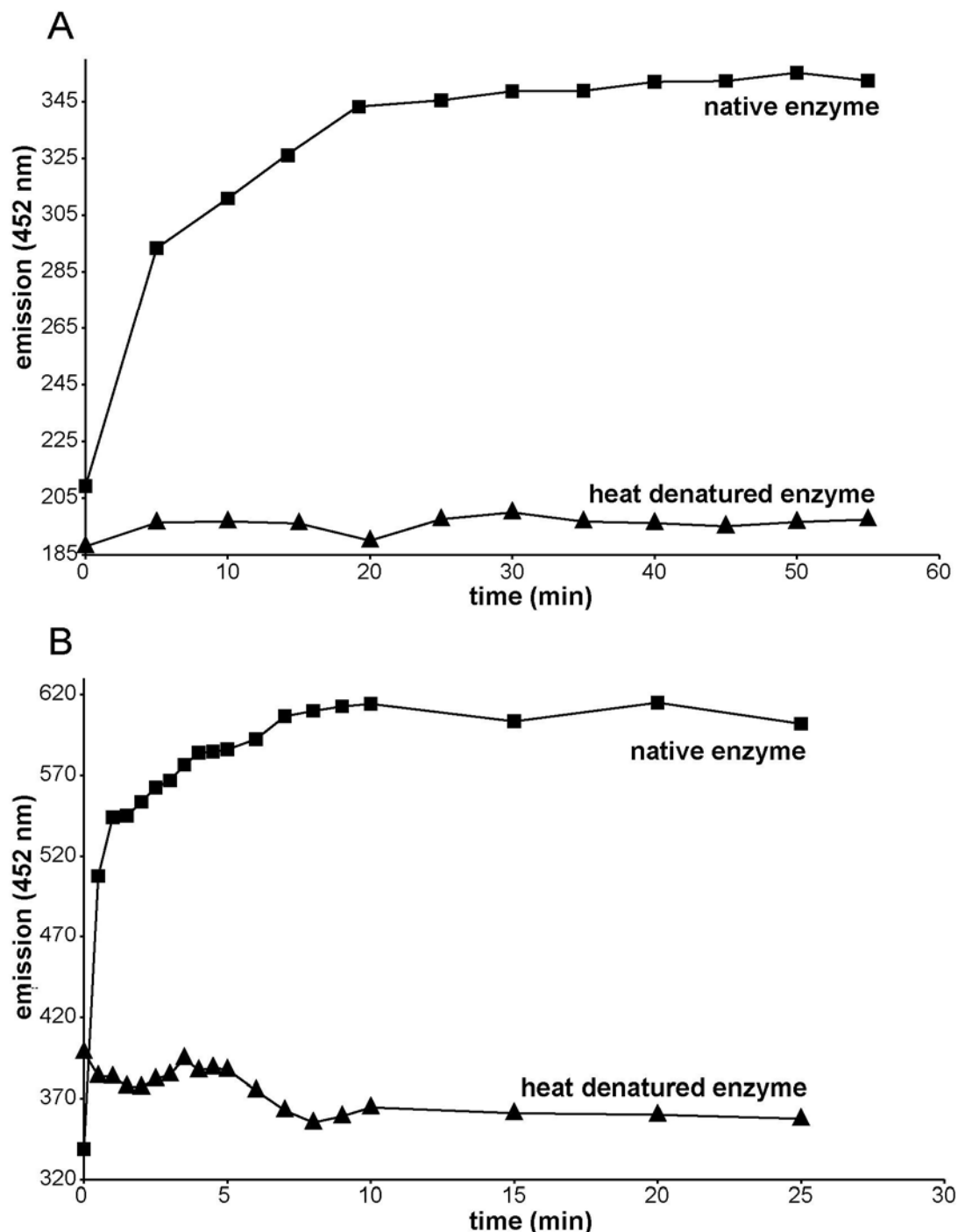


Figure 5.21: Real-time monitoring of peptide cyclization. (A) Sample contained 75 μM **InDap-U3W13** and 5 μM CDA TE (■). The negative control was conducted in the presence of 5 μM heat denatured CDA cyclase (▲). (B) The cuvette contained 50 μM **InTyc-U2W8** and 0.5 μM Tyc TE (■). The negative control was done in the presence of 0.5 μM heat denatured Tyc TE (▲). Excitation wavelength = 280 nm, emission wavelength = 452 nm.

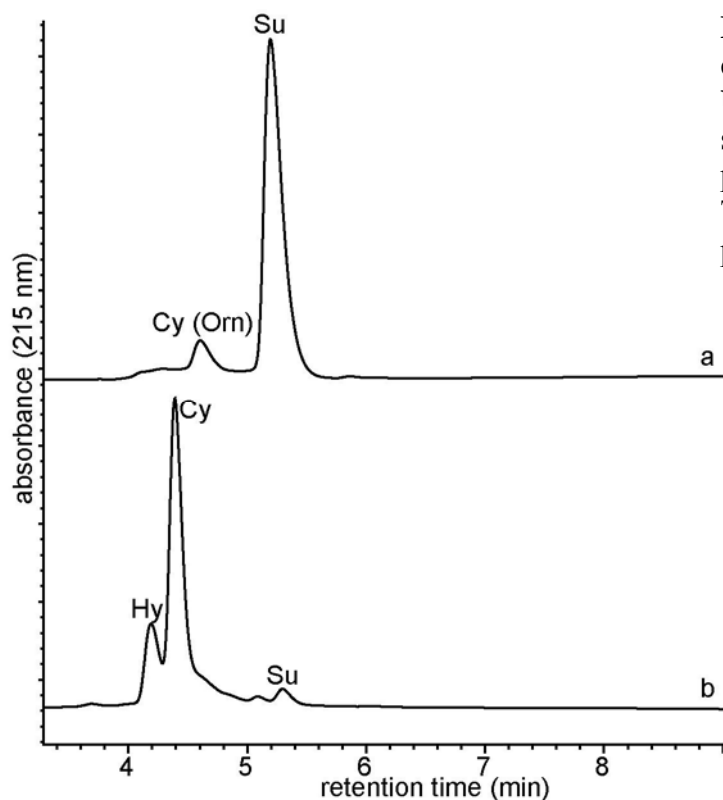


Figure 5.22: HPLC trace of CDA cyclase incubated with 75 μM **InDap-U3W13** for 50 min (trace b). Trace a shows incubation of substrate in the presence of 5 μM heat denatured CDA TE. Su = substrate, Hy = hydrolyzed product, and Cy = cyclized product.

The real-time monitoring of CDA cyclase mediated peptide cyclization raised the question whether this approach may be applicable to other peptide cyclization catalysts. To answer this question, the well-characterized tyrocidine synthetase thioesterase domain (Tyc TE) was chosen, which efficiently catalyzes head-to-tail cyclization with decapeptidyl thioesters. It was previously shown that Tyc TE tolerates replacement of residues 2–8 of peptidyl thioesters [[66, 69]. To follow Tyc TE catalyzed macrolactamization by FRET, the Trp/Kyn pair was incorporated into the wild-type tyrocidine A sequence. Specifically, Pro₂ was replaced by Kyn and Val₈ by Trp (Figure 5.19 shows the corresponding cyclic peptide **cyTyc-U₂W₈**, see also appendix). Incubation of the resulting substrate **InTyc-U₂W₈** with Tyc TE indicated a time-dependent increase in fluorescence emission ($\lambda_{\text{Em}} = 452 \text{ nm}$) (Figure 5.21 B), although the cyclization-to-hydrolysis ratio was quite low (0.28) as determined by analytical HPLC. Finally, no change in fluorescence was observed for heat denatured Tyc TE.

5.3.4. FRET Can Be Used to Measure Kinetics of Enzyme Mediated Peptide Cyclization

The above-mentioned results show that the close spatial proximity of donor and acceptor in the cyclic peptide induces up to 5.5-fold amplification of visible fluorescence in comparison to the linear precursor. In addition, FRET-assisted detection of peptide cyclization easily realizes picomolar detection limits using conventional fluorescence detectors without optimization. For example, the cyclic daptomycin derivative **cyDap-U₂W₁₃** was characterized by a detection limit of 7 pmol, whereas its linear counterpart **lnDap-U₂W₁₃** showed a limit of 28 pmol. This high sensitivity raised the question whether FRET can be used to accurately determine kinetics of enzyme-mediated peptide cyclization. To address this question, thiophenol substrates of daptomycin derivatives (**lnDap-U₁W₁₃** and **lnDap-U₃W₁₃**, see appendix) were chosen for kinetic measurements, which were performed by analytical HPLC combined with fluorescence detection. Initial investigations revealed a linear correlation between fluorescence emission at 452 nm and the concentrations of the respective cyclic peptides (**cyDap-U₁W₁₃** and **cyDap-U₃W₁₃**) as determined by calibration curve plots, thus allowing simple quantification of the fluorophor-containing macrolactones. Kinetic characterization of the cyclization reactions was then carried out by calculating the initial reaction rates at 5–7 substrate concentrations. It was found that the $k_{\text{cat}}/K_{\text{M}}$ values derived from integrated fluorescence emission were in good agreement with the corresponding $k_{\text{cat}}/K_{\text{M}}$ values determined by conventional UV absorbance at 215 nm, resulting in 1.2 to 1.6-fold differences between both detection methods (Table 5.5).

Compound	$k_{\text{cat}}/K_{\text{M}}$ ($\text{mM}^{-1}\text{min}^{-1}$)	Method
lnDap-U₁W₁₃	5.09	Absorbance (215 nm)
	6.13	Fluorescence emission wavelength = 452 nm
lnDap-U₃W₁₃	4.34	Absorbance (215 nm)
	6.75	Fluorescence emission wavelength = 452 nm

Table 5.5:

Determination of cyclization kinetics: UV-absorption vs. Kyn-fluorescence.

U = kynurenine, W = tryptophan, and ln = linear.

5.3.5. FRET-Assisted Detection of Peptide Cyclization of Immobilized CDA Cyclase

It has recently been shown that the use of NRPS-derived peptidyl-carrier protein (PCP) for biotin labeling is amenable to high-throughput enzymatic screening [104], which can be a powerful method for identifying and evolving biological catalysts. It was therefore reasoned that this approach could be transferred to TE domains in order to improve or alter their substrate specificity by directed evolution efforts. Since in the native context of NRPS, the PCP domain is N-terminally associated with the TE domain, the PCP-TE didomain was excised from the corresponding synthetase. Specifically, heterologous expression of CDA PCP-TE was carried out, which is a 44.5 kDa protein from the *S. coelicolor* CDA biosynthetic machinery [17]. The yield of the didomain was around 4 – 5 mg/L. After purification by Ni-NTA affinity chromatography, CDA PCP-TE was labeled with biotin ppan in the presence of Sfp and biotin CoA (see chapter 4.3.3). Site-directed posttranslational modification was allowed to proceed for 90 minutes at 30°C, followed by confirmation with an API Qstar Pulsar i Q-q-TOF mass spectrometer (measured mass m/z 45382, calculated mass 45379). The labeling-reaction mixture was then run over an avidin column (bed volume 1 mL). After washing the column, the immobilized CDA PCP-TE didomain was incubated with 5 mM of **lnDap-U₁W₁₃** (see appendix) for 3 hours at 25°C. Reaction products were eluted off the column, and the mixture was characterized by LC-MS (Figure 5.23 A). Interestingly, **lnDap-U₁W₁₃** was significantly converted to the macrolactone product **cyDap-U₁W₁₃**. The observed cyclization-to-hydrolysis ratio was 7.0, validating that the immobilized CDA cyclase retains excellent cyclization activity. Additionally, minor amounts of an octapeptide lactam derived from cyclization via Orn₆ were detected. In contrast to the desired macrolactone, this byproduct is also generated in the absence of bound CDA cyclase, indicating its nonenzymatic origin (see chapter 5.2.2). Finally, the PCP-TE didomain was eluted with 5 mM biotin, and the protein was identified with SDS-PAGE to yield a single band of correct size (data not shown).

Remarkably, the substrate conversion into products was accompanied by a 3.5-fold increase in fluorescence emission at 452 nm (Figure 5.23 B). This result suggests that rapid detection of peptide cyclization by FRET can be transferred to immobilized TE domains, thus making the PCP-TE-tagging approach amenable to high-throughput enzymatic screening.

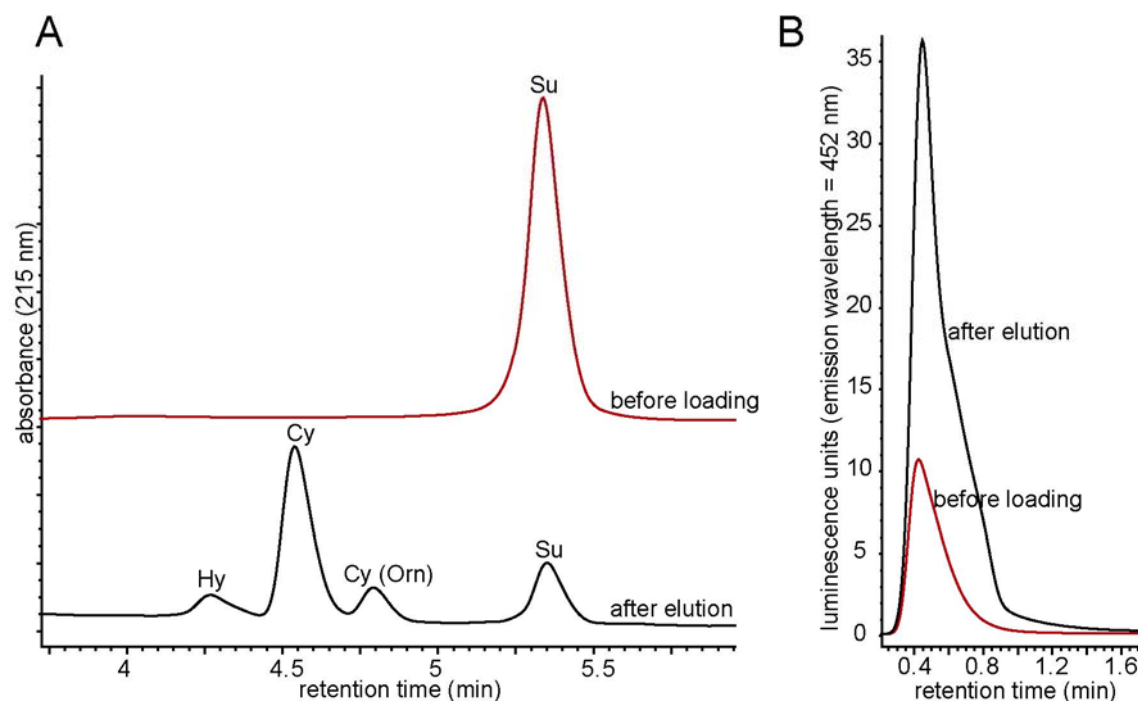


Figure 5.23: Immobilization of CDA cyclase by site-directed posttranslational modification and subsequent detection of reaction products. (A) HPLC trace of **lnDap-U1W13** prior to cyclization by immobilized CDA cyclase (red trace). Immobilized CDA TE was incubated with **lnDap-U1W13** for 3 hours at 25°C (black trace). (B) Detection of generated cyclopeptide by FRET. The red trace shows the fluorescence signal of **lnDap-U1W13** prior to loading onto the column. The black trace shows the fluorescence signal after CDA TE-mediated cyclization. Excitation wavelength = 280 nm, emission wavelength = 452 nm.

6. Discussion

6.1. The Enzymology of CDA Cyclase

In nature the C-terminal CDA cyclase of CDA synthetase catalyzes the formation of a branched cyclic macrolactone through the nucleophilic attack of the L-Thr₂ residue onto the C-terminal L-Trp₁₁ of the bound acyl-undecapeptidyl oxoester. The released CDA macrolactone is structurally related to other antibiotics, including daptomycin, friulimicins, and amphomycins (Figure 6.1) [17]. In order to gain a deeper understanding of the regio-, stereo-, and chemoselective cyclization mechanism of this class of acidic lipopeptides, the CDA thioesterase domain was expressed as excised cyclase from the CDA NRPS. This CDA cyclase has been successfully assayed in a chemoenzymatic approach for the *in vitro* cyclization of various synthetic peptidyl-thioesters based on a modified CDA sequence. This finding is potentially important for engineering the synthesis of novel peptides based on CDA, which can be screened for altered biological activity.

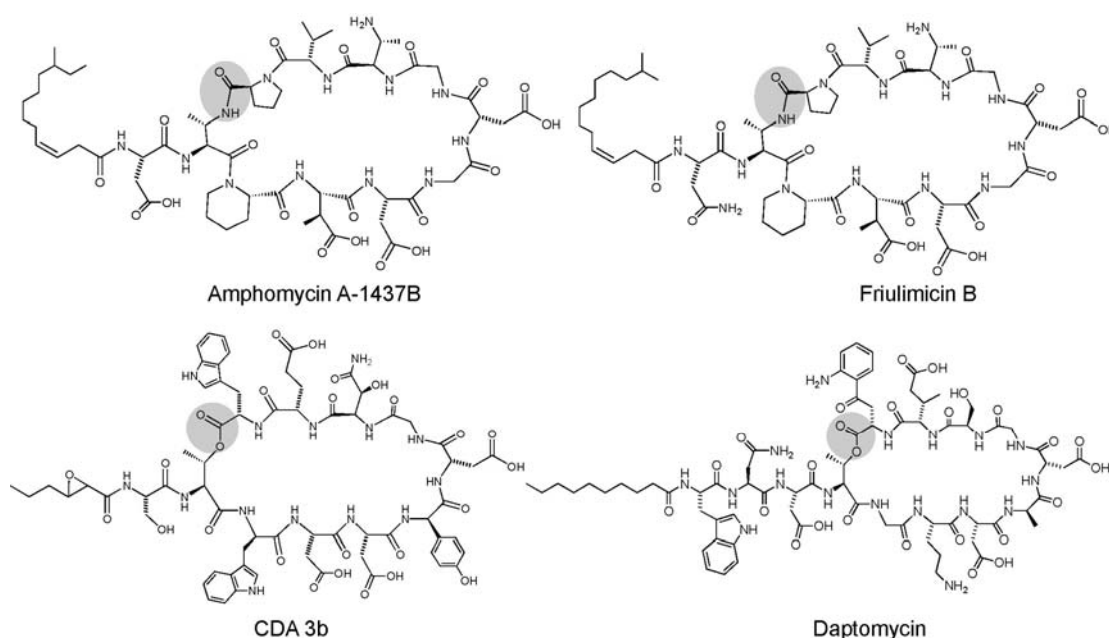


Figure 6.1: Acidic lipopeptide antibiotics. All structures are comprised of a decapeptide lactone or lactam ring (ester or amide linkage highlighted by shading), including several acidic residues probably important for calcium binding and antibiotic activity as well as several D-configured and nonproteinogenic residues. CDA is produced by *S. coelicolor*, friulimicin B and amphomycin A-1437B are produced by *Actinoplanes friuliensis*, and daptomycin is derived from *Streptomyces roseosporus*.

6.1.1. Enzymatic Cyclization of CDA: Substrate Recognition and Leaving Group Properties

Streptomycetes are a group of soil bacteria, which possess an important role in modern medicine as they produce over two-thirds of the naturally derived antibiotics in current use [21]. The excised CDA TE domain is the first recombinant cyclase of this group of microorganisms. It was probed with four different peptidyl-thioesters based on a sequence similar to CDA, including the leaving groups SNAC, ppan, CoA, and thiophenol. **CDA-thiophenol** was the best cyclization substrate, although thiophenol has no structural similarity to the ppan cofactor. Comparison of the catalytic cyclization efficiency of **CDA-thiophenol** with **CDA-SNAC** revealed a 10-16-fold higher $k_{\text{cat}}/K_{\text{M}}$ value for the peptidyl-thiophenol substrate. This result is in good agreement with experiments of the recombinant surfactin cyclase (Srf TE), where it was shown that the enzyme-mediated cyclization with the peptidyl-thiophenol substrate ($k_{\text{cat}}/K_{\text{M}} = 44.9 \text{ mM}^{-1} \text{ min}^{-1}$) was 15 times more efficient than with the respective SNAC substrate ($k_{\text{cat}}/K_{\text{M}} = 2.9 \text{ mM}^{-1} \text{ min}^{-1}$) [73]. In conclusion, the chemical reactivity of the leaving group displays a very important property for enzyme acylation *in trans*.

The observation that structural similarity to the cofactor of the PCP is not an important feature for enzyme acylation *in trans* was further confirmed by the ppan leaving group. The structure of this compound exactly matches the prosthetic group of the PCP. Nevertheless, **CDA-ppan** revealed a 10-fold lower catalytic efficiency ($k_{\text{cat}}/K_{\text{M}}$) for cyclization than **CDA-SNAC** (Table 5.2, chapter 5.1.3). The poorer leaving group properties of ppan ($K_{\text{M}} = 1440 \text{ }\mu\text{M}$) compared to SNAC ($K_{\text{M}} = 147 \text{ }\mu\text{M}$) may be due to additional steric repulsions of this larger ppan arm surrogate, which is reflected in a 10-fold higher K_{M} value. Thus, enzymatic recognition of the ppan group by the TE domain *in trans* is less favored than *in cis*, where this structural element is properly aligned by the adjacent PCP for TE acylation. In accordance to the observed trend, CoA as the largest leaving group employed in this work revealed the highest K_{M} value of 8150 μM . Generally, the $k_{\text{cat}}/K_{\text{M}}$ values of the CDA thioester analogues for cyclization

significantly increase in the order **CDA-CoA** < **CDA-ppan** < **CDA-SNAC** < **CDA-thiophenol**. This indicates that the formation of the peptidyl-O-TE intermediate displays the rate-determining step in TE-mediated cyclization *in vitro*.

6.1.2. Exploring the Regioselectivity of CDA TE-Catalyzed Macrolactonization

In nature the C-terminal TE domain catalyzes the release of the NRPS-tethered linear peptide precursor by macrocyclization. So far, it has been shown that the regio- and stereoselectivity of this cyclization process is retained in excised TE domains, which makes these recombinant cyclases attractive for the *in vitro* synthesis of new cyclic compounds with a defined structure [7]. Nevertheless, the recombinant CDA cyclase from *S. coelicolor* A3(2) catalyzes the cyclization of a linear CDA analogue (**CDA**) with a relaxed regioselectivity generating two regioisomeric cyclic products (Figure 6.2). The main cyclic product was derived from nucleophilic attack of L-Thr₂ onto the C-terminus, which corresponds to the regioselectivity of naturally occurring CDA [115]. In contrast to that, the recombinant CDA cyclase also mediated the formation of a regioisomeric macrolactone, resulting in an increase of the ring size by one residue to a total number of 11. Therefore, CDA TE is the first cyclase where simultaneous formation of two macrocycles with different ring sizes was observed. The ratio between these two regioisomeric products was independent of the four leaving groups (CoA, ppan, SNAC, thiophenol) attached to the C-terminus of the linear peptide precursor **CDA** (see appendix). This indicates that solely the common acyl-enzyme intermediate of all thioester substrates determines the relaxed regioselectivity of the product formation (Figure 6.2).

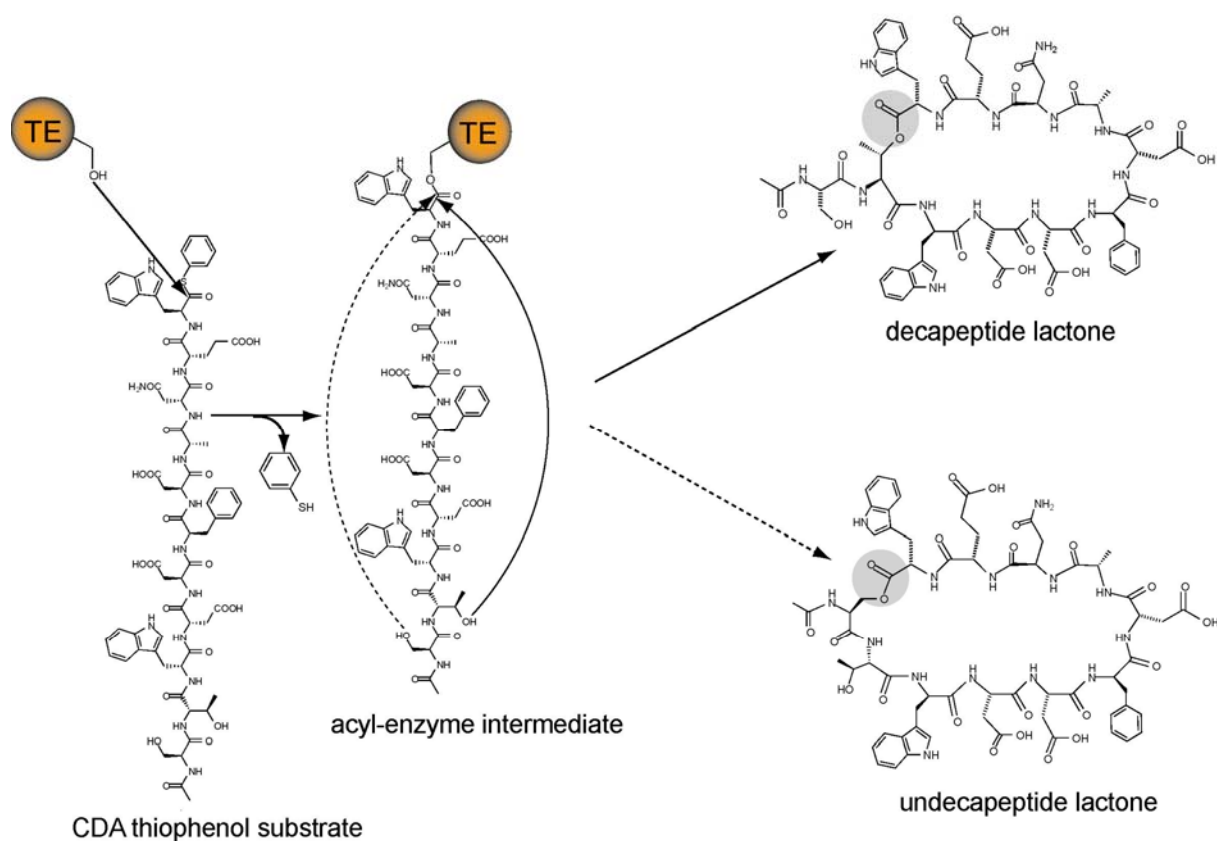


Figure 6.2: Relaxed regioselectivity of CDA TE exemplified for the **CDA-thiophenol** substrate. The active site serine residue of CDA TE is acylated by the reactive **CDA-thiophenol** substrate to generate the acyl-enzyme intermediate, which is then captured either by Thr₂ to generate a decapeptide lactone (solid line) or by Ser₁ to release the regioisomeric undecapeptide lactone (dotted line).

It was reported that fengycin PCP-TE can catalyze the cyclization of the linear fengycin CoA substrate by covalent loading of the peptidyl substrate onto the PCP [74]. It was further shown that cyclization occurred regioselectively via nucleophilic attack of Tyr at position 3, despite the presence of two adjacent nucleophiles at position 2 (Orn) and position 4 (Thr), respectively. Relocation of Tyr from position 3 to position 2 resulted in the formation of a peptidolactone ring, where the ring size was expanded by one residue. This result indicates that relaxed regioselectivity presumably arises from identical or at least similar nucleophilic residues in adjacent positions, as in the case of CDA. The acidic lipopeptide CDA is characterized by two nucleophilic residues in position 1 (Ser) and position 2 (Thr), which

differ only by a β -methyl group. By substitution of one of these residues by alanine, it was demonstrated that CDA cyclase can be forced to selectively produce one of the observed two regioisomeric peptidolactones. Probing CDA cyclase with **CDA-A1** (see appendix) resulted in the formation of the decapeptide lactone ring derived from cyclization of Thr₂ onto the C-terminus. Conversely, incubation with **CDA-A2** (see appendix) led selectively to the release of the isomeric undecapeptide lactone ring where cyclization occurred via Ser₁. The cyclization-to-hydrolysis ratio was much smaller in the latter case, indicating that CDA cyclase prefers Thr₂ as the “natural” cyclization nucleophile.

6.1.3. Probing the Stereoselectivity of CDA Cyclase

The stereoselectivity of the CDA TE mediated ring formation was explored by incubating this recombinant cyclase with five linear CDA thiophenol analogues. The simultaneous replacement of L-Ser₁ and L-Thr₂ from **CDA** by the corresponding D-configured amino acids in **CDA-DS1DT2** (see appendix) resulted in substantial hydrolysis but no cyclization in the presence of CDA cyclase. The same results were obtained when CDA cyclase was probed with substrates **CDA-DS1A2** and **CDA-A1DT2** (see appendix), which permitted the selective examination of the stereochemistry at positions 1 and 2. Remarkably, although Ser₁ does not take part in the cyclization process of naturally occurring CDA, its involvement in the formation of the undecapeptide lactone ring mediated by CDA cyclase is strictly stereoselective. Therefore, CDA cyclase provides another example of stringent stereoselective discrimination against cyclizing nucleophiles with deviating stereochemistry. Additionally, CDA cyclase was probed with the thiophenol substrates **CDA-DS1** and **CDA-DT2** (see appendix), where the stereochemistry of either Ser₁ or Thr₂ was changed. Surprisingly, CDA cyclase employed only the residue with the correct stereoinformation for the cyclization of the linear peptide precursor. Therefore, it is possible to selectively generate the decapeptide

lactone ring or the regioisomeric undecapeptide lactone ring without replacing either serine or threonine by a nonnucleophilic residue (e.g., alanine).

6.1.4. Regioselective Peptide Cyclization Triggered by the Fatty Acid Chain Length

The observed relaxed regioselectivity of the CDA thioester substrates with CDA cyclase clearly deviates from the natural NRPS system, where cyclization regioselectively occurs by nucleophilic attack of L-Thr₂. Therefore, it was tried to better approximate the natural CDA substrate. A new CDA thiophenol analogue (**Hex-CDA**, see appendix) was synthesized where the N-terminal acyl chain was elongated by four methylene groups to its natural length. Remarkably, CDA TE catalyzed the formation of only one macrocyclic product (Figure 6.3). Cyclization occurred regioselectively via L-Thr₂, producing the decapeptide lactone ring as is also observed in the natural NRPS machinery. This result suggests that the N-terminal fatty acid of CDA controls the regioselectivity of the enzyme-mediated ring formation. Further, the k_{cat} value for formation of the decapeptide lactone increased by a factor of 6 compared to **CDA-thiophenol** with the acetylated N-terminus. This may be explained due to a better alignment of the attacking L-Thr₂ nucleophile through favorable hydrophobic interactions between the hexanoic fatty acid residue and the enzyme's active site. Finally, the elongated acyl chain induced a much better chemoselectivity of the CDA cyclase catalyzed reaction. The cyclization-to-hydrolysis ratio of the corresponding thiophenol substrates rose from 5:1 (**CDA**) to 10:1 (**Hex-CDA**). This very selective flux toward cyclization could be due to the improved exclusion of water from the active site mediated by the hydrophobic fatty acid, which facilitates the capture of the acyl-O-TE intermediate by the internal L-Thr₂ nucleophile. Therefore, the relatively low cyclization-to-hydrolysis ratios of the *in vitro* cyclization of lipopeptides such as surfactin, fengycin, mycosubtilin, and syringomycin may be due to the shortened N-terminal acyl chains of the linear peptide analogues.

In summary, the results suggest that elongating the N-terminal acyl chain of linear peptide precursors improves the chemoselectivity, regioselectivity, and kinetics of recombinant TE-mediated macrocyclization. Therefore, the role of these fatty acids is not constrained to biological tasks, e.g., hydrophobic interaction with lipid bilayer membranes.

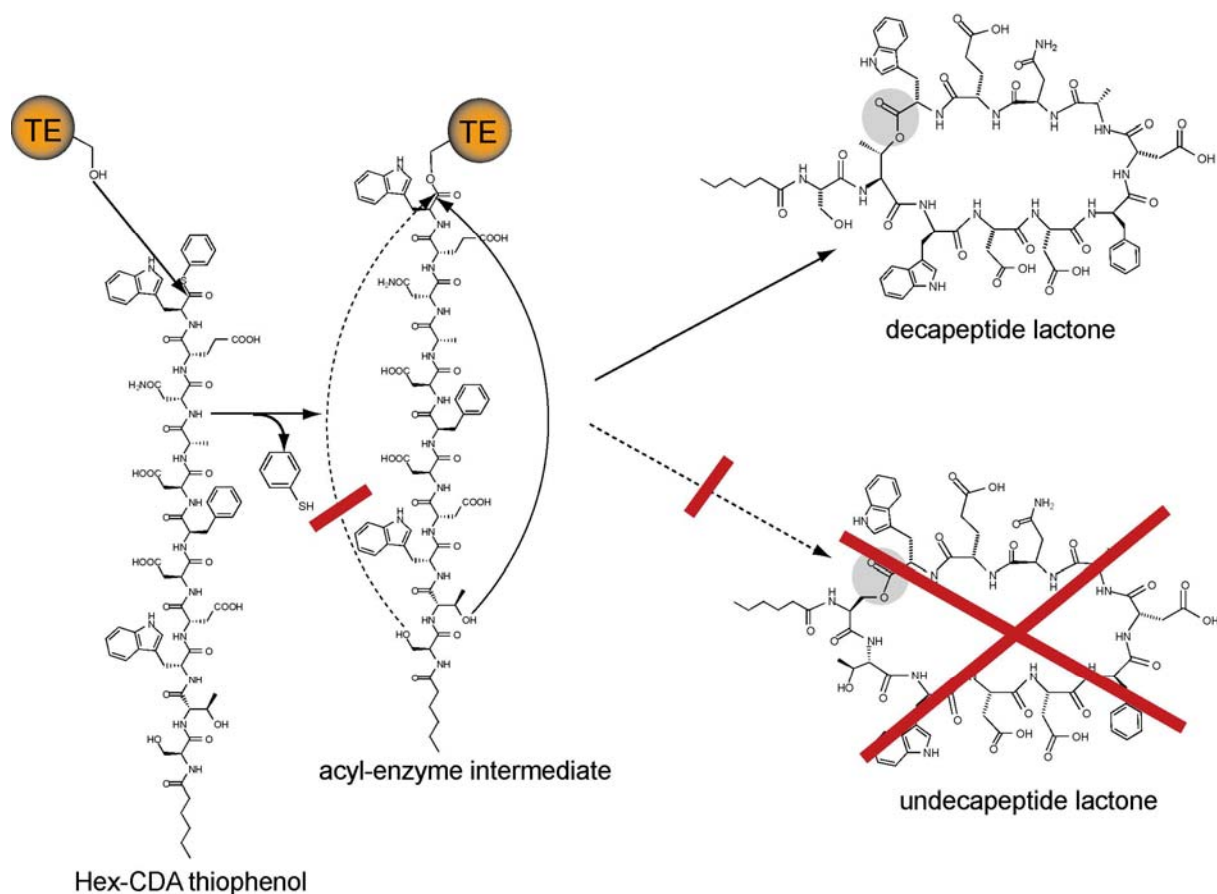


Figure 6.3: Regiospecific peptide cyclization triggered by the fatty acid chain length. The invariant serine residue of CDA cyclase is acylated by the **Hex-CDA-thiophenol** substrate to form the acyl-enzyme intermediate, which is then captured by L-Thr₂ to selectively release the decapeptide lactone.

6.2. A Chemoenzymatic Route to Daptomycin

Natural products play an important role in drug development, which is exemplified by the finding that most antibiotics and anticancer drugs in human use were derived from such compounds [3, 120]. Among these complex compounds is the recently approved antibiotic daptomycin (Figure 6.4 A). Modifications of this nonribosomal lipopeptide have been performed at only two sites so far: the α -amino group of L-Trp₁ and the δ -amino group of L-Orn₆ [116, 121, 122]. In order to make this cyclic tridecapeptide more accessible to derivatization, a new chemoenzymatic strategy was applied, which allows the production of novel variants of this important antibiotic.

6.2.1. Probing the Substrate Specificity of CDA Cyclase

The calcium-dependent antibiotic (CDA) is very similar in structure to the acidic lipopeptide daptomycin. Both compounds are decapeptide lactones, which share five common amino acid side chains in identical ring positions. Encouraged by this striking similarity, single amino acid substitution experiments were carried out. Instead of performing an alanine scan, daptomycin-characteristic residues were incorporated into the peptide backbone of CDA. Applying this strategy revealed that CDA TE is a very permissive cyclase. When hexanoic acid was fused to the N-terminus of the thioester substrates, CDA cyclase accepted all six amino acid side chains characteristic of daptomycin, including one exocyclic position. This is quite remarkable, considering that the side chain alterations in some positions resulted in dramatically different substituents, such as Gly for D-Trp₃. Interestingly, substitution of the hexanoyl fatty acid by acetic acid decreased the substrate tolerance of CDA cyclase. Specifically, for the substrate thioester **AcCDA-G3** (see appendix) only trace amounts of cyclic product were detected under standard assay conditions. Therefore, the chain length of

the N-terminal acyl residue also influences the substrate tolerance of TE mediated macrocyclization.

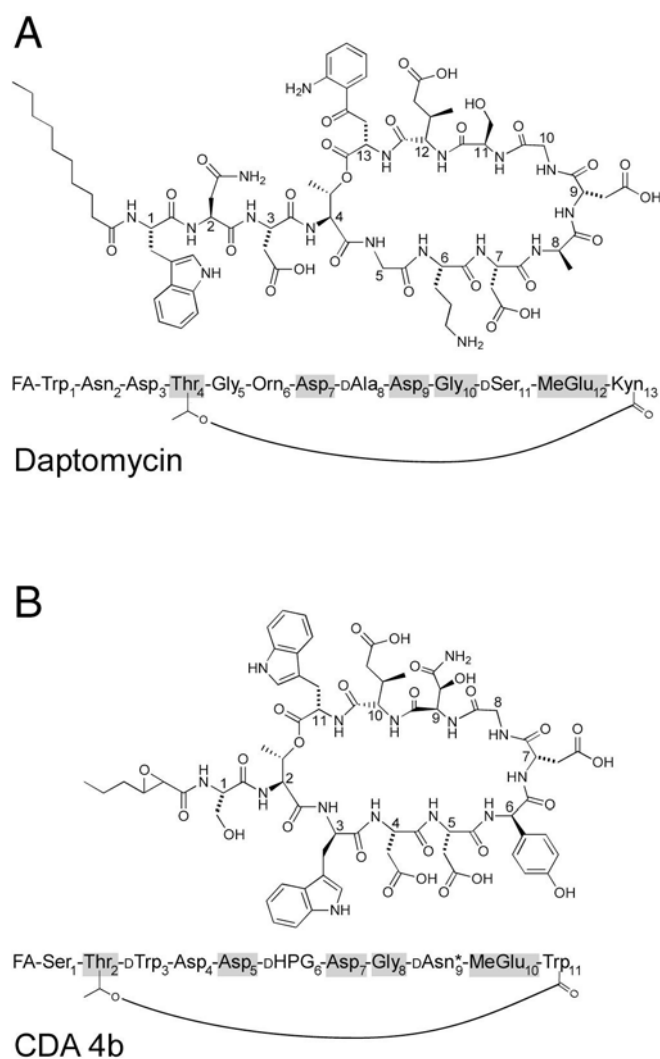


Figure 6.4: Structures of CDA and daptomycin are shown in two different fashions. Common amino acids which are found at equivalent positions in the lactone rings are indicated by shading. mGlu = L-3-methylglutamate; DAsn* = D-3-hydroxyasparagine; D-HPG = D-4-hydroxyphenylglycine.

(A) The branched cyclic tridecapeptide daptomycin derived from the fermentation of *Streptomyces roseosporus*.

(B) The calcium-dependent antibiotic (CDA) produced by *Streptomyces coelicolor* consists of 11 residues. CDA 4b represents one variant of this family of compounds.

The single amino acid substitution experiments raised the question of the effect on cyclization of simultaneous changes in potentially substitutable positions. Assaying the linear precursor peptide **Dap** (see appendix) for CDA TE mediated cyclization revealed that this cyclase behaves very tolerantly toward multiple residue substitutions in the peptide backbone. Macrolactonization of **Dap** occurred with a $k_{\text{cat}}/K_{\text{M}}$ only 1.3-fold reduced from that of the linear CDA analogue [113] and the ratio of cyclization to hydrolysis moderately dropped from 10:1 to 3:1 (Figure 6.5). This cyclization to hydrolysis ratio of **Dap** is still remarkable in comparison to studies with TycC TE, where simultaneous side chain alterations led to the predominance of hydrolysis over cyclization [75]. The efficient conversion to cyclic product

may be caused by the Asp-D-Ala-Asp-Gly motif of the linear peptide precursor. It is known that in the closely related acidic lipopeptide amphomycin the similar Asp-Gly-Asp-Gly motif induces a type II β -turn, which may preorganize the substrate in a product-like conformation [123]. Furthermore, CDA TE is capable of maintaining a macrolactone ring size of 10 residues by tolerating a branch point movement from Thr₂ to Thr₄ as proved by MS-MS sequencing. This suggests that the active site cavity of the CDA cyclase is large enough to accommodate the N-terminal extension of daptomycin, which is composed of two additional amino acids linked to a decanoyl fatty acid residue. Hence, the cyclase of the calcium-dependent antibiotic is a permissive cyclization catalyst allowing the synthesis of daptomycin *in vitro*. Although the methyl group of L-3-methylglutamate (mGlu) was omitted, it is very likely that the TE tolerates this nonproteinogenic amino acid for catalytic activity due to its occurrence in four natural variants of cognate CDA at the same position. It is assumed that a putative glutamate-3-methyltransferase catalyzes the stereospecific β -methylation of glutamate prior to activation by a specific A-domain which differs from conventional glutamate-activating A-domains [17]. This indicates that the corresponding tailoring step occurs prior to peptide cyclization by the TE domain. Notably, β -methylation of glutamate displays a key role in the biological activity of daptomycin. Substitution of mGlu₁₂ by Glu₁₂ in **Dap** yielded a 7-fold increase of the MIC against *B. subtilis*. This suggests that the more hydrophobic mGlu induces a closer contact of daptomycin with the bacterial lipid bilayer than its nonmethylated counterpart. The importance of the nonproteinogenic constituents on the antimicrobial action of daptomycin was further shown for the tryptophan metabolite L-kynurenine. Replacement by L-tryptophan resulted in an additional 5-fold increase of the MIC in comparison to **Dap**.

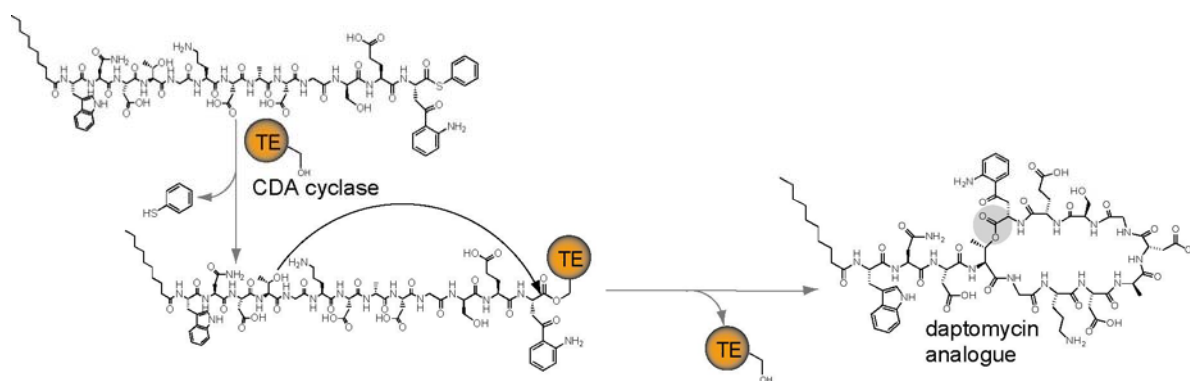


Figure 6.5: Regioselective cyclization of a daptomycin analogue catalyzed by CDA TE is shown.

6.2.2. Chemoenzymatic Derivatization of Daptomycin

The bioactivity of daptomycin is dependent on the presence of calcium ions. These divalent cations presumably trigger the oligomerization of daptomycin molecules to form ion channels, which disrupt the membrane potential of the bacterial cell [118]. Despite the 7-fold higher MIC of **Dap** in comparison to authentic daptomycin, its bactericidal activity was clearly calcium-dependent (Table 5.4, chapter 5.2.3). It is speculated that calcium interacts with the four acidic residues of daptomycin [124]. In order to explore this, the chemoenzymatic approach was used to delete these residues through replacement by noncharged amino acids (e.g., Asn and Gln). Significantly, only L-Asp₇ and L-Asp₉ in the lactone ring are essential for antibiotic activity. This is in agreement to experiments with CDA, where it was shown that deletion of L-Asp₇ in the cyclic part completely abolished antimicrobial behaviour [50]. Moreover, these ring-membered aspartic acid residues are strictly conserved among the group of acidic lipopeptides including also the calcium-dependent antibiotics friulimicins and amphomycins [20, 125] (Figure 6.6). Surprisingly, the consensus sequence DXDG of these nonribosomal peptides is also part of the calcium binding EF-hand motif of ribosomally assembled calmodulin [126]. Therefore, acidic lipopeptides and calmodulin use a similar language for calcium recognition despite their biosynthetic difference.

consensus								D	X	D	G					
daptomycin	1	W	N	D	T	G	O	D	dA	D	G	dS	Z	Z	13	
CDA4b	1			S	T	dW	D	D	dZ	D	G	dZ	Z	W	11	
amphomycins	1			D	Z	dZ	D	D	G	D	G	dZ	V	P	11	
friulimicins	1			N	Z	dZ	D	D	G	D	G	dZ	V	P	11	
calmodulin	15	E	A	F	S	L	F	D	K	D	G	D	G	T	27	
		51	D	M	I	N	E	V	D	A	D	G	N	G	T	63
		88	E	A	F	R	V	F	D	K	D	G	N	G	F	100
		124	E	M	I	R	E	A	D	I	D	G	D	G	Q	136

Figure 6.6: Alignment of nonribosomal acidic lipopeptides with the calcium binding EF-hand motif of ribosomally assembled calmodulin [126]. The conserved amino acids of the consensus sequence DXDG are highlighted by shading. O = ornithine, Z = unusual amino acid.

The function of L-Orn₆ in daptomycin is still unclear [119]. It was recently shown that the positively charged amino group of this residue is not essential for bactericidal activity but reduced the potency 8-fold compared to daptomycin [122]. In the studies presented here, a 4-fold drop in efficiency was observed when the positive charge was masked by Alloc-protection.

In conclusion, CDA cyclase is a viable tool for the synthesis of daptomycin and derivatives that are hardly accessible by chemical modification of the parental compound. This allowed exploration of the influence of nonproteinogenic and charged residues on the bioactivity of this approved antibiotic. In future, this chemoenzymatic strategy using the versatility of CDA TE can be employed for the combinatorial generation of comprehensive libraries of daptomycin analogues that can be screened for improved therapeutic activity.

6.3. TE-Catalyzed Peptide Cyclization Followed by FRET

Fluorescence resonance energy transfer (FRET) is a radiationless transfer of energy from an excited donor fluorophore to a suitable acceptor fluorophore, a physical process that depends on spectral overlap and proper dipole alignment of the two fluorophores [127]. In order to expand the scope of this technique to TE-mediated peptide cyclization, the two fluorophores Trp and Kyn were incorporated into the backbone of peptidyl-thioester substrates by using solid-phase peptide chemistry. In this case, FRET occurs by a process that comprises the excitation of the Trp residue that subsequently transfers its energy to a nonproteinogenic Kyn residue; this excited chromophore then relaxes via emission of blue light [119]. The Trp and Kyn fluorophores are originally found in the lipopeptide antibiotic daptomycin, which was clinically approved under the trade name Cubicin (see chapter 2.2). The Trp residue of daptomycin was previously shown to have a low fluorescence yield due to energy transfer to the Kyn residue. This efficient energy transfer results from the spectral overlap between the Trp donor emission ($\lambda_{Em} \approx 330$ nm) and Kyn acceptor absorption (excitation wavelength $\lambda_{Ex} \approx 350$ nm) [24, 119].

6.3.1. Distance Dependence and Detection Limits

The efficiency of FRET depends on the distance between donor and acceptor. In the case of fluorescence-assisted detection of peptide cyclization, the linear peptide precursor adopts a conformation that spatially separates the Trp and Kyn fluorophores, limiting the Kyn emission process (Figure 6.7). However, the cyclized peptide adopts a conformation in which the Kyn fluorophore is in close spatial proximity to the Trp residue allowing efficient FRET to occur. Therefore, the Kyn fluorescence difference between the linear and cyclized peptide can be exploited to reliably detect peptide cyclization. Moreover, a library of daptomycin-like peptides revealed that fluorescence-assisted detection of peptide cyclization allows variable positioning of the fluorophores in the N- and C-terminal parts of the peptide sequence, which

is significant given that TE domains do not tolerate exchanges of specific residues of their peptidic substrates [7]. Therefore, this high flexibility in primary sequence makes this approach a general tool for various peptide cyclases by simple incorporation of the fluorophores Trp and Kyn into the terminal parts of the respective linear peptidyl-thioester substrates. Finally, picomolar detection limits and a linear correlation between acceptor fluorescence and cyclopeptide concentration are realized, thus allowing determination of cyclization kinetics.

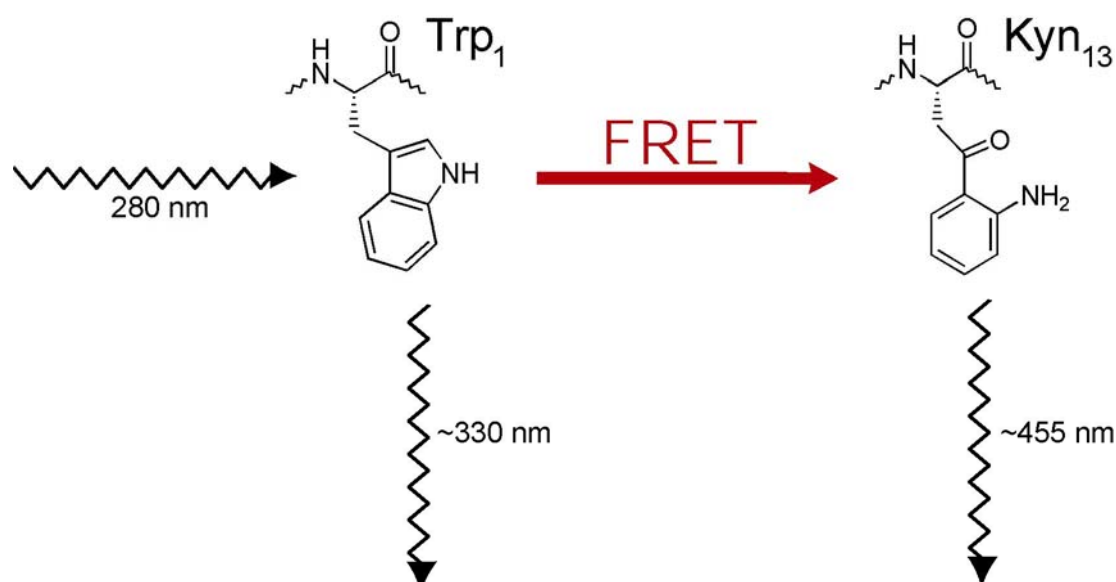


Figure 6.7: A proposed model for the energetic interactions between Trp and Kyn is shown. In case of the linear peptide precursor, excitation at 280 nm preferentially leads to emission of Trp. After cyclization this emission at ~330 nm is efficiently quenched due to fluorescence resonance energy transfer, which induces fluorescence of Kyn in the visible region of light.

6.3.2. FRET-Assisted Detection of Peptide Cyclization Combined with PCP-TE Tagging

The chemoenzymatic synthesis of macrocyclic peptides combines the strength of solid phase peptide synthesis with the strength of stereoselective and regioselective TE domain cyclization. However, a limitation of this approach is the high enzymatic selectivity of TE domains for cognate substrates, which can be a disadvantage when the cyclization of substrate

analogues is desired. Exchanges of C- and N-terminal residues of the linear peptide substrate often abolish formation of the macrocyclic product [5]. In other cases the yield of enzymatically generated ring formation dramatically suffers from linear hydrolytic by-products due to nucleophilic attack of water molecules onto the acyl-enzyme intermediate [75]. Since the utility of TE domains strongly depends on substrate tolerance, efficient turnover, and high product yield, there is a constant need for engineered TE domains. This could be achieved by directed protein evolution, as previously shown for lipases [128]. However, such an approach requires reliable detection of cyclized peptides under high-throughput conditions.

In order to combine sensitive detection of peptide cyclization via FRET with high-throughput enzymatic screening, a new strategy was developed to rapidly isolate peptide cyclases from the cell lysate. It is known that the NRPS-derived peptide carrier protein (PCP) is a versatile tag for labelling PCP fusion proteins due to its small size (80 amino acids) and its good portability to various target proteins [102]. This autonomously folded domain directs the specific labelling of the target protein in a complex mixture of cellular proteins, which is efficiently catalyzed by the promiscuous 4'-phosphopantetheinyl transferase Sfp from *B. subtilis* [38]. Using this approach, a PCP-TE didomain was excised from the CDA synthetase followed by site-directed posttranslational labelling with biotin ppan in the presence of Sfp and biotin CoA (Figure 6.8). The biotinylated PCP-TE didomain was subsequently immobilized on an avidin column. Remarkably, the immobilized CDA cyclase retained excellent catalytic activity and the cyclization of the linear peptidyl-thioester substrate, comprising the Trp-Kyn FRET pair, was accompanied by a 3.5-fold increase in fluorescence emission.

In future, this PCP-TE tagging approach combined with sensitive FRET-assisted detection of peptide cyclization can serve as a valuable tool in high-throughput enzymatic screening to

alter the substrate specificity of nonribosomal peptide cyclases by directed evolution efforts, thereby allowing the synthesis of novel cyclopeptides. Moreover, the PCP-TE didomain covalently anchored via its ppan cofactor to an insoluble solid support makes it possible to successively cyclize various linear peptide precursors in a combinatorial fashion. Such an approach would greatly facilitate the formation of comprehensive cyclic peptide libraries that can be screened for improved or altered activities.

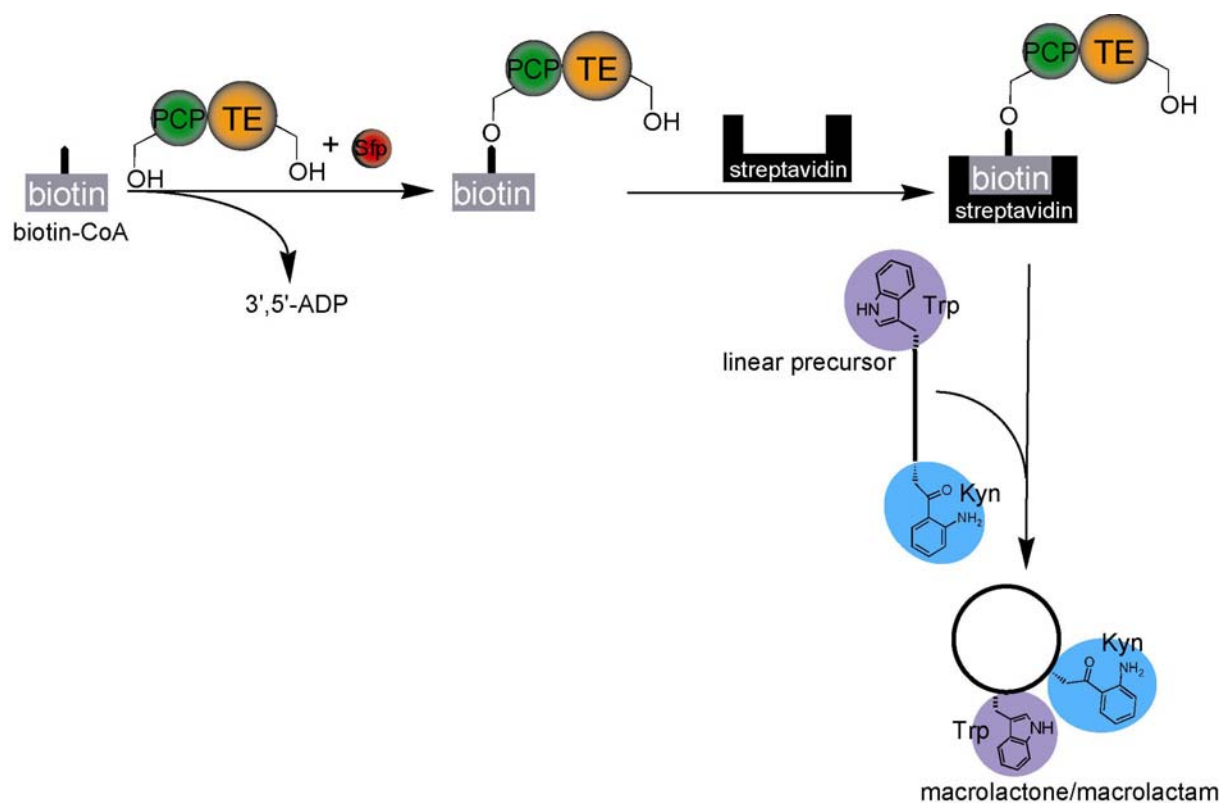


Figure 6.8: PCP-TE tagging combined with FRET-assisted detection of peptide cyclization is illustrated. Sfp-catalyzed site-directed biotin labelling of the recombinant PCP-TE didomain is followed by protein immobilization on an avidin/streptavidin surface. Successful TE-mediated macrolactonization/macrolactamization is detected by sensitive FRET.

7. Literature

1. Schwarzer, D., Finking, R., and Marahiel, M.A. (2003). Nonribosomal peptides: from genes to products. *Nat Prod Rep* 20, 275-287.
2. Walsh, C. (2000). Molecular mechanisms that confer antibacterial drug resistance. *Nature* 406, 775-781.
3. Wohlleben, W., and Pelzer, S. (2002). New compounds by combining "modern" genomics and "old-fashioned" mutasynthesis. *Chem Biol* 9, 1163-1164.
4. Chatterjee, C., Paul, M., Xie, L., and van der Donk, W.A. (2005). Biosynthesis and mode of action of lantibiotics. *Chem Rev* 105, 633-684.
5. Sieber, S.A., and Marahiel, M.A. (2005). Molecular mechanisms underlying nonribosomal Peptide synthesis: approaches to new antibiotics. *Chem Rev* 105, 715-738.
6. Marahiel, M.A., Stachelhaus, T., and Mootz, H.D. (1997). Modular Peptide Synthetases Involved in Nonribosomal Peptide Synthesis. *Chem Rev* 97, 2651-2674.
7. Kohli, R.M., and Walsh, C.T. (2003). Enzymology of acyl chain macrocyclization in natural product biosynthesis. *Chem Commun (Camb)*, 297-307.
8. Wyckoff, E.E., Stoeber, J.A., Reed, K.E., and Payne, S.M. (1997). Cloning of a *Vibrio cholerae* vibriobactin gene cluster: identification of genes required for early steps in siderophore biosynthesis. *J Bacteriol* 179, 7055-7062.
9. Walsh, C.T. (2004). Polyketide and nonribosomal peptide antibiotics: modularity and versatility. *Science* 303, 1805-1810.
10. Storm, D.R., and Strominger, J.L. (1973). Complex formation between bacitracin peptides and isoprenyl pyrophosphates. The specificity of lipid-peptide interactions. *J Biol Chem* 248, 3940-3945.
11. Storm, D.R., and Strominger, J.L. (1974). Binding of bacitracin to cells and protoplasts of *Micrococcus lysodeikticus*. *J Biol Chem* 249, 1823-1827.
12. Kahne, D., Leimkuhler, C., Lu, W., and Walsh, C. (2005). Glycopeptide and lipoglycopeptide antibiotics. *Chem Rev* 105, 425-448.
13. Williams, D.H., Williamson, M.P., Butcher, D.W., and Hammond, S.J. (1983). Detailed binding sites of the antibiotics Vancomycin and Ristocetin A: Determination of intermolecular distances in antibiotic/substrate complexes by use of the time-dependent Nuclear Overhauser Effect (NOE). *J Am Chem Soc* 105, 1332-1339.
14. Barna, J.C., and Williams, D.H. (1984). The structure and mode of action of glycopeptide antibiotics of the vancomycin group. *Annu Rev Microbiol* 38, 339-357.
15. Sieber, S.A., and Marahiel, M.A. (2003). Learning from nature's drug factories: nonribosomal synthesis of macrocyclic peptides. *J Bacteriol* 185, 7036-7043.
16. May, J.J., Wendrich, T.M., and Marahiel, M.A. (2001). The *dhb* operon of *Bacillus subtilis* encodes the biosynthetic template for the catecholic siderophore 2,3-dihydroxybenzoate-glycine-threonine trimeric ester bacillibactin. *J Biol Chem* 276, 7209-7217.
17. Hojati, Z., Milne, C., Harvey, B., Gordon, L., Borg, M., Flett, F., Wilkinson, B., Sidebottom, P.J., Rudd, B.A., Hayes, M.A., Smith, C.P., and Micklefield, J. (2002). Structure, biosynthetic origin, and engineered biosynthesis of calcium-dependent antibiotics from *Streptomyces coelicolor*. *Chem Biol* 9, 1175-1187.
18. Raja, A., LaBonte, J., Lebbo, J., and Kirkpatrick, P. (2003). Daptomycin. *Nat Rev Drug Discov* 2, 943-944.
19. Fukuda, D.S., Du Bus, R.H., Baker, P.J., Berry, D.M., and Mynderse, J.S. (1990). A54145, a new lipopeptide antibiotic complex: isolation and characterization. *J. Antibiot. (Tokyo)* 43, 594-600.

20. Vertesy, L., Ehlers, E., Kogler, H., Kurz, M., Meiwes, J., Seibert, G., Vogel, M., and Hammann, P. (2000). Friulimicins: novel lipopeptide antibiotics with peptidoglycan synthesis inhibiting activity from *Actinoplanes friuliensis* sp. nov. II. Isolation and structural characterization. *J Antibiot (Tokyo)* *53*, 816-827.
21. Bentley, S.D., Chater, K.F., Cerdeno-Tarraga, A.M., Challis, G.L., Thomson, N.R., James, K.D., Harris, D.E., Quail, M.A., Kieser, H., Harper, D., Bateman, A., Brown, S., Chandra, G., Chen, C.W., Collins, M., Cronin, A., Fraser, A., Goble, A., Hidalgo, J., Hornsby, T., Howarth, S., Huang, C.H., Kieser, T., Larke, L., Murphy, L., Oliver, K., O'Neil, S., Rabinowitsch, E., Rajandream, M.A., Rutherford, K., Rutter, S., Seeger, K., Saunders, D., Sharp, S., Squares, R., Squares, S., Taylor, K., Warren, T., Wietzorrek, A., Woodward, J., Barrell, B.G., Parkhill, J., and Hopwood, D.A. (2002). Complete genome sequence of the model actinomycete *Streptomyces coelicolor* A3(2). *Nature* *417*, 141-147.
22. Micklefield, J. (2004). Daptomycin structure and mechanism of action revealed. *Chem Biol* *11*, 887-888.
23. Tally, F.P., and DeBruin, M.F. (2000). Development of daptomycin for gram-positive infections. *J Antimicrob Chemother* *46*, 523-526.
24. Jung, D., Rozek, A., Okon, M., and Hancock, R.E. (2004). Structural transitions as determinants of the action of the calcium-dependent antibiotic daptomycin. *Chem Biol* *11*, 949-957.
25. Jones, R.N., and Barry, A.L. (1987). Antimicrobial activity and spectrum of LY146032, a lipopeptide antibiotic, including susceptibility testing recommendations. *Antimicrob Agents Chemother* *31*, 625-629.
26. Lipmann, F., et al. (1971). Polypeptide synthesis on protein templates: the enzymatic synthesis of gramicidin S and tyrocidine. *Adv. Enzymol. Relat. Areas Mol. Biol.* *35*, 1-34.
27. Lipmann, F. (1980). Bacterial production of antibiotic polypeptides by thiol-linked synthesis on protein templates. *Adv Microb Physiol* *21*, 227-266.
28. Miao, V.B., R.; Chapple, J.; She, K.; Coëffet-Le Gal, M.-F.; Baltz, R. H. (2005). The lipopeptide antibiotic A54145 biosynthetic gene cluster from *Streptomyces fradiae*. *in press*.
29. Schwarzer, D., and Marahiel, M.A. (2001). Multimodular biocatalysts for natural product assembly. *Naturwissenschaften* *88*, 93-101.
30. Mootz, H.D., Schwarzer, D., and Marahiel, M.A. (2002). Ways of assembling complex natural products on modular nonribosomal peptide synthetases. *Chembiochem* *3*, 490-504.
31. Hahn, M., and Stachelhaus, T. (2004). Selective interaction between nonribosomal peptide synthetases is facilitated by short communication-mediating domains. *Proc Natl Acad Sci U S A* *101*, 15585-15590.
32. Broadhurst, R.W., Nietlispach, D., Wheatcroft, M.P., Leadlay, P.F., and Weissman, K.J. (2003). The structure of docking domains in modular polyketide synthases. *Chem Biol* *10*, 723-731.
33. Dieckmann, R., Lee, Y.O., van Liempt, H., von Dohren, H., and Kleinkauf, H. (1995). Expression of an active adenylate-forming domain of peptide synthetases corresponding to acyl-CoA-synthetases. *FEBS Lett* *357*, 212-216.
34. May, J.J., Kessler, N., Marahiel, M.A., and Stubbs, M.T. (2002). Crystal structure of DhbE, an archetype for aryl acid activating domains of modular nonribosomal peptide synthetases. *Proc Natl Acad Sci U S A* *99*, 12120-12125.
35. Stryer, L. (1996). *Biochemie*. Spektrum Akademischer Verlag Heidelberg Berlin Oxford, 4. Auflage.

36. Ehmman, D.E., Shaw-Reid, C.A., Losey, H.C., and Walsh, C.T. (2000). The EntF and EntE adenylation domains of *Escherichia coli* enterobactin synthetase: sequestration and selectivity in acyl-AMP transfers to thiolation domain cosubstrates. *Proc Natl Acad Sci U S A* 97, 2509-2514.
37. Stachelhaus, T., Huser, A., and Marahiel, M.A. (1996). Biochemical characterization of peptidyl carrier protein (PCP), the thiolation domain of multifunctional peptide synthetases. *Chem Biol* 3, 913-921.
38. Lambalot, R.H., Gehring, A.M., Flugel, R.S., Zuber, P., LaCelle, M., Marahiel, M.A., Reid, R., Khosla, C., and Walsh, C.T. (1996). A new enzyme superfamily - the phosphopantetheinyl transferases. *Chem Biol* 3, 923-936.
39. Bergendahl, V., Linne, U., and Marahiel, M.A. (2002). Mutational analysis of the C-domain in nonribosomal peptide synthesis. *Eur J Biochem* 269, 620-629.
40. Stachelhaus, T., Mootz, H.D., Bergendahl, V., and Marahiel, M.A. (1998). Peptide bond formation in nonribosomal peptide biosynthesis. Catalytic role of the condensation domain. *J Biol Chem* 273, 22773-22781.
41. Stein, T., Vater, J., Kruft, V., Otto, A., Wittmann-Liebold, B., Franke, P., Panico, M., McDowell, R., and Morris, H.R. (1996). The multiple carrier model of nonribosomal peptide biosynthesis at modular multienzymatic templates. *J Biol Chem* 271, 15428-15435.
42. Clugston, S.L., Sieber, S.A., Marahiel, M.A., and Walsh, C.T. (2003). Chirality of peptide bond-forming condensation domains in nonribosomal peptide synthetases: the C5 domain of tyrocidine synthetase is a (D)C(L) catalyst. *Biochemistry* 42, 12095-12104.
43. Belshaw, P.J., Walsh, C.T., and Stachelhaus, T. (1999). Aminoacyl-CoAs as probes of condensation domain selectivity in nonribosomal peptide synthesis. *Science* 284, 486-489.
44. Conti, E., Stachelhaus, T., Marahiel, M.A., and Brick, P. (1997). Structural basis for the activation of phenylalanine in the non-ribosomal biosynthesis of gramicidin S. *Embo J* 16, 4174-4183.
45. Weber, T., Baumgartner, R., Renner, C., Marahiel, M.A., and Holak, T.A. (2000). Solution structure of PCP, a prototype for the peptidyl carrier domains of modular peptide synthetases. *Structure Fold Des* 8, 407-418.
46. Keating, T.A., Marshall, C.G., Walsh, C.T., and Keating, A.E. (2002). The structure of VibH represents nonribosomal peptide synthetase condensation, cyclization and epimerization domains. *Nat Struct Biol* 9, 522-526.
47. Jackowski, S. (1996). Biosynthesis of coenzymes and prosthetic groups. *E. coli and Salmonella. Cellular and Molecular Biology New York: ASM Press*, 687-694.
48. Schwarzer, D., Mootz, H.D., Linne, U., and Marahiel, M.A. (2002). Regeneration of misprimed nonribosomal peptide synthetases by type II thioesterases. *Proc Natl Acad Sci U S A* 99, 14083-14088.
49. Yeh, E., Kohli, R.M., Bruner, S.D., and Walsh, C.T. (2004). Type II thioesterase restores activity of a NRPS module stalled with an aminoacyl-S-enzyme that cannot be elongated. *Chembiochem* 5, 1290-1293.
50. Uguru, G.C., Milne, C., Borg, M., Flett, F., Smith, C.P., and Micklefield, J. (2004). Active-site modifications of adenylation domains lead to hydrolysis of upstream nonribosomal peptidyl thioester intermediates. *J Am Chem Soc* 126, 5032-5033.
51. Miao, V., Coeffet-Legal, M.F., Brian, P., Brost, R., Penn, J., Whiting, A., Martin, S., Ford, R., Parr, I., Bouchard, M., Silva, C.J., Wrigley, S.K., and Baltz, R.H. (2005). Daptomycin biosynthesis in *Streptomyces roseosporus*: cloning and analysis of the gene cluster and revision of peptide stereochemistry. *Microbiology* 151, 1507-1523.

52. Trivedi, O.A., Arora, P., Sridharan, V., Tickoo, R., Mohanty, D., and Gokhale, R.S. (2004). Enzymic activation and transfer of fatty acids as acyl-adenylates in mycobacteria. *Nature* *428*, 441-445.
53. Konz, D., and Marahiel, M.A. (1999). How do peptide synthetases generate structural diversity? *Chem Biol* *6*, R39-48.
54. Luo, L., Kohli, R.M., Onishi, M., Linne, U., Marahiel, M.A., and Walsh, C.T. (2002). Timing of epimerization and condensation reactions in nonribosomal peptide assembly lines: kinetic analysis of phenylalanine activating elongation modules of tyrocidine synthetase B. *Biochemistry* *41*, 9184-9196.
55. Stachelhaus, T., and Walsh, C.T. (2000). Mutational analysis of the epimerization domain in the initiation module PheATE of gramicidin S synthetase. *Biochemistry* *39*, 5775-5787.
56. Pfeifer, E., Pavela-Vrancic, M., von Dohren, H., and Kleinkauf, H. (1995). Characterization of tyrocidine synthetase 1 (TY1): requirement of posttranslational modification for peptide biosynthesis. *Biochemistry* *34*, 7450-7459.
57. Hoffmann, K., Schneider-Scherzer, E., Kleinkauf, H., and Zocher, R. (1994). Purification and characterization of eucaryotic alanine racemase acting as key enzyme in cyclosporin biosynthesis. *J Biol Chem* *269*, 12710-12714.
58. Balibar, C.J.V., F. H.; Walsh, C. T. (2005). Generation of D-Amino Acid Residues in Assembly of Arthrofactin by Dual Condensation/Epimerization Domains. *Chem Biol in press*.
59. Weber, G., and Leitner, E. (1994). Disruption of the cyclosporin synthetase gene of *Tolypocladium niveum*. *Curr Genet* *26*, 461-467.
60. Kessler, N., Schuhmann, H., Morneweg, S., Linne, U., and Marahiel, M.A. (2003). The linear pentadecapeptide gramicidin is assembled by four multimodular nonribosomal peptide synthetases that comprise 16 modules with 56 catalytic domains. *J Biol Chem*, submitted.
61. Becker, J.E., Moore, R.E., and Moore, B.S. (2004). Cloning, sequencing, and biochemical characterization of the nostocyclopeptide biosynthetic gene cluster: molecular basis for imine macrocyclization. *Gene* *325*, 35-42.
62. Bruner, S.D., Weber, T., Kohli, R.M., Schwarzer, D., Marahiel, M.A., Walsh, C.T., and Stubbs, M.T. (2002). Structural basis for the cyclization of the lipopeptide antibiotic surfactin by the thioesterase domain SrfTE. *Structure (Camb)* *10*, 301-310.
63. Tseng, C.C., Bruner, S.D., Kohli, R.M., Marahiel, M.A., Walsh, C.T., and Sieber, S.A. (2002). Characterization of the surfactin synthetase C-terminal thioesterase domain as a cyclic depsipeptide synthase. *Biochemistry* *41*, 13350-13359.
64. Sewald, N., and Jakubke, H. (2002). *Peptides: Chemistry and Biology*, Volume p. 313 (Weinheim: Wiley-VCH).
65. Davies, J.S. (2003). The cyclization of peptides and depsipeptides. *J Pept Sci* *9*, 471-501.
66. Trauger, J.W., Kohli, R.M., Mootz, H.D., Marahiel, M.A., and Walsh, C.T. (2000). Peptide cyclization catalysed by the thioesterase domain of tyrocidine synthetase. *Nature* *407*, 215-218.
67. Yeh, E., Lin, H., Clugston, S.L., Kohli, R.M., and Walsh, C.T. (2004). Enhanced macrocyclizing activity of the thioesterase from tyrocidine synthetase in presence of nonionic detergent. *Chem Biol* *11*, 1573-1582.
68. Kohli, R.M., Trauger, J.W., Schwarzer, D., Marahiel, M.A., and Walsh, C.T. (2001). Generality of peptide cyclization catalyzed by isolated thioesterase domains of nonribosomal peptide synthetases. *Biochemistry* *40*, 7099-7108.

69. Trauger, J.W., Kohli, R.M., and Walsh, C.T. (2001). Cyclization of backbone-substituted peptides catalyzed by the thioesterase domain from the tyrocidine nonribosomal peptide synthetase. *Biochemistry* *40*, 7092-7098.
70. Mahlert, C., Sieber, S.A., Grünewald, J., and Marahiel, M.A. (2005). Chemoenzymatic approach to enantiopure streptogramin B variants: characterization of stereoselective pristinamycin I cyclase from *Streptomyces pristinaespiralis*. *J Am Chem Soc* *127*, 9571-9580.
71. Turner, N.J. (2004). Enzyme catalysed deracemisation and dynamic kinetic resolution reactions. *Curr Opin Chem Biol* *8*, 114-119.
72. Mukhtar, T.A., Koteva, K.P., and Wright, G.D. (2005). Chimeric streptogramin-tyrocidine antibiotics that overcome streptogramin resistance. *Chem Biol* *12*, 229-235.
73. Sieber, S.A., Tao, J., Walsh, C.T., and Marahiel, M.A. (2004). Peptidyl thiophenols as substrates for nonribosomal peptide cyclases. *Angew Chem Int Ed Engl* *43*, 493-498.
74. Sieber, S.A., Walsh, C.T., and Marahiel, M.A. (2003). Loading peptidyl-coenzyme A onto peptidyl carrier proteins: a novel approach in characterizing macrocyclization by thioesterase domains. *J Am Chem Soc* *125*, 10862-10866.
75. Kohli, R.M., Takagi, J., and Walsh, C.T. (2002). The thioesterase domain from a nonribosomal peptide synthetase as a cyclization catalyst for integrin binding peptides. *Proc Natl Acad Sci U S A* *99*, 1247-1252.
76. Kohli, R.M., Burke, M.D., Tao, J., and Walsh, C.T. (2003). Chemoenzymatic route to macrocyclic hybrid peptide/polyketide-like molecules. *J Am Chem Soc* *125*, 7160-7161.
77. Du, L., Sanchez, C., and Shen, B. (2001). Hybrid peptide-polyketide natural products: biosynthesis and prospects toward engineering novel molecules. *Metab Eng* *3*, 78-95.
78. Garbe, D., Sieber, S.A., Bandur, N.G., Koert, U., and Marahiel, M.A. (2004). Enzymatic cyclisation of peptidomimetics with incorporated (E)-alkene dipeptide isosteres. *Chembiochem* *5*, 1000-1003.
79. Lin, H., and Walsh, C.T. (2004). A chemoenzymatic approach to glycopeptide antibiotics. *J Am Chem Soc* *126*, 13998-14003.
80. Lin, H., Thayer, D.A., Wong, C.H., and Walsh, C.T. (2004). Macrolactamization of glycosylated peptide thioesters by the thioesterase domain of tyrocidine synthetase. *Chem Biol* *11*, 1635-1642.
81. Boeck, L.D., Papiska, H.R., Wetzel, R.W., Mynderse, J.S., Fukuda, D.S., Mertz, F.P., and Berry, D.M. (1990). A54145, a new lipopeptide antibiotic complex: discovery, taxonomy, fermentation and HPLC. *J Antibiot (Tokyo)* *43*, 587-593.
82. Kagan, R.M., and Clarke, S. (1994). Widespread occurrence of three sequence motifs in diverse S-adenosylmethionine-dependent methyltransferases suggests a common structure for these enzymes. *Arch Biochem Biophys* *310*, 417-427.
83. Kim, H.B., Smith, C.P., Micklefield, J., and Mavituna, F. (2004). Metabolic flux analysis for calcium dependent antibiotic (CDA) production in *Streptomyces coelicolor*. *Metab Eng* *6*, 313-325.
84. Heinzelmann, E., Berger, S., Puk, O., Reichenstein, B., Wohlleben, W., and Schwartz, D. (2003). A glutamate mutase is involved in the biosynthesis of the lipopeptide antibiotic friulimicin in *Actinoplanes friuliensis*. *Antimicrob Agents Chemother* *47*, 447-457.
85. Buckel, W. (2001). Unusual enzymes involved in five pathways of glutamate fermentation. *Appl Microbiol Biotechnol* *57*, 263-273.
86. Kato, Y., and Asano, Y. (1997). 3-Methylaspartate ammonia-lyase as a marker enzyme of the mesaconate pathway for (S)-glutamate fermentation in Enterobacteriaceae. *Arch Microbiol* *168*, 457-463.

87. Velkov, T., and Lawen, A. (2003). Non-ribosomal peptide synthetases as technological platforms for the synthesis of highly modified peptide bioeffectors--Cyclosporin synthetase as a complex example. *Biotechnol Annu Rev* 9, 151-197.
88. de Crecy-Lagard, V., Blanc, V., Gil, P., Naudin, L., Lorenzon, S., Famechon, A., Bamas-Jacques, N., Crouzet, J., and Thibaut, D. (1997). Pristinamycin I biosynthesis in *Streptomyces pristinaespiralis*: molecular characterization of the first two structural peptide synthetase genes. *J Bacteriol* 179, 705-713.
89. Schauwecker, F., Pfennig, F., Grammel, N., and Keller, U. (2000). Construction and in vitro analysis of a new bi-modular polypeptide synthetase for synthesis of N-methylated acyl peptides. *Chem Biol* 7, 287-297.
90. Chen, H., O'Connor, S., Cane, D.E., and Walsh, C.T. (2001). Epothilone biosynthesis: assembly of the methylthiazolylcarboxy starter unit on the EpoB subunit. *Chem Biol* 8, 899-912.
91. Du, L., Sanchez, C., Chen, M., Edwards, D.J., and Shen, B. (2000). The biosynthetic gene cluster for the antitumor drug bleomycin from *Streptomyces verticillus* ATCC15003 supporting functional interactions between nonribosomal peptide synthetases and a polyketide synthase. *Chem Biol* 7, 623-642.
92. Schneider, T.L., and Walsh, C.T. (2004). Portability of oxidase domains in nonribosomal peptide synthetase modules. *Biochemistry* 43, 15946-15955.
93. Finking, R., and Marahiel, M.A. (2004). Biosynthesis of nonribosomal peptides1. *Annu Rev Microbiol* 58, 453-488.
94. Du, L., Chen, M., Sanchez, C., and Shen, B. (2000). An oxidation domain in the BlmIII nonribosomal peptide synthetase probably catalyzing thiazole formation in the biosynthesis of the anti-tumor drug bleomycin in *Streptomyces verticillus* ATCC15003. *FEMS Microbiol. Lett.* 189, 171-175.
95. Schneider, T.L., Shen, B., and Walsh, C.T. (2003). Oxidase domains in epothilone and bleomycin biosynthesis: thiazoline to thiazole oxidation during chain elongation. *Biochemistry* 42, 9722-9730.
96. Silakowski, B., Schairer, H.U., Ehret, H., Kunze, B., Weinig, S., Nordsiek, G., Brandt, P., Blocker, H., Hofle, G., Beyer, S., and Muller, R. (1999). New lessons for combinatorial biosynthesis from myxobacteria. The myxothiazol biosynthetic gene cluster of *Stigmatella aurantiaca* DW4/3-1. *J Biol Chem* 274, 37391-37399.
97. Duerfahrt, T., Eppelmann, K., Muller, R., and Marahiel, M.A. (2004). Rational design of a bimodular model system for the investigation of heterocyclization in nonribosomal peptide biosynthesis. *Chem Biol* 11, 261-271.
98. Pelzer, S., Sussmuth, R., Heckmann, D., Recktenwald, J., Huber, P., Jung, G., and Wohlleben, W. (1999). Identification and analysis of the balhimycin biosynthetic gene cluster and its use for manipulating glycopeptide biosynthesis in *Amycolatopsis mediterranei* DSM5908. *Antimicrob Agents Chemother* 43, 1565-1573.
99. Bischoff, D., Pelzer, S., Bister, B., Nicholson, G.J., Stockert, S., Schirle, M., Wohlleben, W., Jung, G., and Sussmuth, R.D. (2001). The Biosynthesis of Vancomycin-Type Glycopeptide Antibiotics-The Order of the Cyclization Steps This work was supported by the Deutsche Forschungsgemeinschaft (SFB 323) and by a grant of the EU (MEGATOP, QLK3-1999-00650). R. D. S. gratefully acknowledges the support of a Feodor-Lynen Fellowship granted by the Alexander-von-Humboldt Stiftung. We thank Corina Bihlmaier and Volker Pfeifer for help with transformation and Southern hybridization, J. A. Moss (La Jolla (USA)) for critical comments on the manuscript and Prof. Dr. M. E. Maier and Prof. Dr. H.-P. Fiedler (Tubingen) for generous support. *Angew Chem Int Ed Engl* 40, 4688-4691.

100. Zerbe, K., Woithe, K., Li, D.B., Vitali, F., Bigler, L., and Robinson, J.A. (2004). An oxidative phenol coupling reaction catalyzed by oxyB, a cytochrome P450 from the vancomycin-producing microorganism. *Angew Chem Int Ed Engl* *43*, 6709-6713.
101. Quadri, L.E., Weinreb, P.H., Lei, M., Nakano, M.M., Zuber, P., and Walsh, C.T. (1998). Characterization of Sfp, a *Bacillus subtilis* phosphopantetheinyl transferase for peptidyl carrier protein domains in peptide synthetases. *Biochemistry* *37*, 1585-1595.
102. La Clair, J.J., Foley, T.L., Schegg, T.R., Regan, C.M., and Burkart, M.D. (2004). Manipulation of carrier proteins in antibiotic biosynthesis. *Chem Biol* *11*, 195-201.
103. Mercer, A.C., La Clair, J.J., and Burkart, M.D. (2005). Fluorescent multiplex analysis of carrier protein post-translational modification. *Chembiochem* *6*, 1335-1337.
104. Yin, J., Liu, F., Li, X., and Walsh, C.T. (2004). Labeling proteins with small molecules by site-specific posttranslational modification. *J Am Chem Soc* *126*, 7754-7755.
105. Yin, J., Liu, F., Schinke, M., Daly, C., and Walsh, C.T. (2004). Phagemid encoded small molecules for high throughput screening of chemical libraries. *J Am Chem Soc* *126*, 13570-13571.
106. Vivero-Pol, L., George, N., Krumm, H., Johnsson, K., and Johnsson, N. (2005). Multicolor Imaging of Cell Surface Proteins. *J Am Chem Soc* *127*, 12770-12771.
107. George, N., Pick, H., Vogel, H., Johnsson, N., and Johnsson, K. (2004). Specific labeling of cell surface proteins with chemically diverse compounds. *J Am Chem Soc* *126*, 8896-8897.
108. Clarke, K.M., Mercer, A.C., La Clair, J.J., and Burkart, M.D. (2005). In vivo reporter labeling of proteins via metabolic delivery of coenzyme A analogues. *J Am Chem Soc* *127*, 11234-11235.
109. Linne, U., and Marahiel, M.A. (2004). Reactions catalyzed by mature and recombinant nonribosomal peptide synthetases. *Methods Enzymol* *388*, 293-315.
110. Sambrook, J., Fritsch, E.F., and Maniatis, T. (1989). *Molecular cloning: a laboratory manual*. Cold Spring Laboratory press, Cold spring Harbor, NY.
111. Bradford, M.M. (1976). A rapid and sensitive method for the quantitation of microgram quantities of protein utilizing the principle of protein-dye binding. *Anal Biochem* *72*, 248-254.
112. Kohli, R.M., Walsh, C.T., and Burkart, M.D. (2002). Biomimetic synthesis and optimization of cyclic peptide antibiotics. *Nature* *418*, 658-661.
113. Grünwald, J., Sieber, S.A., and Marahiel, M.A. (2004). Chemo- and regioselective peptide cyclization triggered by the N-terminal fatty acid chain length: the recombinant cyclase of the calcium-dependent antibiotic from *Streptomyces coelicolor*. *Biochemistry* *43*, 2915-2925.
114. LaVallie, E.R., DiBlasio, E.A., Kovacic, S., Grant, K.L., Schendel, P.F., and McCoy, J.M. (1993). A thioredoxin gene fusion expression system that circumvents inclusion body formation in the *E. coli* cytoplasm. *Biotechnology (N Y)* *11*, 187-193.
115. Kempter, C., Kaiser, D., Haag, S., Nicholson, G., Gnau, V., Walk, T., Gierling, K.H., Decker, H., Zähner, H., Jung, G., and Metzger, J.W. (1997). CDA: Calcium-dependent peptide antibiotics from *Streptomyces coelicolor* A3(2) containing unusual residues. *Angew. Chem. Int. Ed. Engl.* *36*, 498-501.
116. Debono, M., Abbott, B.J., Molloy, R.M., Fukuda, D.S., Hunt, A.H., Daupert, V.M., Counter, F.T., Ott, J.L., Carrell, C.B., Howard, L.C., and et al. (1988). Enzymatic and chemical modifications of lipopeptide antibiotic A21978C: the synthesis and evaluation of daptomycin (LY146032). *J Antibiot (Tokyo)* *41*, 1093-1105.
117. Richter, S.S., Kealey, D.E., Murray, C.T., Heilmann, K.P., Coffman, S.L., and Doern, G.V. (2003). The in vitro activity of daptomycin against *Staphylococcus aureus* and *Enterococcus* species. *J Antimicrob Chemother* *52*, 123-127.

118. Silverman, J.A., Perlmutter, N.G., and Shapiro, H.M. (2003). Correlation of daptomycin bactericidal activity and membrane depolarization in *Staphylococcus aureus*. *Antimicrob Agents Chemother* *47*, 2538-2544.
119. Lakey, J.H., and Ptak, M. (1988). Fluorescence indicates a calcium-dependent interaction between the lipopeptide antibiotic LY146032 and phospholipid membranes. *Biochemistry* *27*, 4639-4645.
120. Harvey, A. (2000). Strategies for discovering drugs from previously unexplored natural products. *Drug Discov Today* *5*, 294-300.
121. Siedlecki, J., Hill, J., Parr, I., Yu, X., Morytko, M., Zhang, Y., Silverman, J., Controneo, N., Laganas, V., Li, T., Li, J., Keith, D., Shimer, G., and Finn, J. (2003). Array synthesis of novel lipodepsipeptide. *Bioorg Med Chem Lett* *13*, 4245-4249.
122. Hill, J., Siedlecki, J., Parr, I., Morytko, M., Yu, X., Zhang, Y., Silverman, J., Controneo, N., Laganas, V., Li, T., Lai, J.J., Keith, D., Shimer, G., and Finn, J. (2003). Synthesis and biological activity of N-Acylated ornithine analogues of daptomycin. *Bioorg Med Chem Lett* *13*, 4187-4191.
123. Lakey, J.H., Maget-Dana, R., and Ptak, M. (1988). Conformational change on calcium binding by the lipopeptide antibiotic amphomycin. A C.D. and monolayer study. *Biochem Biophys Res Commun* *150*, 384-390.
124. Ball, L.J., Goult, C.M., Donarski, J.A., Micklefield, J., and Ramesh, V. (2004). NMR structure determination and calcium binding effects of lipopeptide antibiotic daptomycin. *Org Biomol Chem* *2*, 1872-1878.
125. Banerjee, D.K., Scher, M.G., and Waechter, C.J. (1981). Amphomycin: effect of the lipopeptide antibiotic on the glycosylation and extraction of dolichyl monophosphate in calf brain membranes. *Biochemistry* *20*, 1561-1568.
126. Yazawa, M., and Yagi, K. (1980). The amino acid sequence of the calmodulin obtained from sea anemone (*metridium senile*) muscle. *Biochem Biophys Res Commun* *96*, 377-381.
127. Förster, T. (1948). Intermolecular energy migration and fluorescence. *Ann. Phys.* *2*, 55 - 75.
128. Reetz, M.T. (2002). Lipases as practical biocatalysts. *Curr Opin Chem Biol* *6*, 145-150.

Appendix

Name	Peptide Sequence
CDA	Ac-Ser-Thr-DTrp-Asp-Asp-DPhe-Asp-Ala-DAsn-Glu-Trp
Hex-CDA	Hex-Ser-Thr-DTrp-Asp-Asp-DPhe-Asp-Ala-DAsn-Glu-Trp
CDA-A1A2	Ac-Ala-Ala-DTrp-Asp-Asp-DPhe-Asp-Ala-DAsn-Glu-Trp
CDA-A1	Ac-Ala-Thr-DTrp-Asp-Asp-DPhe-Asp-Ala-DAsn-Glu-Trp
CDA-A2	Ac-Ser-Ala-DTrp-Asp-Asp-DPhe-Asp-Ala-DAsn-Glu-Trp
CDA-DS1A2	Ac-DSer-Ala-DTrp-Asp-Asp-DPhe-Asp-Ala-DAsn-Glu-Trp
CDA-A1DT2	Ac-Ala-DThr-DTrp-Asp-Asp-DPhe-Asp-Ala-DAsn-Glu-Trp
CDA-DS1	Ac-DSer-Thr-DTrp-Asp-Asp-DPhe-Asp-Ala-DAsn-Glu-Trp
CDA-DT2	Ac-Ser-DThr-DTrp-Asp-Asp-DPhe-Asp-Ala-DAsn-Glu-Trp
CDA-DS1DT2	Ac-DSer-DThr-DTrp-Asp-Asp-DPhe-Asp-Ala-DAsn-Glu-Trp
AcCDA-G3	Ac-Ser-Thr-Gly-Asp-Asp-DPhe-Asp-Ala-DAsn-Glu-Trp
AcCDA-O4	Ac-Ser-Thr-DTrp-Orn-Asp-DPhe-Asp-Ala-DAsn-Glu-Trp
AcCDA-DA6	Ac-Ser-Thr-DTrp-Asp-Asp-DAla-Asp-Ala-DAsn-Glu-Trp
AcCDA-DS9	Ac-Ser-Thr-DTrp-Asp-Asp-DPhe-Asp-Ala-DSer-Glu-Trp
HexCDA-G3	Hex-Ser-Thr-Gly-Asp-Asp-DPhe-Asp-Ala-DAsn-Glu-Trp
HexCDA-O4	Hex-Ser-Thr-DTrp-Orn-Asp-DPhe-Asp-Ala-DAsn-Glu-Trp
HexCDA-DA6	Hex-Ser-Thr-DTrp-Asp-Asp-DAla-Asp-Ala-DAsn-Glu-Trp
HexCDA-DS9	Hex-Ser-Thr-DTrp-Asp-Asp-DPhe-Asp-Ala-DSer-Glu-Trp
HexCDA-D1	Hex-Asp-Thr-DTrp-Asp-Asp-DPhe-Asp-Ala-DAsn-Glu-Trp
HexCDA-U11	Hex-Ser-Thr-DTrp-Asp-Asp-DPhe-Asp-Ala-DAsn-Glu-Kyn
Dap	Dec-Trp-Asn-Asp-Thr-Gly-Orn-Asp-DAla-Asp-Gly-DSer-Glu-Kyn
Dap-N3	Dec-Trp-Asn-Asn-Thr-Gly-Orn-Asp-DAla-Asp-Gly-DSer-Glu-Kyn
Dap-N7	Dec-Trp-Asn-Asp-Thr-Gly-Orn-Asn-DAla-Asp-Gly-DSer-Glu-Kyn
Dap-N9	Dec-Trp-Asn-Asp-Thr-Gly-Orn-Asp-DAla-Asn-Gly-DSer-Glu-Kyn
Dap-Q12	Dec-Trp-Asn-Asp-Thr-Gly-Orn-Asp-DAla-Asp-Gly-DSer-Gln-Kyn
Dap-DD11	Dec-Trp-Asn-Asp-Thr-Gly-Orn-Asp-DAla-Asp-Gly-DAsp-Glu-Kyn
Dap-Aloc	Dec-Trp-Asn-Asp-Thr-Gly-Orn(Aloc)-Asp-DAla-Asp-Gly-DSer-Glu-Kyn
Dap-W13	Dec-Trp-Asn-Asp-Thr-Gly-Orn-Asp-DAla-Asp-Gly-DSer-Glu-Trp
Dap-W13K6	Dec-Trp-Asn-Asp-Thr-Gly-Lys-Asp-DAla-Asp-Gly-DSer-Glu-Trp
Dap-U₁W₁₃	Dec-Kyn-DAsn-Asp-Thr-Gly-Orn-Asp-DAla-Asp-Gly-DSer-Glu-Trp
Dap-U₂W₁₃	Dec-DAsn-Kyn-Asp-Thr-Gly-Orn-Asp-DAla-Asp-Gly-DSer-Glu-Trp
Dap-U₃W₁₃	Dec-DAsn-Asp-Kyn-Thr-Gly-Orn-Asp-DAla-Asp-Gly-DSer-Glu-Trp
Dap-U₅W₁₃	Dec-DAsn-Asp-Gly-Thr-Kyn-Orn-Asp-DAla-Asp-Gly-DSer-Glu-Trp
Dap-U₇W₁₃	Dec-DAsn-Asp-Gly-Thr-Orn-Asp-Kyn-DAla-Asp-Gly-DSer-Glu-Trp
Dap-U₁W₁₄	Dec-Kyn-DAsn-Asp-Gly-Thr-Gly-Orn-Asp-DAla-Asp-Gly-DSer-Glu-Trp
Dap-U₁W₁₅	Dec-Kyn-DAsn-Asp-Gly-Gly-Thr-Gly-Orn-Asp-DAla-Asp-Gly-DSer-Glu-Trp
Tyc-U₂W₈	DPhe-Kyn-Phe-DPhe-Asn-Gln-Tyr-Trp-Orn-Leu

Acknowledgements

I would like to thank Prof. M. A. Marahiel for his excellent scientific guidance and generous support during my diploma and doctoral thesis in his lab. I gratefully acknowledge his important scientific advice and education as well as fruitful discussions. He always supported new ideas and helped to develop them further which significantly influenced my way of scientific thinking. I am particular grateful for the generous opportunity to attend two Gordon Research Conferences at Oxford (UK) and Ventura Beach (California, USA). I would like to thank him for being in my thesis committee and for providing an expert opinion. I would be very grateful for his support in my future.

I also acknowledge the opportunity to discuss scientific results with Prof. C. T. Walsh from Harvard Medical School (Cambridge, USA). I would like to thank Prof. M. A. Marahiel, Prof. L. O. Essen and Prof. C. T. Walsh for supporting my fellowship application for a postdoctoral position.

I would like to thank Prof. L. O. Essen, Prof. T. Schrader, and Prof. Klebe for being in my thesis committee.

I gratefully acknowledge all members of the Marahiel laboratory and junior groups for their generous help. In particular, I would like to thank Christoph Mahlert for his motivation and excellent help with solid phase peptide synthesis, Dr. Stephan A. Sieber for very fruitful collaborations and help with the TE projects, Florian Kopp for superb support of the FRET project and commitment on TE projects, Dr. Uwe Linne for his expert opinion concerning mass spectrometry and his commitment on FRET measurements, Dr. Dirk Schwarzer and Dr. Jürgen May for their help in the initial part of my diploma thesis, Dr. Henning D. Mootz for excellent scientific comments, Christian Wirges, Jonas Treutwein, Gabi Schimpff-Weiland and Dr. Antonio Pierik for fruitful support of the FRET and TE projects, Antje Schäfer, Jenny Hilberg and Christiane Bomm for technical assistance and Björn Wagner, Daniel Garbe, Nadine Schracke, Dr. Torsten Stachelhaus, Daniel Stein, Dr. Jun Yin, Marcus Miethke and Georg Schönafinger for interesting research discussions. I would also like to thank Prof. Lars-Oliver Essen for supporting my fellowship application for a postdoctoral position and I gratefully acknowledge the generous gift of daptomycin from Cubist Pharmaceuticals (Lexington, USA).

I gratefully acknowledge Florian Kopp, Christoph Mahlert, and Dr. Stephan A. Sieber for proof reading the manuscript of the thesis.

I would like to thank the “Fond der Chemischen Industrie” for the financial support during my thesis. I would also like to acknowledge the Graduiertenkolleg “Protein function at the atomic level” for the many opportunities to present my research to an international audience.

I would like to thank my parents for their support. I wish to dedicate this thesis to them.